



The Use of Optical Coherence Tomography as a Diagnostic Tool for Dental Caries

**Submitted in partial fulfilment of the requirements for the Degree of
Clinical Doctorate in Dentistry (Paediatric Dentistry)**

University College London

Eastman Dental Institute

2016 - 2019

Submitted by:

Rawan Waleed Al-Khuwaitem

B.Dent.Sc. (University of Liverpool), MFD part 1 – RCSI,

MPaed Dent (RCSED)

Project supervisors:

Dr. Laurent Bozec (Faculty of Dentistry, University of Toronto, Toronto, Canada)

Dr. Susan Parekh (Department of Paediatric Dentistry, Eastman Dental Institute-
University College London)

DECLARATION OF WORK

I, Rawan Waleed Al-Khuwaitem confirm that the work presented in this thesis is my own. Where information has been derived from other sources, I confirm that this has been acknowledged and indicated in the thesis.

Rawan Waleed Al-Khuwaitem

DDent Peadiatric Dentistry

Eastman Dental Institute, University of College London

July 2019

Word Count: 32702

Abstract

Dental caries is one of the most common human diseases, 60-90% of school children worldwide have dental cavities. Severity can vary, from early demineralisation, which preventive measures can improve, to cavitation, leading to fillings. Different diagnostic tools are available, such as clinical examination, radiographic investigation and Enhanced Visual examination/International Caries Detection and Assessment System (ICDAS). To date, there is no universal diagnostic tool that can be used to detect carious lesions at the very early stages. Optical Coherence Tomography (OCT) is a non-invasive and ionising radiation free technique that has been used in dentistry, but not to diagnose caries.

The aim of this research was to investigate the use of OCT imaging in dentistry as a routine, and adjunct clinical diagnostic tool for dental caries, by developing standardised markers for each ICDAS score, and to compare the results with conventional clinical methods i.e. radiographs and ICDAS. In addition, markers in the OCT scan and scattering profile intensity plots for both sound and carious affected teeth were determined, to aid diagnosis.

All specimens were collected from patients undergoing dental treatment at Eastman Dental Hospital. Extracted human primary and permanent teeth ($N > 180$) with varying caries severity were collected under ethical approval, after obtaining informed consent according to the inclusion and exclusion criteria. Photographic and radiographic images of tooth samples were taken and categorised according to the ICDAS system. Samples were then imaged using OCT (VivoSight OCT Scanner) with each lesion scanned separately ($N > 200$). The scattering intensity profiles were plotted. In healthy samples, OCT B-scans showed a homogenous pattern of scattering intensity throughout enamel structure indicating healthy structure while in carious teeth, a non-homogenous scattering intensity was observed indicating changes in enamel structure.

Different scattering intensity profiles for each ICDAS score were observed, and empirical markers were developed for each score. This led to establishing scattering fingerprints for each type of ICDAS lesion. A multi-assessor's analysis, followed by a kappa analysis, was carried to evaluate the selectivity and accuracy of the markers. The results showed moderate to substantial strength of agreement in both intra-rater and inter-rater reliability.

In conclusion, OCT has been shown to be a safe, useful, reliable and non-destructive technique that can investigate the internal structure by measuring the back-scattered light from enamel and dentine. OCT provides an understanding of the lesion in terms of depth and extent, therefore helping in predicting the lesion's prognosis, which is not found in conventional

methods. In addition, OCT helps to differentiate between carious and sound teeth, and additionally between different ICDAS scores. The definition of specific scattering markers for each type of caries lesions will enable us to bring this technique one-step closer to the clinic.

AKNOWLEDGEMNT

Alhamdulillah, with His gracious help, I managed to finish and submit this final thesis after three years of continuous hard work and sacrifice. I would like to acknowledge everyone who played a role in my academic accomplishments. First and foremost, I dedicate it to my beloved parents, **Waleed Al-khuwaitem** and **Bedour Al-Turaiji**, who supported me with love and understanding. The pillars upon which I stand tall. Without you, I could never have reached this current level of success. Thank you for everything. Your love, support and constant encouragement throughout my life has been an inspiration. All that I am or ever hope to be, I owe to you. I wish I could show you just how much I love you and appreciate you.

Furthermore, I would like to express my deepest appreciation to my grandmother, **Latifa Al-Tuwajri**, and my Aunt, Auntie **Hanadi**, my sisters, **Dana**, **Jana** and **Hanouf** and brother, **Mohammad** for their continuous prayers, encouragement and for being my backbone and supporters in all my difficult times . **Abdullah** and **Deema** my beautiful nephew and niece nothing makes me happier than seeing your smile after a long tough day. Thanks for believing in me and always lending an ear to all my dramatic meltdowns. There is a piece of you all in this thesis.

Moreover, I would also like to show appreciation to my research supervisors, **Dr Laurent Bozec** and **Dr Susan Parekh**, for their excellent guidance endless support and encouragement and valuable advice throughout the three years of my studies to complete this research- I cannot thank you enough. Your valuable comments were much appreciated, considered, and contributed to the completion of this study.

In addition to that, I would like to express my gratitude to the programme director, **Prof. Paul Ashley**, we all appreciate and recognise his effort to make DDent programme a smooth sail for us.

Also, I would like to express my deepest gratitude to my lovely **colleagues** in DDent programme for their support and always having each other's back during this fun -filled journey. We had together moments of happiness and despair for the last three years. Thank you for always being there. This is the beginning of a lifelong friendship.

To all the staff that I have met and worked with in the Unit of Paediatric Dentistry of the Eastman Dental Institute/Hospital, thank you very much for your lovely companionship.

Finally, I would like to give my special thanks to the **Kuwait Ministry of Health**, for the financial support and the opportunity given to further my studies.

This journey and thesis would not have been possible without you all.

Rawan Waleed Al-Khuwaitem

DDent Paediatric Dentistry

Eastman Dental Institute, University of College London

July 2019

Impact statement

Dental caries is considered the most common human disease, affecting about 60-90% of school children worldwide, and nearly 100% of the adult population (Petersen, 2003). Dentists and patients are faced with caries and its subsequent problems daily. Patient related problems include pain that may cause disturbance in eating and sleeping, aesthetics, discomfort and the expense of managing caries, costing 5-10% of health care expenditure worldwide (Petersen, 2003). Clinician related problems include pain management and restoring the aesthetics and function of carious teeth. It is one of the more common pandemic health problems in the world, and it can be effectively controlled by early diagnosis, followed by appropriate treatment. Continuing research and development are needed to prevent and manage this important international health problem.

Caries can be diagnosed both clinically and radiographically, however with limitations. Many techniques are used to detect dental caries; clinical techniques depend on the position of the caries (proximal surfaces, occlusal surfaces), and include visual and radiographic assessment. ICDAS is a system for detection and visual assessment of dental caries. It was developed for epidemiological studies, and it is considered a gold standard system in the detection of dental caries (Ismail et al., 2007). ICDAS is a simple, practical and evidence-based system that can be used in clinical setting, public health programmes and dental research (www.icdas.org). However, ICDAS is unable to detect the depth of early white spot lesion before it becomes cavitated lesions.

The other method to assess the depth of the carious lesion is the use of radiographs. However, in clinical situations, radiographs are not indicated to detect caries white spot lesions. Also, radiographs not only possess radiation and ionisation effects, but children may not be able to tolerate intra-oral films. Therefore, minimally invasive techniques to assess caries at the early stages are required.

I have presented my research to colleagues and professors in our institute and proposed a calibration exercise on how to correctly use OCT markers to report different scores of ICDAS caries lesions. This research was presented as a poster at the International Dental Association of Research (IADR) in London, United Kingdom 2018, and at the International Association of Paediatric Dentistry (IAPD) in Cancun, Mexico 2019, where researchers from all over the world attend, interact and exchange new knowledge (Appendices 7 and 8).

This research can be a starting point for bringing the OCT scanner to the dental clinic, as a routine diagnostic tool. Furthermore, the markers can be further studied and used with a larger sample size to confirm their validity and reproducibility.

Table of contents

Declaration of work	3
Abstract.....	4
Acknowledgement.....	6
Impact statement.....	8
List of figures.....	12
List of tables.....	15
List of Abbreviations.....	17
1 Introduction.....	18
2 Review of literature	20
2.1 Dental caries	20
a. Definition	20
b. Epidemiology.....	20
2.2 Aetiology	20
2.2.1 Bacteria.....	21
2.2.2 Diet.....	22
2.2.3 Susceptibility	23
2.2.4 Genetic factor.....	23
2.2.5 Enamel Hypoplasia	23
2.3 Management	25
2.4 Diagnosis	27
2.4.1 Visual and tactile.....	28
2.4.2 Radiographic imaging	28
2.4.3 Diagnodent (DD)	31
2.4.4 Dyes for Caries Detection	32
2.4.5 Quantitative Light Induced Fluorescence (QLF)	33
2.4.6 Fiber Optic Transillumination (FOTI).....	34
2.4.7 Digital Imaging Fiber Optic Trans-illumination (DIFOTI)	34
2.4.8 Electric Conductance Monitor (ECM).....	35
2.4.9 International Caries Detection and Assessment System (ICDAS).....	36
2.4.10 Optical Coherence Tomography (OCT)	38
3 Aim and objectives.....	46
3.1 Rational for Research	46
3.2 Aim.....	46

3.3 Objectives	46
4 Patient Recruitment and Selection.....	48
4.1 Study registration and ethical approval	48
4.2 Patient identification and recruitments	48
4.3 Samples collection and storage	49
5 The assessment of the samples using conventional methods in diagnosing caries.....	52
5.1 Rationale of this section.....	51
5.2 Materials and methods.....	51
5.2.1 Materials and methods for clinical visual assessment using ICDAS.....	52
5.2.2 Materials and methods for Radiographic assessments	53
5.3 Results.....	53
5.3.1 Results of clinical visual assessment using ICDAS.....	53
5.3.2 Results of Radiographic assessment.....	55
5.4 Discussion.....	57
5.4.1 Clinical visual assessment using ICDAS.....	57
5.4.2 Radiographic assessment.....	58
6 OCT as a diagnostic imaging tool	61
6.1 Optical Coherence Tomography Scanner.....	61
6.2 The assessment of samples using OCT scanner	62
6.2.1 Method	62
6.2.2 Results of Optical Coherence Tomography (OCT)	64
6.2.2.1 Results of control sample.....	65
6.2.2.2 Results of ICDAS score 1 sample.....	66
6.2.2.3 Results of ICDAS score 2 sample.....	67
6.2.2.4 Results of ICDAS score 3 sample.....	68
6.2.2.5 Results of ICDAS score 4 sample.....	69
6.2.2.6 Results of ICDAS score 5 sample.....	70
6.2.2.7 Results of ICDAS score 6 sample.....	71
6.3 Advanced Diagnostics Using OCT Signal Intensity Profiles	72
6.3.1 Method	72
6.3.2 Application of signal intensity profile	72
6.3.2.1 Signal Intensity Profile of Control Sample.....	73
6.3.2.2 Signal Intensity Profile of ICDAS score 1 Sample.....	75

6.3.2.3 Signal Intensity Profile of ICDAS score 2 Sample.....	77
6.3.2.4 Signal Intensity Profile of ICDAS score 3 Sample.....	79
6.3.2.5 Signal Intensity Profile of ICDAS score 4 Sample.....	81
6.3.2.6 Signal Intensity Profile of ICDAS score 5 Sample.....	83
6.3.2.7 Signal Intensity Profile of ICDAS score 6 Sample.....	85
6.4 Discussion.....	86
6.4.1 Optical coherence tomography scanning.....	86
6.4.2 Diagnostic potential of OCT.....	87
6.4.3 Conclusion.....	89
7 Defining markers in the OCT scan and scattering profile intensity plots.....	91
7.1 Methods- multi-examiners evaluation of the markers	94
7.1.1 Exercise 1: Intra-examiner reliability	92
7.1.2 Exercise 2: Inter-examiner reliability	94
7.1.3 Exercise 3- Populating the Empirical Markers.....	94
7.2 Results.....	95
7.2.1 Exercise 1.....	95
7.2.2 Exercise 2.....	97
7.2.3 Exercise 3.....	98
7.3 Discussion	99
7.3.1 Exercise 1.....	99
7.3.2 Exercise 2.....	100
7.3.3 Exercise 3.....	100
8 Progression of Lesion from 2D to 3D Diagnostics.....	102
8.1 Methods.....	103
8.1.1 Mapping a-scans across the B-scan.....	103
8.1.2 Mapping a-scans across the c-scan.....	104
8.2 Results.....	104
8.3 Discussion.....	105
8.3.1 From building blocks to a whole image – cross-sectional analysis.....	105
8.3.2 Clinical need for 3-Dimension volumetric data.....	106
9 Clinical Relevance.....	108

9.1 Clinical relevance of caries and OCT.....	109
9.2 Limitations.....	110
10 Future work	111
11 Conclusion.	113
12 Scientific Dissemination.....	115
12.1 Poster Presentations.....	116
13 References.....	117
14 Appendices.....	131

List of Figures:

Figure 2.1: Stephan curve.....21

Figure 2.2: Diagram illustrates Ecological plaque hypothesis.....22

Figure 2.3: Model of the sequence of events leading to HAS-ECC.....25

Figure 2.4: Decision making for carious lesions in retainable teeth with vital pulps. ART, atraumatic restorative treatment..... 27

Figure 2.5: Diagram illustrates visual tactile tools.....29

Figure 2.6: Diagram illustrates Bitewing x-rays arrows indicate caries.....29

Figure 2.7: Diagram illustrates Lateral oblique radiograph.....31

Figure 2.8: Diagram illustrates how Diagnodent works.....32

Figure 2.9: Diagram illustrates caries detector dyes.....33

Figure 2.10: Diagram illustrates QLF.....34

Figure 2.11: Diagram illustrates DIFOTI.....35

Figure 2.12: Diagram illustrates ECM.....36

Figure 2.13: Diagram illustrates an b- OCT b-scan image of a dental enamel.....40

Figure 2.14: Diagram illustrates a scattering plot (a-scan) obtained by plotting the scattering intensity profile vs the enamel depth.....41

Figure 2.15: Diagram demonstrating the principles of OCT.....43

Figure 4.1: Schematic Diagram outlining how the sample teeth were collected.....49

Figure 5.1: A) Radiographic image of a control tooth shown in the a) clinical photograph....54

Figure 5.2: A) Radiographic image of a score 2 ICDAS tooth shown in the a) clinical photograph57

Figure 5.3: A) Radiographic image of a score 3 ICDAS tooth shown in the a) clinical photograph58

Figure 5.4: A) Radiographic image of a score 6 ICDAS tooth shown in the a) clinical photograph..... 58

Figure 6.1: Image shows the different parts of OCT machine63

Figure 6.2: Control sample clinical photo and OCT b-scan.....66

Figure 6.3: ICDAS score 1 sample clinical photo and OCT b-scan.....69

Figure 6.4: ICDAS score 2 sample clinical photo and OCT b-scan.....70

Figure 6.5: ICDAS score 3 sample clinical photo and OCT b-scan.....71

Figure 6.6: ICDAS score 4 sample clinical photo and OCT b-scan.....72

Figure 6.7: ICDAS score 5 sample clinical photo and OCT b-scan.....73

Figure 6.8: ICDAS score 6 sample clinical photo and OCT b-scan.....74

Figure 6.9: OCT b- scans and a- scans of samples75

Figure 6.10 Signal intensity profile of a control healthy enamel.....76

Figure 6.11 Back scattered light intensity profiles extracted from eight different selected regions in an OCT image of a control sample healthy enamel.....	75
Figure 6.12 Signal intensity profile of ICDAS score 1.....	76
Figure 6.13 Back scattered light intensity profiles extracted from ten different selected regions in an OCT image of ICDAS score 1 sample.....	77
Figure 6.14 Signal intensity profile of ICDAS score 2.....	78
Figure 6.15 Back scattered light intensity profiles extracted from ten different selected regions in an OCT image of ICDAS score 2 sample.....	79
Figure 6.16 Signal intensity profile of ICDAS score 3.....	80
Figure 6.17 Back scattered light intensity profiles extracted from ten different selected regions in an OCT image of ICDAS score 3 sample.....	81
Figure 6.18 Signal intensity profile of ICDAS score 4.....	82
Figure 6.19 Back scattered light intensity profiles extracted from ten different selected regions in an OCT image of ICDAS score 4 sample.....	83
Figure 6.20 Signal intensity profile of ICDAS score 5.....	84
Figure 6.21 Back scattered light intensity profiles extracted from ten different selected regions in an OCT image of ICDAS score 5 sample.....	85
Figure 6.22 Signal intensity profile of ICDAS score 6.....	86
Figure 6.23 Back scattered light intensity profiles extracted from ten different selected regions in an OCT image of ICDAS score 6 sample.....	87
Figure 6.24: Summary of back scattered light intensity profiles of control and scores 1-6 ICDAS.....	88
Figure 7.1 illustrates formula used to generate Cohen's Kappa.....	94
Figure 7.2: Bar charts summary of cycle 1 and 2 results.....	96
Figure 8.1 Demonstrating schematic description of the distribution of the regions chosen throughout a b-scan of sample 13 ICDAS score 1, with the yellow boxes resembling a 10-pixel width of scan.....	102
Figure 8.2 Illustrating consecutive regions of a-scans taken throughout a b-scan of sample 13 ICDAS score 1, with their corresponding a-scans.....	102
Figure 8.3: showing how the data was fed to excel origin, with the a-axis being as a constant, and consequently adding the y-axis data for ICDAS score 3 sample.....	103
Figure 8.4: Illustrating a-scan waterfall plot (stacks of a-scans) across an ICDAS score 3 sample.....	104
Figure 8.5: Demonstrate presentation of carious lesion from building block to a whole 3D volumetric image via MATLAB, 3D image courtesy of Dr Bozec.....	107

List of Tables:

Table 2.1: The table demonstrates ICDAS scoring system with clinical pictures37

Table 5.1: Table demonstrates ICDAS scoring system.....55

Table 5.2: Table demonstrates data of sound teeth samples used in the study.....56

Table 5.3: Table demonstrates data of carious teeth samples used in the study.....56

Table 7.1 illustrates different empirical markers of control and ICDAS 1-4 samples.....92

Table 7.2 illustrates interpretation of Cohen’s Kappa values.....94

Table 7.3 Showing different types of scoring markers and each examiner filled in a table with presented sample number based on what they see in the a-scans.....95

Table 7.4: Illustrates summary of results of first cycle.....97

Table 7.5: Illustrates summary of results of second cycle.....98

Table 7.6: Illustrates intra-rater reliability in match of type to specified pattern of markers over cycle 1 and 2, measured by Kappa index (Single rater, 52 lesions).....98

Table 7.7: Illustrates summary of results of exercise 2..... 99

Table 7.8: Illustrates Cohen’s overall Kappa values of assessment of markers between 10 different examiners (inter-rater reliability). (10 different raters, 52 lesions).....100

Table 7.9: Illustrates Cohen’s Kappa values of intra-rater reliability of assessment of markers, Examiner 6 (single rater, 1 week apart; 52 lesions).....100

Table 7.10: Illustrates Cohen’s Kappa values of intra-rater reliability of assessment of markers, Examiner 9 (single rater, 1 week apart; 52 lesions).....100

LIST OF ABBREVIATIONS

ART	Atraumatic restorative treatment
BW	Bite-wing radiograph
CCD	Charge-Coupled Device
CEJ	Cementum Enamel Junction
DD	Diagnodent
DIFOTI	Digital Imaging Fiber Optic Transillumination
DNA	Deoxyribonucleic acid
EDJ	Enamel Dentine Junction
EDH	Eastman Dental Hospital
ECM	Electric Conductance Monitor
ECJ	Enamel cementum junction
FD-LCI	Fourier domain Low Coherence Interferometry
fFD-LCI	frequency tuning Fourier Domain Low Coherence Interferometry
FD-OCT	Fourier Domain- Optical Coherence Tomography
FOTI	Fiber Optic Transillumination
ICDAS	International Caries Detecting and Assessment System
LCI	Low coherence interferometry
µm	micro metre
NIR	Near-Infra Red
nm	Nano metre
OCT	Optical Coherence Tomography
OPL	Optical Path-Length
PD	Photo detector
PS- OCT	Polarisation Sensitive Optical Coherence Tomography
QLF	Quantitative Light Fluorescence
SD-OCT	Spectral Domain OCT
SEM	Scanning Electron Microscope
sFD – LCI	spectral Low Coherence Interferometry Fourier domain
SLD	Super luminescent light diode
TD-LCI	Time Domain- Low Coherence interferometry
TD-OCT	Time Domain OCT
US	United States
WHO	World Health Organization

CHAPTER 1

Introduction

Introduction

Research Problem

Dental caries is one of the most common human diseases, 60-90% of school children worldwide have dental cavities (Petersen, 2003). Early detection and diagnosis of caries prevents pain and reduce the progression of the bacterial invasion, thus reducing the loss of the hard tissues of the tooth. Different diagnostic tools to determine caries include; clinical examination, radiographic investigation, Light fluorescence detectors and Enhanced Visual examination/International Caries Detection and Assessment System (ICDAS). These diagnostic tools have their limitations, and therefore there is a need for better diagnostic tools to give more information about the extent of these lesions into the enamel and dentine. To date, there is no one universal diagnostic tool that can be used to detect carious lesions at the very early stages. In this project, the aim is to evaluate Optical Coherence tomography (OCT) and to understand its light response to enamel changes of refractive properties of demineralized enamel at various stages of degeneration, so a better clinical diagnostic tool can be developed to identify early changes in enamel structure when caries affects it. OCT is considered as a non-ionizing technique, so teeth will be examined without exposing the patient to radiation hazard. OCT is a simple, quick technique to investigate the enamel structure. Employing OCT in the clinical setting will aid in early caries diagnosis, and help in early intervention and reversing demineralisation process.

CHAPTER 2

Review of Literature

Review of the Literature

2.1 Dental caries

a. Definition

Dental caries is the irreversible loss of the hard tissues of the tooth structure, due to acid that been produced by bacteria, mainly *Streptococcus Mutans* (Kidd and Fejerskov, 2004).

b. Epidemiology

Dental caries is one of the most common human diseases, with 60-90% of school children worldwide having dental cavities (www.who.int). The oral health survey of three-year-old children (2013) by Public Health England, reported that 12% of three-year-old children had experience of obvious dental decay, with one or more teeth decayed to dentinal level, extracted, or filled because of caries (www.nwph.net).

In 2015, the National Dental Epidemiology Programme for England oral health survey of five-year-old children, reported that the proportions who were free from visually obvious dental decay were 75.2%. The remaining 24.7% had experience of dental decay with one or more teeth that were decayed to dentinal level, extracted, or filled because of caries (www.nwph.net).

According to the Children's Dental Health Survey in 2013, 10% of 12-15-year olds had a general anaesthetic for dental treatment (www.nhs.uk). Levels of dental caries have decreased over the last twenty years; however, this drop appears to be levelling off.

2.2 Aetiology

The term "caries" can be used to refer to both the caries process, and the caries lesion that forms because of that process; the caries process is initiated in the biofilm or dental plaque (Fejerskov and Thylstrup, 1994). Biofilms form on any solid surface exposed to appropriate amounts of water and nutrients (Kidd and Fejerskov, 2004). The dental hard tissues such as enamel, dentine, and cementum, are the appropriate oral solid surfaces, and these surfaces are coated by a pellicle to which the microbial cells attach (Kidd and Fejerskov, 2004). A pellicle is a thin film that is formed from proteins, which develops in seconds after teeth brushing and cleaning (Kidd and Fejerskov, 2004). Over the pellicle, the plaque biofilm which consists of large number of bacteria develops then colonises by primary and secondary organisms, to create a matrix within which cells grow (Selwitz et al., 2007).

Figure 2.1 illustrates Stephan curve, which was first described by Robert Stephan in 1943, showing the fall in pH below the critical level of pH 5.5, at which demineralization of enamel occurs following the intake of fermentable carbohydrates, acidic liquids, or sugar in the presence of acidogenic bacteria. After consumption, there is an elimination of the acid and a return to normal saliva or plaque pH, at which point repair of any destruction of the enamel structure

takes place (remineralization). Repeated intakes of fermentable carbohydrates cause the low pH to be maintained for longer periods, thereby not allowing remineralization to take place (Stephan and Miller, 1943 , Manji et al., 1991). The cumulative result of these de- and re-mineralization processes lead to dissolution of the dental hard tissues and the formation of a caries lesion. Caries is most likely to occur where the biofilm is undisturbed, such as occlusal fissures and approximal sites.

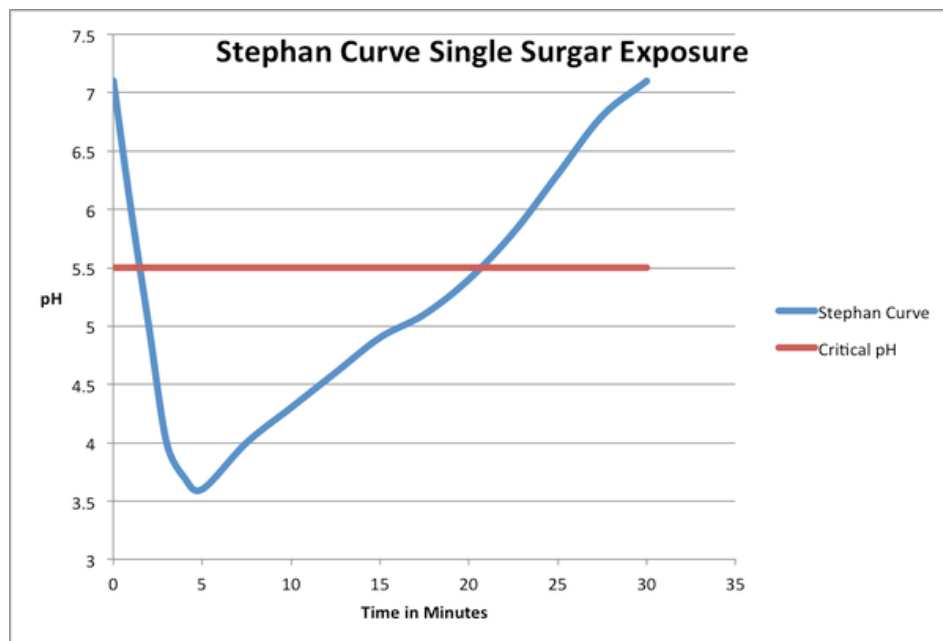


Figure 2.1: Illustrates Stephan curve, Image retrieved from: <https://www.quora.com/What-is-the-Stephan-curve-in-dentistry>

2.2.1 Bacteria

Dental biofilms produce acids from carbohydrates that result in caries (Takahashi and Nyvad, 2008). There have been two main schools of thought on the role of plaque bacteria in the aetiology of caries and periodontal diseases. The "**Specific Plaque Hypothesis**" proposed that, out of the diverse collection of organisms comprising the resident plaque microflora, only a few species are actively involved in disease. This proposal focused on controlling disease by targeting preventive measures and treatment against a limited number of organisms (Loesche, 1976). In contrast, the "**Non-Specific Plaque Hypothesis**" considered that disease is the outcome of the overall activity of the total plaque microflora that collect on the gingival crevice and tooth surfaces in the oral cavity. These bacteria produce specific factors and substances that causes inflammation and damage to the gingival tissues. In this way, a heterogeneous mixture of microorganisms could play a role in disease. In some respects, the arguments about the relative merits of these hypotheses may be about semantics, since plaque-mediated diseases are essentially mixed culture (polymicrobial) infections, but in which only a

limited number of species are able to predominate. More recently, an alternative hypothesis has been proposed the "**Ecological Plaque Hypothesis**" that reconciles the key elements of the earlier two hypotheses. According to the caries ecological hypothesis, the caries process consists of three reversible stages as demonstrated below in figure 2.2 (Takahashi and Nyvad, 2010).

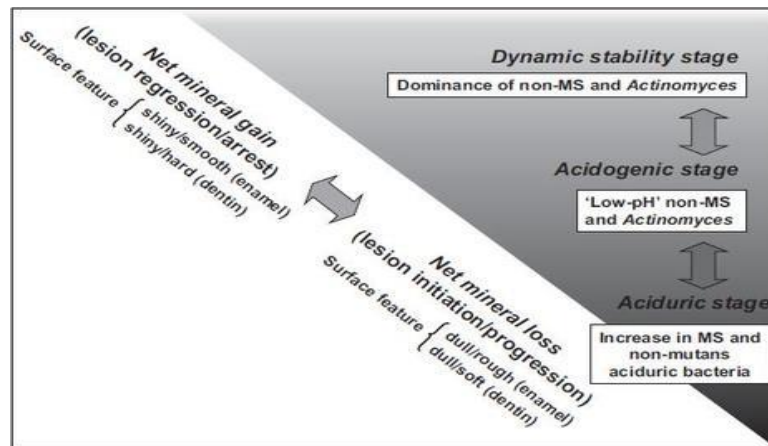


Figure 2.2: Diagram illustrates An Extended Caries Ecological plaque hypothesis (Takahashi and Nyvad, 2010)

Image taken from <http://cariology.wikifoundry.com/page/Microbiology+of+Root+Caries>

Figure 1 elucidates an extended caries ecological hypothesis set forth by some scientists. They hypothesize that dental plaque is a dynamic microbial ecosystem in which non-mutans bacteria are the key players for maintaining stability. Homeostatic mechanisms in plaque help to maintain the stability of the environment surrounding tooth surfaces. However, when there is substantial increase in sugary substrates, the saliva becomes an ineffective buffer and causes a decrease in the pH of plaque. Under such conditions, the population of the 'low-pH' non-mutans streptococci and Actinomyces then increases via acid selection, leading to a shift towards more acidogenic microflora. This is the acidogenic stage which causes net mineral loss and initial lesion formation. If prolonged acidic conditions prevail, this will lead to an aciduric stage, in which more aciduric bacteria such as mutans streptococci and lactobacilli will prevail in the microflora. Hence, high proportions of mutan streptococci and/or other aciduric bacteria may be considered as biomarkers of sites that undergo particularly rapid caries development. This also proves the dynamic changes in the microflora as lesions progresses (Takahashi and Nyvad, 2010).

2.2.2 Diet

Diets high in fermentable carbohydrates can cause caries (Beighton et al, 1996). A systematic review of studies in humans, updated the evidence on the association between sugars intake and dental caries, and the effect of restricting sugar intake to < 10% and < 5% energy (E) on

caries, to inform the World Health Organization guidelines on sugars consumption (Moynihan and Kelly, 2014). There was evidence of moderate quality showing that caries was lower when free-sugars intake was < 10% E. With the < 5% E cut-off, a significant relationship was observed, but the evidence was judged to be of very low quality (Moynihan and Kelly, 2014). According to the WHO guideline, sugar intake for adults and children, there are some evidence to suggest specific diet interventions for pre-school children are effective (www.who.int).

2.2.3 Susceptibility

Saliva plays a vital role in the maintenance of a healthy oral environment, and to regulate the growth of specific strains of microflora present in the mouth. By acting as a buffer, saliva maintains the pH of the mouth, ensuring the optimal growth of the resident colonies (Marsh and Nyvad, 2008) and chemically maintain an environment rich in calcium and phosphate (Edgar et al., 2004). Most of the naturally-occurring microbes present in the mouth also utilize the glycoproteins and proteins in the saliva as their main source of nutrition (Marsh and Martin, 1999). The presence of saliva and its constituent proteins and glycoproteins is also responsible for the formation of the pellicle. The constant flow of saliva is also responsible for the removal of non-endogenous bacteria which is unable to adhere to specific sites in the mouth (Hill and Marsh, 1990). Saliva thus acts a collector of these cells and facilitates their removal (Marsh and Martin, 1999). This contributes to the way different bacteria dominate different oral surfaces, as other bacteria not adapted to adhere is quickly washed away by the saliva and swallowed. (Marsh and Nyvad, 2008). As a result, areas which receive markedly less saliva flow, such as deep gingival crevices, proximal spaces and occlusal fissures, tend to have significantly higher levels of bacterial build-up (Hill and Marsh, 1990). Saliva also plays a role in carrying bacteria. Being the main source of microbial transmission, the passage of saliva between individuals has been credited with the main source of microflora in the colonization of the oral cavity (Marsh and Nyvad, 2008). Saliva also circulates bacteria within the oral cavity, resulting in re-colonization of oral surfaces where the microflora might be removed via mechanical forces such as cleaning. Most of the bacteria carried in the saliva come from the dorsum of the tongue (Hill and Marsh, 1990). The last function has been recognized as having the ability to reduce the incidence of dental caries (Stokey, 2004).

2.2.4 Genetic factor

The importance of genetic factors in the genesis of dental caries of both primary and permanent dentitions is well established; however, the degree to which genes contribute to the development of dental caries, and whether these genes differ between primary and permanent dentitions, is largely unknown. Wang et al. in 2010, using family-based likelihood methods, assessed the heritability of caries-related phenotypes for both children and adults in 2,600

participants from 740 families. They found that caries phenotypes in the primary dentition were highly heritable, with genes accounting for 54–70% of variation in caries scores (Wang et al., 2010). The heritability of caries scores in the permanent dentition was also substantial (35–55%, all $p < 0.01$), although this was lower than analogous phenotypes in the primary dentition. Assessment of the genetic correlation between primary and permanent caries scores indicated that 18% of the covariation in these traits was due to common genetic factors ($p < 0.01$) (Wang et al., 2010). Therefore, dental caries in primary and permanent teeth may be partly attributable to different suites of genes or genes with differential effects. Sex and age explained much of the phenotypic variation in permanent, but not primary, dentition. Further, including pre-cavitated white-spot lesions in the phenotype definition substantially increased the heritability estimates for dental caries. In conclusion, the results showed that dental caries are heritable, and suggested that genes affecting susceptibility to caries in the primary dentition may differ from those in permanent teeth (Wang et al., 2010). Moreover, metrics for quantifying caries that incorporate white-spot lesions may serve as better phenotypes in genetic studies of the causes of tooth decay.

2.2.5 Enamel Hypoplasia

Enamel hypoplasia (EHP) is one of several forms of developmental defects of enamel (DDE) identified by the Federation Dentaire Internationale (FDI) Commission on Oral Health (1992) and defined as a quantitative disturbance of mineralized tissue formation during tooth development (FDI, 1992). Primary teeth forming in utero are adversely affected by various insults to embryonic cells responsible for dentin and enamel formation (Seow et al., 2005). These insults are comprised mainly of covariates associated with low socio-economic societies and poverty, including malnutrition and possibly other dietary deficiencies, low birthweight and prematurity, pre- and post-natal infectious diseases, and a host of other risk factors affecting both mother and newborn (Seow et al., 2005). The collective impact results in various manifestations of tooth damage, clinically presenting in most cases as EHP. EHP is most often seen in the maxillary anterior teeth of the primary dentition but can extend to other teeth, including molars (Sabel et al., 2008). Teeth with EHP are vulnerable to early and elevated colonization by cariogenic bacteria, notably streptococcus mutans and lactobacilli, promoting early caries at the ecological sites of enamel defects, leading to what is called Hypoplasia associated severe early childhood caries (HAS-ECC) (Caufield et al., 2012). However, early or elevated colonization of streptococcus mutans and other cariogenic bacteria is necessary, but not enough, without a caries-promoting diet high in fermentable carbohydrates, EHP probably would not progress to HAS-ECC (Caufield et al., 2012) (Figure 2.3).

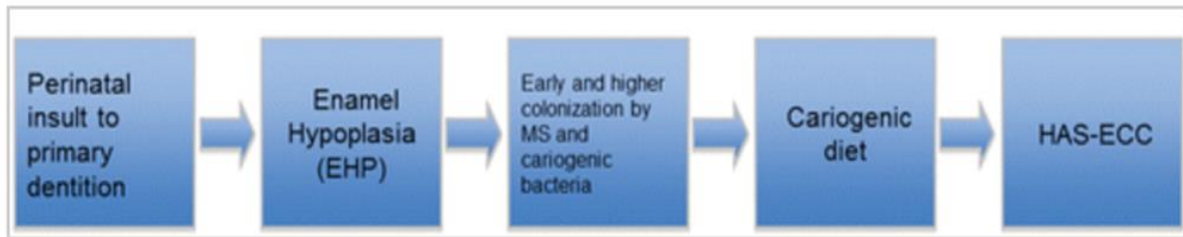


Figure 2.3: Model of the sequence of events leading to HAS-ECC, MS; mutans streptococci
Image taken from: https://journals-sagepub-com.liproxy.ucl.ac.uk/doi/10.1177/0022034512444929#_i8

2.3 Management

Dental caries can be managed behaviourally by controlling its causative factors, the supply of fermentable carbohydrates and the presence and maturation of bacterial dental biofilms (Schwendicke et al., 2016). If, however, such management is neither provided nor adhered to by the patient i.e. the lesion activity is not controlled, the remaining cariogenic biofilm promotes progression of the lesion, which may eventually lead to both chronic pulp inflammation and the irreversible stages of pulp necrosis and apical periodontitis following bacterial penetration into the pulp cavity (Bjorndal and Ricucci, 2014).

Children with dental caries may have high levels of anxiety while having dental treatment done on affected teeth, due to hypersensitivity of teeth leading to frequent pain episodes, as well as their young age (Willmott et al., 2008). Diagnosis at an earlier stage is key in the management, to re-enforce teeth remineralisation levels and reduce their hypersensitivity. Caries prevention should be achieved via regular fluoride application and fissure sealants placement.

Minimal intervention dentistry (Banerjee and Doméjean, 2013) allow dentists to pursue holistic and cause-based management of the dental caries, with the aim of maintaining healthy functional teeth for life. Effective management of caries is characterized by detection of early lesions and subsequent accurate diagnosis, by caries activity and risk assessment, and by preventing occurrence of new carious lesions. The management of cavitated carious lesions focuses on arresting or restoring existing lesions through minimal invasive restorative treatments, including repairing rather than replacing defective restorations.

Given the pathologic basis for dental caries as a biofilm disease, both prevention of new lesions and management of existing lesions, should focus primarily on control or management rather than tissue removal. For existing carious lesions, different lesion stages and activities might require different management, all of which should aim toward control of the disease process, preservation of dental hard tissue, avoidance of initiating the cycle of restoration, and preservation of the tooth for as long as possible (Banerjee and Doméjean, 2013).

The International Caries Consensus Collaboration (ICCC) held in Leuven, Belgium, in February 2015, comprising 21 experts in cariology from 12 countries covering North and South America, Europe, and Australasia undertook a consensus process and presented clinical recommendations for carious tissue removal and managing cavitated carious lesions, including restoration, based on texture of demineralized dentine. It is crucial that dentists manage the dental caries and control activity of existing cavitated lesions to preserve hard tissues and retain teeth long-term (Schwendicke et al., 2016). ICCC suggested that entering the restorative cycle should be avoided as far as possible and controlling the disease in cavitated carious lesions should be attempted using methods which are aimed at biofilm removal or control first.

When cavitated carious lesions either are non-cleansable or can no longer be sealed restorative interventions are indicated (Schwendicke et al., 2016). When a restoration is indicated, the priorities are as follows: preserving healthy and remineralizable tissue, achieving a restorative seal, maintaining pulpal health, and maximizing restoration success (Schwendicke et al., 2016). With respect to carious tissue it is suggested that it should be removed purely to create conditions for long-lasting restorations while bacterially demineralized tissues close to the pulp do not need to be removed. In deeper lesions in teeth with vital pulps, preserving pulpal health should be prioritized, while in shallow or moderately deep lesions, restoration longevity becomes priority (Schwendicke et al., 2016). For teeth with shallow or moderately deep cavitated lesions, carious tissue removal is performed according to selective removal to firm dentine. In deep cavitated lesions in primary or permanent teeth, selective removal to soft dentine should be performed, although in permanent teeth, stepwise removal is an option (Schwendicke et al., 2016). The evidence and, therefore, these recommendations support less invasive carious lesion management, delaying entry to, and slowing down, the restorative cycle by preserving tooth tissue and retaining teeth long-term (Figure 2.4).

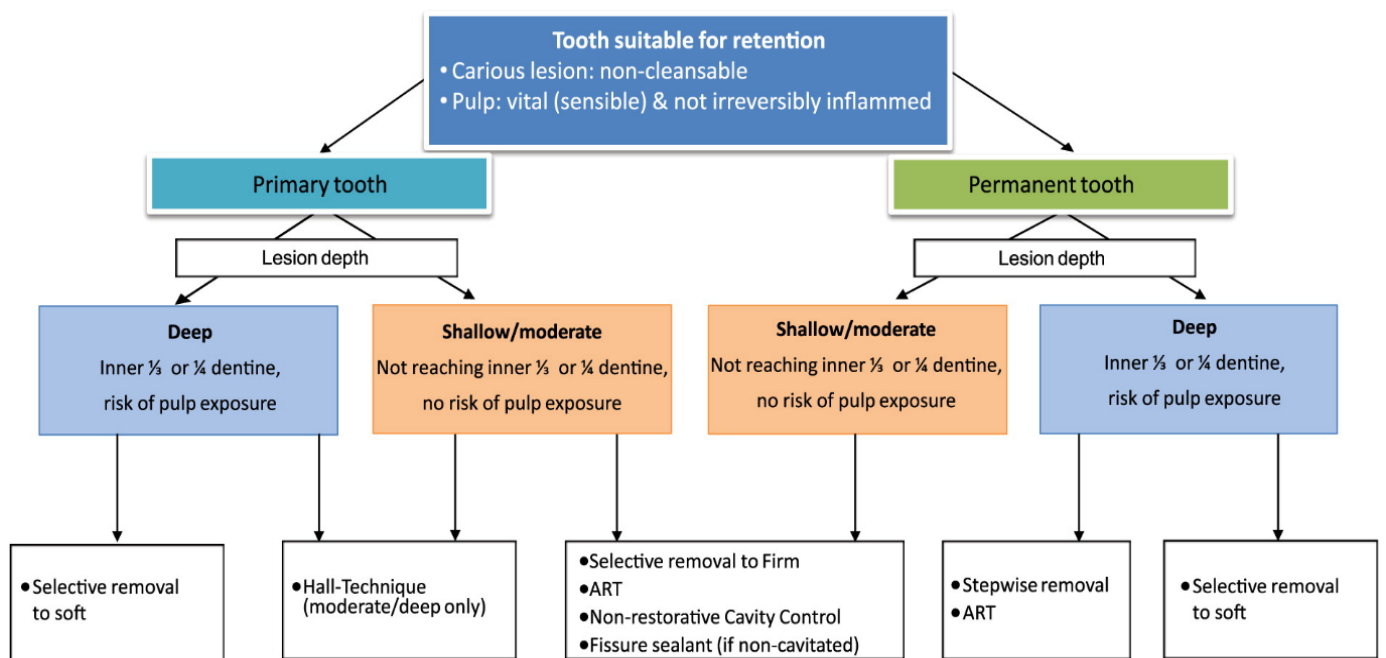


Figure 2.4: Decision making for carious lesions in retainable teeth with vital pulps. ART, atraumatic restorative treatment. Image taken from: <http://journals.sagepub.com.libproxy.ucl.ac.uk/doi/10.1177/0022034516639271>

2.4 Diagnosis

The proper management of dental caries in clinical practice requires an accurate diagnosis. Diagnosis is a clinical judgment that precedes a treatment decision. It implies detecting a caries lesion, estimating its depth and degree of demineralization, and planning about its activity (Nyvad and Fejerskov, 1997). Early detection and diagnosis of caries reduces the progression of the bacterial invasion, thus loss of the hard tissue of the tooth. Before deciding on a treatment plan, which may include a range of clinical techniques, the characteristics of the manifestations of the caries disease of the individual child must be assessed which includes the child, as well as individual teeth and surfaces. Over the years, many techniques have been developed to assess and detect caries lesions such as; clinical examination, radiographic investigation, Light fluorescence detectors and Enhanced Visual examination/International Caries Detection and Assessment System (ICDAS). Any diagnostic methods need to have certain characteristics to be considered as a useful tool, such as validity. In order to consider a system as a valid diagnostic tool, it should have high sensitivity and specificity. Sensitivity is the proportion of true disease identified correctly by the diagnostic system, and specificity is the proportion of non-caries teeth identified correctly by the system (Attrill and Ashley, 2001). Moreover, the diagnostic tool should be reliable and reproducible, safe and non-invasive. The aforementioned diagnostic tools have their limitations, these will be considered in greater details below, and therefore there is a need for better diagnostic tools to give more information about the extent of carious lesions into the enamel and dentine.

2.4.1 Visual and tactile

In this method, occlusal caries is detected by drying the tooth and examining it under dental light using a sharp explorer (Figure 2.5). This method is no longer used due to the potential risk of creating irreversible traumatic damage in the dental enamel (Ekstrand et al., 1987). It can jeopardize the remineralisation process and it can cause inoculation of fissures with cariogenic bacteria. For proximal caries, orthodontics separators can be used to detect carious lesions with direct vision. However, the patient might experience pain and discomfort from the elastic separators which reaches the peak one day after placing the separator then decrease, and pain fade within one week (Giannopoulou et al., 2006). A systematic review on selected caries diagnostic tools concluded that there is poor quality of evidence on the validity of the visual- tactile technique (Bader et al., 2001). Another systematic review on visual and visual-tactile technique found that these techniques are incapable of measuring the different stages of the carious lesions (Ismail et al., 2007).



Figure 2.5: Diagram illustrates visual tactile tools

Image taken from: https://www.google.com.kw/search?dcr=0&tbm=isch&q=caries+diagnostic+techniques+visual+exam&chips=q:caries+diagnostic+techniques+visual+exam,online_chips:visual+tactile&sa=X&ved=0ahUKEwjakuig5vaAhXRyKQKHd7sBv4Q4IYJJSqB&biw=1366&bih=637&dpr=1#imgc=wulcc9musBX2IM

2.4.2 Radiographic imaging

Radiographs are an ionised technique widely used to detect dental caries whether the lesion is cavitated or non-cavitated, if the lesion is active or arrested, and it has a role in investigating the extent of the lesion into the tooth structure (Vandenberghe et al., 2010). Generally, radiographic examination of teeth is an important part in the diagnostic process of any dental disease. It aids in visualising the oral structures and distinguishing them in health and disease, diagnose caries, periodontal disease, radicular or bony resorptions, bony tumours, and cysts. The most common radiographic images prescribed in investigating the extent of caries lesions into the tooth structure in children are lateral oblique and bite-wing (BW) radiographs (Figure 2.6).

Bitewing Xray

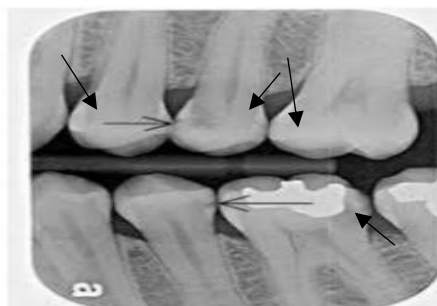


Figure 2.6: Diagram illustrates Bitewing xrays arrows indicate caries

Image taken from: <https://www.slideshare.net/drsunny984/dental-radiology-related-to-pedodontics>

Lateral obliques (Figure 2.7) are an extra-oral image which shows the dentition in both dental arches as well as the adjacent bony structures such as the body of the mandible and the ramus (Vandenberghe et al., 2010). Whereas, BWs are intra-oral images showing areas confined to the affected region. In BW radiographs, the posterior teeth in one side of the mouth are imaged at the same time making them the most suitable images when the crown is the area of interest (Vandenberghe et al., 2010). They mainly show the crown of the imaged teeth and possibly the area between the roots as well as interdental alveolar bone. One of the downsides of these radiographic images is that information from these images is masked by superimposition of other anatomical structures and it is difficult to assess occlusal caries if enamel is affected only (Otis et al., 2000).

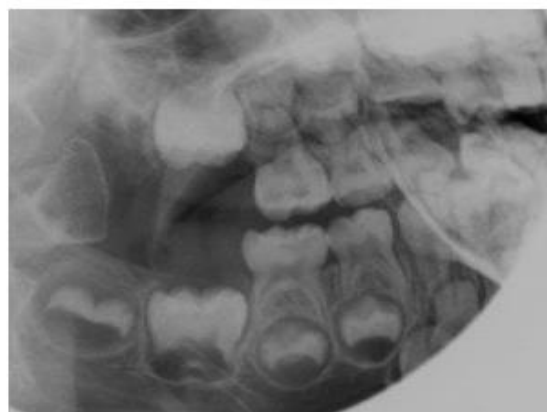


Figure 2.7: Diagram illustrates Lateral oblique radiograph
Image taken from: <https://www.nature.com/articles/bdjteam2014118/figures/22?proof=true>

Radiographic imaging has potential risks associated with it due to increased patient's radiation exposure. For example, in the United States radiographic imaging cost and radiation exposure has increased for the last thirty years due to the increase in its use in diagnosing a variety of clinical conditions (White and Mallya, 2012). The contribution of the radiography and fluoroscopy to the effective dose in the United States population in 2006 was reported to be 5% and half of this percentage was contributed to conventional dental imaging (White and Mallya, 2012).

The effects of radiation can be deterministic or stochastic. Deterministic effects occur from high exposure doses, result in cell death, and have a threshold dose for it to occur, such as in radiotherapy, (White and Mallya, 2012). However, stochastic effects have no threshold or safe dose, and can occur from very low doses and they damage the cell's Deoxyribonucleic acid (DNA) causing cancer (Ribeiro, 2012). This cancer risk was reported to be lifelong for the exposed individual (US National Research Council, 2006). However, it is presumed that the benefits of use of radiography in diagnosing

medical and dental conditions balance its risks (Tubiana, 2000). Therefore, it is important to try and limit the unnecessary radiation exposures whenever possible. This can be achieved by using two principles, justification, and optimization in accordance to the Ionising Radiation Medical Exposure Regulations (IRMER) 2017 (www.legislation.gov.uk).

Due to the risk of ionisation radiation of the radiographic imaging and consequent carcinogenic risk, it is important to investigate novel diagnostic technique which avoids the use of radiation to the patient.

2.4.3 Diagnodent (DD)

Diagnodent is used as a complementary tool beside visual examination for diagnosis of occlusal caries (Figure 2.7). Diagnodent decay detection is based on the principle that IR red Diode laser with 655nm wavelength emissions interact with the enamel on the tooth surface, it is absorbed by metabolites of intraoral bacteria and these metabolites produce a red fluorescence. This fluorescence emissions by the dental surface is indicated as a number between 0 and 99 on the screen of the device. Greater numbers are an indication of a greater decay area (Pretty, 2006). Therefore, Laser fluorescence provides a quantitative and non-invasive method for the diagnosis of dental caries.

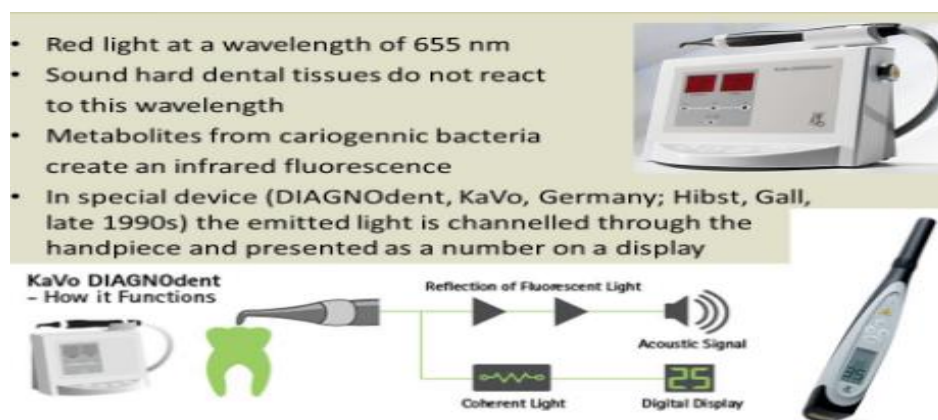


Figure 2.7: Diagram illustrates how Diagnodent works

Image taken from:

https://www.google.com.kw/search?dcr=0&tbm=isch&q=diagnodent&chips=q:diagnodent,online_chips:kavo+diagnodent&sa=X&ved=0ahUKEwiPpsixsJvaAhXQxgQKHQFEDCkQ4IYI-igG&biw=1366&bih=637&dpr=1#imgrc=hivKJdofSUfeVM:

Review of papers that have used DD to evaluate primary caries in permanent teeth showed that it has a high sensitivity and low specificity (Nokhbatolfoghahaie et al., 2013). Having a high sensitivity makes this device suitable for diagnosis, but since the probability of false positive diagnosis such as; foodstuffs is high, its use is recommended in combination with other techniques (Bader and Shugars, 2004). DD is a simple device to use and does not need a lot

of cooperation from the child. In addition, repetitive use of this device has no harm for the child.

Considering the reported sensitivity and specificity in different studies, it seems that DD is a suitable device for detection of caries in coaddition to other methods, and its use alone is not enough to determine appropriate management (Attrill and Ashley, 2001).

2.4.4 Dyes for Caries Detection

This technique was first introduced in 1972, it works by employing non-specific proteins which stain infected dentine, leading to easy identification and removal of carious dentine (MCComb, 2000). One of the disadvantages of this method, was that it was found that these dyes stain sound dentine at the Enamel Dentine Junction (EDJ) as well as the infected dentine. The use of dyes in detecting caries lacks specificity (Yip et al., 1994). Similarly, it was found that these dyes stain collagen in less mineralised organic matrix instead of the infected dentine hence, there is increased risk for excessive removal of sound dental tissue which may lead to unnecessary mechanical pulp involvement (MCComb, 2000). Caries detector dyes usually acceptable by children but can cause irreversible staining of dental tissues, which is undesirable clinically (Figure 8). This caries detection technique lacks scientific evidence that support the use of this method (MCComb, 2000).

CARIES DETECTOR DYES



Figure 2.8: Diagram illustrates caries detector dyes

Image taken from:

https://www.google.com.kw/search?dcr=0&biw=1366&bih=637&tbm=isch&sa=1&ei=qQvCWofUOYngkgX90Z2ADQ&q=dyes+for+caries&oq=dyes+for+caries&gs_l=psy-ab.3..0i24k1.344817.350424.0.350859.15.13.0.1.1.0.254.1383.0j5j2.7.0....0...1c.1.64.psy-ab..7.8.1387...0j0i67k1.0.48aP-h0Ruwl#imgsrc=td-DYkFwgcP3DM

2.4.5 Quantitative Light Induced Fluorescence (QLF)

For numerous years, the changes in mineral content of dental hard tissues has been known to cause alteration in visual and optical properties (Stokey, 2004). In 1982, Swedish researchers discovered the ability of laser induced auto fluorescence to assess mineral loss of dental hard tissues. They have reported that when the proper filters are used with fluorescence laser instead of white light as laser has high energy at 1 wavelength, an improved contrast can be gained between sound and infected enamel as it blocks excitation and allows long pass filtered emission (Sundstrom et al., 1985). The QLF method employs violet blue light of a wavelength of 290- 450 nm (Figure 2.9). The incident light will be absorbed by the tooth and transmitted as fluorescence. A charged coupled device (CCD) micro-camera detects and captures the fluorescent image, and data is analysed by a computer software.



Figure 2.9: Diagram illustrates QLF

Image taken from:

https://www.google.com.kw/search?dcr=0&biw=1366&bih=637&tbm=isch&sa=1&ei=ug-bCW6wC8_TsAe51K5w&q=quantitative+light+induced+fluorescence&og=quantitative+light&gs_l=psy-ab.3.0.0i2j0i30k1j0i24k1l5.5290.13037.0.15343.30.14.0.7.7.0.263.1583.0j6j2.8.0...0...1c.1.64.psyab15.14.1470...0.cebxURbvYZA#imgrc=Av8subzyt8AKgM:

The limitations of this method are that the result can be affected by several factors, such as the presence of plaque and stains, the degree of tooth dehydration can affect the outcome. Moreover, this method cannot detect lesions at mesio-buccal or disto-buccal surfaces as the QLF light must be perpendicular on the tooth surface (Heinrich-Weltzien et al., 2003). Moreover, a comparison between visual examination and QLF in detection of non-cavitated carious lesions in a clinical study concluded that small and non cavitated occlusal caries are more likely to be detected using QLF however, it is impractical and time consuming (Kuhnisch et al., 2007) . Also, a systematic review showed that the accuracy of QLF has insufficient scientific evidence (Twetman et al., 2013).

2.4.6 Fiber Optic Transillumination (FOTI)

This method involves using white light with high intensity on a clean dry tooth. The light is directed onto the tooth, and the internally scattered but transmitted light is collected from the other side on a mirror system to be processed in a digital electronic instrument (Pretty, 2006). Dark shadows appear if caries is present due to the increase in the scatter same as QLF. The main advantage of this technique is that it can be used to detect all tooth surfaces including the interproximal area.

There are several limitations of FOTI such as; it cannot measure the depth of the lesion, and the fact that the data produced cannot be recorded as an image, which makes the system more subjective as it depends on visual evaluation of the appearance of the scattered light (Pretty, 2006).

2.4.7 Digital Imaging Fiber Optic Trans-illumination (DIFOTI)

This is the digital version of the FOTI technique (Figure 2.10). It employs a light with high intensity with two heads camera, one to examine the occlusal surface and the second to inspect smooth surface. The images produced can then be saved and archived on a computer for retrieval at the further visits. The downside of this system is that the images cannot be quantified, and the analysis of the image is subjective depending on the examiner visual evaluation of the scattering appearance (Pretty, 2006).

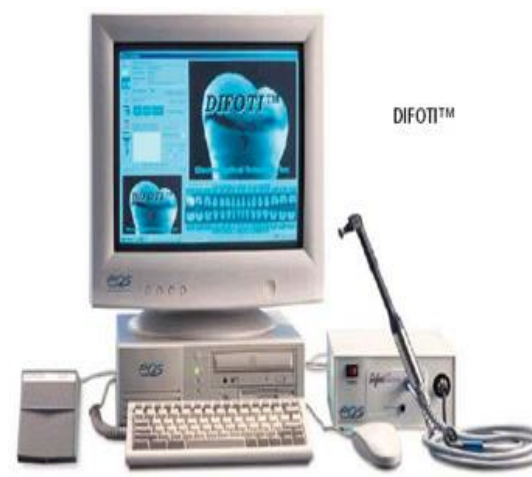


Figure 2.10: Diagram illustrates DIFOTI

Image taken from:

https://www.google.com.kw/search?dcr=0&tbm=isch&q=fiber+optic+light+caries&chips=q:fi-ber+otic+light+caries,online_chips:fiberoptic+transillumination&sa=X&ved=0ahUKEwj7g_iGtZvaAh-FLewKHYM6ATgQ4IYJigC&biw=1366&bih=637&dpr=1#imgrc=9Ee7XGf75rfPVM

2.4.8 Electric Conductance Monitor (ECM)

This technique uses a fixed frequency with single alternating current, to analyse the substance resistance within the dental hard tissues. To examine a surface, the device probe is applied on the site of interest and held in place for five seconds for a measurement cycle. The tip of the ECM probe will produce compressed air directed to the surface to be examined and measure the drying profile (Pretty, 2006). The mechanism of this device is to measure the porosity, which is generally known to be associated with dental caries (Figure 2.11). The data collected can give valuable information about the lesion features and characteristics (Pretty, 2006).

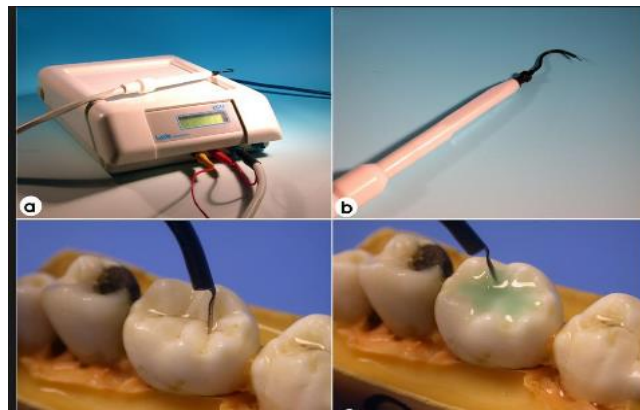


Figure 2.11: Diagram illustrates ECM

Image taken from:

https://www.google.com.kw/search?dcr=0&biw=1366&bih=637&tbn=isch&sa=1&ei=ZwrCWsWAFoWdkgWPhbvDg&q=ECM+caies&oq=ECM+caies&gs_l=psyab.3...312960.320315.0.321153.10.10.0.0.0.0.671.2248.0j3j3j1j0j1.8.0...0...1c.1.64.psy-ab..2.7.2067...0j0i67k1j0i30k1j0i8i30k1.0.zzFn-TlqLuc#imgsrc=1nIL3mAiSEr0xM:

The limitations of this system are that the results can be influenced by many factors including tissue thickness, moisture, tooth temperature and immature or hypoplastic teeth (Pretty, 2006). According to Pretty (2006) ECM had sensitivity values of 74.8 (\pm 11.9) in site specific and 63 (\pm 2.8) surface specific, whereas the specificity values at site specific 87.6 (\pm 10) and 79.5 (\pm 9.2) at surface specific evaluation (Pretty, 2006).

2.4.9 International Caries Detection and Assessment System (ICDAS)

The system was developed in 2002 by a group of restorative dentists, researchers, and epidemiologists during the International Consensus Workshop on Caries Clinical Trials (Pitts and Stamm, 2004), which confirmed the need of non-cavitated lesions detection. The workshop had reviewed many inconsistent and unreliable caries detection systems (Ismail et al., 2007). The ICDAS is based on the work of previous studies which assessed the reproducibility of occlusal demineralisation depth assessment in three methods and its accuracy (Ekstrand et al., 1997). The ICDAS concept is that the use of a standardised system, based on best available scientific evidence for detecting early and later stage caries severity, should lead to the acquirement of better-quality information, which could then be used to inform decisions about appropriate diagnosis, prognosis, and clinical management of dental caries. It was constructed to identify the carious process in six stages, starting from early changes in dental enamel to the most extensive cavity caused by demineralisation.

ICDAS detects and assesses caries according to whether the lesion is cavitated or non-cavitated, tooth morphology that includes smooth surfaces, pits and fissures, and sealant restoration status (Ismail et al., 2007), as shown in table 1.

As well as the coding classification there are simple, standard examination processes employed as part of the system. A key element of the examination is the cleaning of teeth to aid detection since caries forms where there has been plaque stagnation, with the use of compressed air to reveal the earliest visual signs of caries (Ismail et al., 2007). ICDAS classifies caries status into six codes from zero to six (Table 1).

Score	Description	Clinical photograph
0	Sound tooth surface	
1	Opacity or discoloration only visible after air drying	
2	Opacity or discoloration distinctly visible without air drying	
3	A white or brown spot lesion with localised enamel breakdown	
4	Underlying dark shadow from dentine with or without localised enamel breakdown	
5	Distinct cavity with visible dentine	
6	Extensive cavity with visible dentine	

Table 2.1: The table demonstrates ICDAS scoring system with clinical pictures.

Notes to accompany table 1:

Sound

0 No enamel demineralisation or a narrow surface zone of opacity (edge phenomenon) Tooth surface that exhibits dental defects such as amelogenesis imperfecta, fluorosis, extrinsic and intrinsic staining, and tooth wear such as; erosion, attrition, and abrasion should be considered as sound surface. Tooth surface with pits and fissure stains that is associated with non-carious habits for instance frequent coffee or tea drinkers should also be considered as sound surfaces (Ismail et al., 2007).

Early Stage Decay

1 Enamel demineralization limited to the outer 50% of the enamel layer

The tooth surface has no signs of demineralisation or colour changes when the surface is dry. However, after prolonged drying time of about 5 seconds, opacity or change in colour either to white or light brown discoloration is noted on the tooth surface.

2 Demineralisation involving between 50% of the enamel and 1/3 of the dentine

When the tooth surface is wet a carious opacity with white spot is visible without drying. Or brown discoloration of pits and fissures which appears wider than natural features of stained fissures.

Established Decay

3 Demineralisation involving the middle 1/3 of the dentine, clinically microcavitated

Carious opacity or change in discoloration to brown colour with wider feature of fissure is evident when compared to clinical appearance of sound pits and fissures. Once prolonged air drying is applied, enamel structure loss can be viewed within or at the margins of pits or fissures. A localized breakdown of enamel structure is evident without visible dentine in the carious cavity.

4 Demineralisation involving the middle 1/3 of the dentine, clinically shadowed

The lesion shows an intact enamel surface or localized enamel cavity or breakdown but with a shadow of underlying discoloured dentine. The colour of the intrinsic shadow might appear as brown, blue, or grey discoloration which is visible through the intact enamel surface. The shadow can be detected when the tooth is wet. The examiner should evaluate the origin of the shadow whether the carious lesion started from the tooth surface that is being examined or it has started from an adjacent surface with no evidence of caries on the surface of interest. If the caries has originated from adjacent tooth surface but the shadow reflects on the surface being tested, then it should be scored with code 0 as sound surface.

Severe Decay

5 Demineralisation involving the inner 1/3 of dentine± into the pulp, clinically cavitated but the cavitation < ½ the surface

This code is given to the lesion when a distinct cavity on dental enamel is detected with visible dentine showing underneath enamel cavity. If the surface is examined wet, the dark dentine will appear through dental enamel. But if air is applied for 5 second, a frank cavity will be visually detected with evidence of carious enamel demineralisation, which may be present as opaque or dark brown on cavity walls specifically in the pits and fissures. To confirm surface evaluation, the examiner can use ball ended explorer and slide it gently along the cavity. If the ball entered the cavity reaching the dentine, then the surface should be noted as code 5.

6 Demineralisation involving the inner 1/3 of dentine± into the pulp, clinically cavitated but the cavitation > ½ the surface

This code represents deep cavity with extensive loss of dental structure with dentine evidently visible at the wall and base of the cavity. The cavity may extend to involve half of tooth surface with an increased possibility to reach the dental pulp (Ismail et al., 2007).

The ICDAS is considered the gold standard system for caries detection. However, it cannot assess the depth and the progression of the lesion into the enamel structure. There is a necessity for new system that can help the clinicians to determine the progression of caries lesion so that a better treatment modality can be provided.

In the following section, I will discuss in detail about OCT and the potential of developing this technique as a clinical diagnostic tool.

2.4.10 Optical Coherence Tomography (OCT)

Optical Coherence Tomography (OCT) is defined as a non-destructive imaging system, using near infrared light to investigate the internal biological structures to a depth of up to 2-3 mm such as; ocular, skin, intravascular, oral soft, and hard tissue (Jones et al., 2006b). OCT is based on the same concept as for ultrasound imaging, but light is used instead of sound. In both techniques, an incident beam is used, and the back scattered signal is measured (Jones et al., 2006b). It produces a two-dimensional (2D) optical tomographic (XZ), cross-sectional images which is called b-scans (Figure 2.12). When multiple b-scans images are taken in the (Y) direction, a three-dimensional (3D) image (in the XYZ dimensions) can be produced.

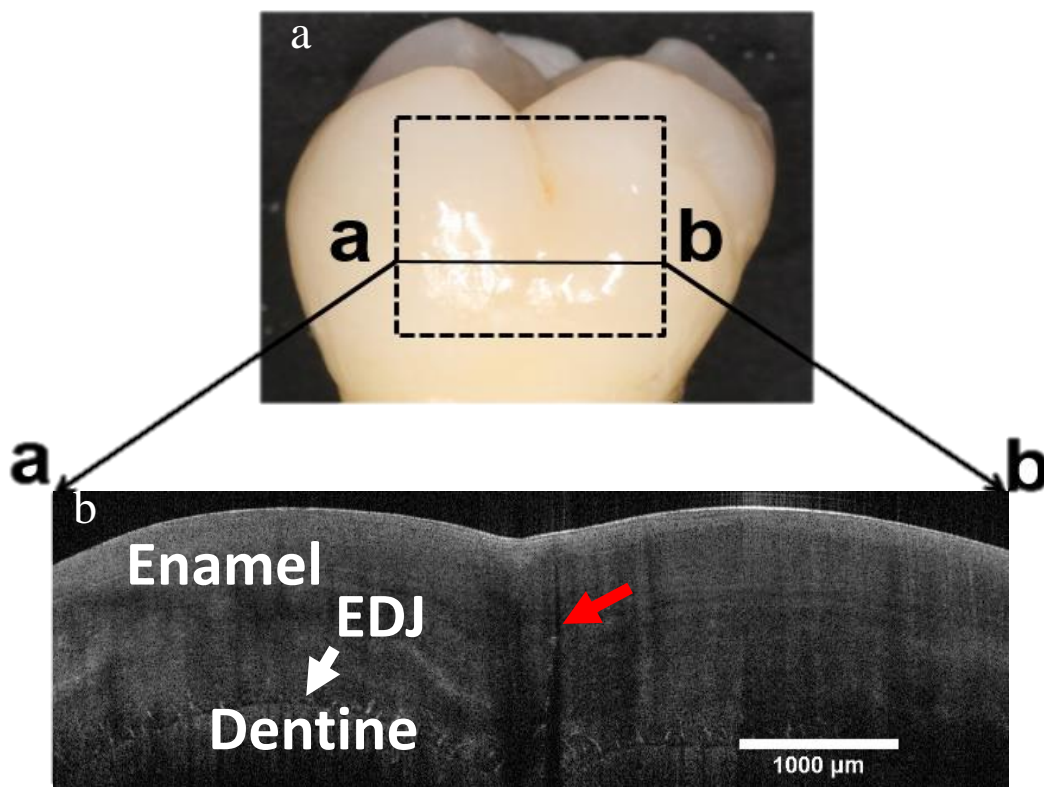


Figure 2.12: Diagram illustrates an b- OCT b-scan image of a- dental enamel
Image courtesy of Dr Khalifa Al-Azri

OCT measures the backscattered signal from scattering surface and produces an a-scan, which represents a signal intensity of the imaged tissue as shown in Figure 2.13 (Fried et al., 2002). OCT uses Low Coherent Interferometry (LCI) visible and near infrared wavelengths (Fercher, 2010). There are two imaging resolutions can be created by OCT; depth, and lateral resolution images. One more type of OCT is called polarised sensitive OCT (PS-OCT), which employs polarised light instead, this backscattered intensity signal was shown as a colour-coded scale image (Manesh et al., 2009). OCT has an axial resolution in the order of 10 μ m

(Baumgartner et al., 2000), and it was reported that it has no detrimental biological effect (Otis et al., 2000).

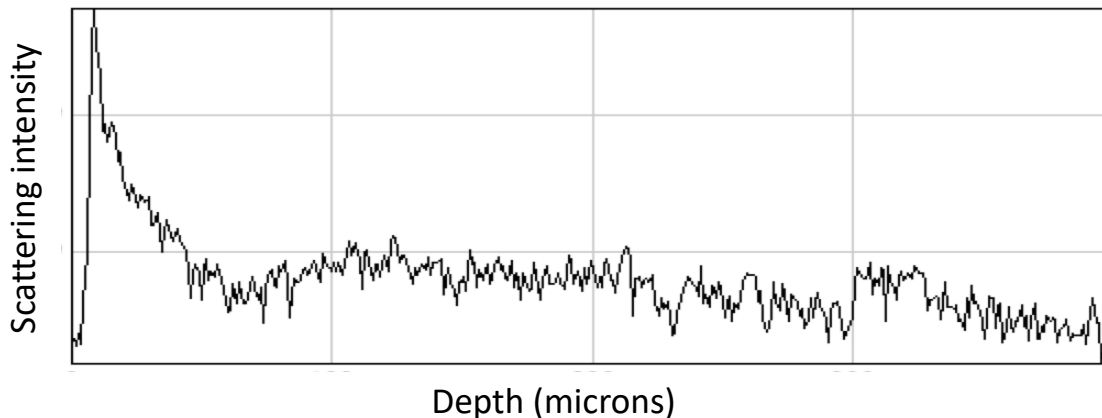


Figure 2.13: Diagram illustrates a scattering plot (a-scan) obtained by plotting the scattering intensity profile vs the enamel depth

Principles of OCT

Most of the earlier investigations on OCT were done in ophthalmology, and in 1990, Fercher presented the first two-dimensional representation of an in vivo human eye fundus contour using this technique (Fercher et al., 1993). Fercher described the two different types of OCT, based on low LCI, the Time-Domain LCI (TD-LCI) and Fourier-domain LCI (FD-LCI)

(Fercher, 2010).

The former technique, (TD- LCI), records structure depth of the sample using a series of partial time-coherence interferograms. These interferograms are developed by a light reflecting specimen sites, and a reference beam reflected at a moving reference mirror (Fercher, 2010). The second method, (FD-LCI), can be based either on a tuneable laser which is known as frequency tuning FD-LCI or fFD-LCI, or based on a spectrometer named Spectral FDLCI or sFD-LCI (Fercher, 2010). Both techniques have similar results in terms of resolution and can form low coherence a-scan and b-scan images. However, TD-OCT has less sensitivity in comparison to FD-OCT (Choma et al., 2003).

Originally, multimode diode lasers were used as the source of light for OCT. These light sources used to produce confusing results, due to their periodic coherence functions (Fercher and Roth, 1986). Later, super luminescent light diodes (SLDs) were used as a light source to produce LCI for OCT (Huang et al., 1991, Fercher, 2010). These SLDs light sources gave a high depth resolution, due to their ability to produce broader spectral emission by monotonic coherence functions (Fercher, 2010). Femtosecond Titanium-sapphire lasers and photonic

crystal fibres were used offering a very high resolution and, sub-micrometre resolution (Huang et al., 1991, Hartl et al., 2001, Povazay et al., 2002, Bourquin et al., 2003).

In the past, FD-OCT showed imperfect tunability due to the use of wavelength tuneable light source. It offered either a slow tuning with high depth resolution or low depth resolution with fast tuning. Current lasers substituted external-cavity tuneable laser diodes by cavity-tuning 'swept laser sources', which allow performing the spectral filtering inside the laser cavity (Fercher, 2010). Nonetheless, SLDs remain the light source of choice.

There are many acquisition systems used in the OCT technique. The standard OCT systems, FD-OCT, and TD-OCT produce images with depth-oriented cross-sections in planes normal to the frontal plane which is called b-scan images. While, an en face OCT system, produces frontal sections of the sample of interest creating an image called c-scan, this technique performs (2D) transverse scan in high speed with only slow change in axial direction of the coherence access (Fercher, 2010). Another acquisition system used is Linear OCT, which is considered as an alternative to TD-OCT, yet it shows less sensitivity and resolution (Koch et al., 2004, Fercher, 2010). Other acquisition systems are endoscopic OCT, High depth-resolution OCT, High speed and volumetric OCT, High lateral resolution and, full field OCT systems. Each system has its specific applications.

OCT has many optical signal property detection systems. One of these systems is polarisation sensitive OCT (PS-OCT) which was mentioned previously in this section. This system is founded by Hee et al. (Hee et al., 1992). In this system, the sample is illuminated by circularly polarized light with two channels of a polarization sensitive detection unit (Fercher, 2010). Other optical signal detection systems were used such as; Differential phase contrast OCT, system sensitivity, spectrometry and, refractometry.

Enamel and dentine are scattering materials. To develop a beneficial imaging optical tool, it is crucial to understand how visible and near infrared light transmits through enamel and dentine. Throughout enamel demineralisation, partial dissolution of enamel forms micro-pores in its structure, that perform as scattering centers for the lights (Darling et al., 2006). Light scattering in enamel is likely to decrease by $1/\lambda^3$, where λ is the wavelength of the incident light (Darling et al., 2006). This is related to the dimension of light scatterers (enamel crystals) in dental enamel. Hence Darling et al. suggested that the near-infra red (NIR) region ranging from 780-1550 nm presents an optimal imaging technique, due to low scattering and absorption in enamel and dentine (Darling et al., 2006). If the NIR wavelength is longer, then the light is absorbed markedly by the water in the tissue and therefore reducing the penetration of the NIR light (Darling et al., 2006, Fried et al., 2002).

The principle of OCT system is illustrated in Figure 2.14 Swept source (SS) produces a low coherent light, which enters the Beam Splitter then splits into two beams at the fibre coupler. One beam is directed to a movable reference mirror arm and another to a sample arm. Both back-reflected beam from the reference arm and the back-scattered beam from the sample arm are reunited at the fibre coupler and transferred to a photo detector which is called Michelson interferometer. The interference signal can be detected if the length of the back reflected light is in the range of coherence length of the main source (Otis et al., 2000). Because of the known reference mirror position, the depth into the sample structure can be determined (depth resolution). These depth signals are known as a-scan signals, which are transferred into digital signal processing system, where OCT b-scan images can be constructed from multiple a-scan signals (Fercher et al., 2003).

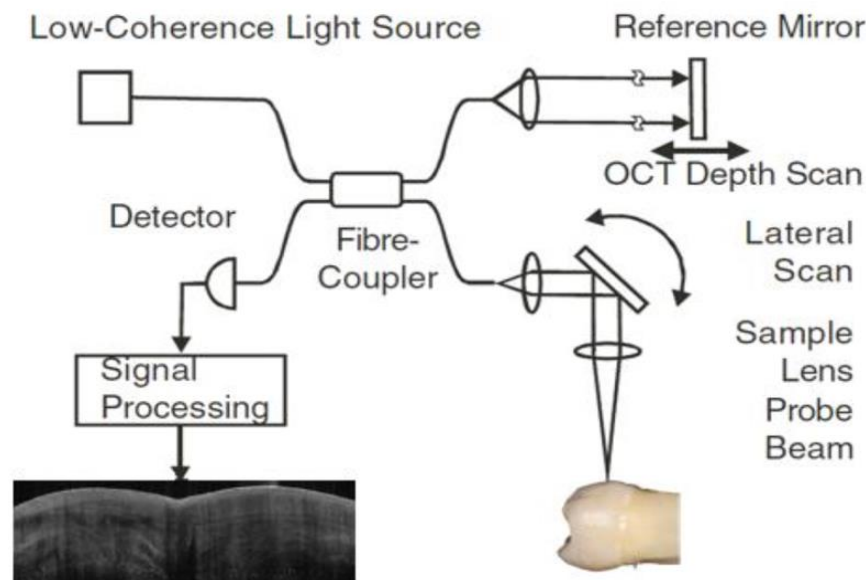


Figure 2.14: Diagram demonstrating the principles of OCT (Fercher et al., 2003). Image modified by Khalifa Al-Azri

Dental hard tissue refractive index:

Refraction occurs when the light propagates from one medium to another. The measure of alteration in light speed when it passes from air to another medium, is called the refractive index. The larger the refractive index, the slower the speed of light in the material. The refractive index of air is 1. OCT measures the light refraction that occurs when light passes from air into a dental structure. The refractive index is a significant optical parameter of biological structures (Meng et al., 2009). Light propagation in biological tissues depends on the tissues' refractive index, which shows an indication of the scattering properties of the tissue (Hariri et al., 2012). The scattering property of the tissue is the ultimate result of refractive index variation between tissues (Knüttel et al., 2004). Many studies had reported that early carious lesions

could alter the refractive index of sound enamel which in turn aids in diagnosing dental caries (Besic and Wiemann, 1972).

Studies have looked at different methods to measure the refractive index of tooth using OCT such as; focus-tracing method (Song et al., 2000, Haruna et al., 1998). One of the downsides of this method is its difficulty to perform, as multiple focus points should be adjusted with specific calibration of lens. There was another simpler method which was based on Optical Path-Length (OPL) matching (Meng et al., 2009, Hariri et al., 2013). It is easy to perform, fast, and has high accuracy (Meng et al., 2009). They stated the refractive indices of enamel, dentine, and cementum to be 1.631 ± 0.007 , 1.540 ± 0.013 and 1.582 ± 0.01 respectively. These results matched with other studies (Ohmi et al., 2000, Kienle et al., 2006, Hsieh et al., 2011).

Applications of OCT

The use of OCT in medical and dental fields has increased in the past twenty years. Its first application in the medical field was in ophthalmology (Swanson et al., 1993, Fercher et al., 1993). Fercher et al described the advantages of OCT in contrast to non-optical techniques (Fercher, 2010). OCT is a non-destructive and contact free technique. However, the main disadvantage of this technique was that light penetration into the sample of interest, is limited (Fercher, 2010). In addition to its use in ophthalmology, it has been used in gastroenterology and dermatology. OCT was applied in dermatology for examining and diagnosing dermatological diseases such as bullous and inflammatory conditions (Welzel, 2001). While in gastroenterology, endoscopic OCT was used to examine gastrointestinal tract disorders. Endoscopic OCT was reported to be a promising imaging modality for early diagnosis of tumours (Sergeev et al., 1997).

In dentistry, OCT was extensively used in investigating caries, artificial demineralisation and remineralisation in enamel and dentine. Jones et al used PS-OCT to examine artificial occlusal caries by measuring the magnitude of backscattered light with variations in the enamel volume (Jones et al., 2006a). It was reported that PS-OCT can measure artificial occlusal caries by observing the changes in backscattered and depolarisation of near infra-red light, and the technique is promising in detecting and diagnosing caries (Jones et al., 2006a).

Fried et al studied root, occlusal, interproximal caries, and recurrent caries under composite fillings (Fried et al., 2002). They concluded that PS-OCT is capable to image such lesions (Fried et al., 2002). Another study by Azevedo et al investigated the use of OCT to measure demineralisation amount in artificially induced dentine caries (Azevedo et al., 2011). They used FD-OCT and stated that OCT is an efficient method to detect the depths of carious lesions (Azevedo et al., 2011). A study conducted by Feldchtein et al to examine in vivo oral soft

and hard tissues and dental restorations such as composite, amalgam and compomer (Feldchtein et al., 1998). They showed that defects that occurs underneath dental restorations can be detected using OCT.

Maia et.al used two types of OCT; TD-OCT and sFD-OCT with light source wavelengths of 1280 nm and 840 nm, respectively in evaluating caries in deciduous teeth (Maia et al., 2010). They found that there was a great potential for OCT to be used routinely in clinical practice for caries detection and monitoring lesion progression (Maia et al., 2010). The same conclusion was reached by Amaechi et.al that looked at root caries using PS-OCT and correlated it with TMR (Amaechi et al., 2004). They demonstrated that the technique could replace conventional dental radiographs and avoid the hazards of ionising radiation directed to patients (Amaechi et al., 2004). The main drawback of these studies is the fact that no one has validated these studies of OCT and dental caries against the gold standard of ICDAS.

As already discussed, this technique is promising, and its merit is that it does not involve ionising radiation. The use of OCT to analyse demineralisation in dentine will provide practitioners with information they would be unable to obtain from direct vision or radiography. The knowledge of the depth of the caries will enable dentists to develop an informed treatment plan i.e. whether to restore, root treat or extract the tooth. Saving patients, the expense and discomfort of unnecessary treatment and ensuring appropriate treatment.

CHAPTER 3

Aim and Objectives

3 Aim and objectives

3.1 Rational for Research

Based on the increased prevalence of dental caries, and the importance of their early diagnosis and management, this research aims to investigate early detection and diagnosis of white spot lesions using OCT.

3.2 Aim

The aim of this study is to investigate the use of Optical Coherence Tomography (OCT) imaging in dentistry as a routine and adjunct clinical diagnostic tool for dental caries, by developing a standardised marker for each ICDAS score.

3.3 Objectives

1. Understanding OCT as an imaging technique for teeth.
2. To study the effect of demineralization on enamel and dentine structures.
3. Compare Control, score 1,2,3 and 4 ICDAS using standard diagnostics tools.
4. Characterise Control, score 1,2,3 and 4 ICDAS using OCT.
5. Define empirical markers in the OCT scan and scattering profile intensity plot for control, score 1,2,3 and 4 ICDAS.

CHAPTER 4

Patient Recruitment and Selection

4 Patient Recruitment and Selection

4.1 Study registration and ethical approval

Ethical approval for this research is obtained from the University College London (UCL) Eastman Dental Institute (EDI) Biobank Committee on the 10TH of October 2017, under the reference number 1702 (Appendix 1).

4.2 Patient identification and recruitments

Eligible patients who attended the Department of Paediatric Dentistry at the Eastman Dental Hospital (EDH) were invited to participate in this research. The patients were identified from patient's clinical list, and the general anaesthesia theatre list. Full explanation of the project was given to the parents and patients verbally along with written information leaflets related to age group about the project and enough time to think about participating in the study, with the right to ask any related questions and understanding that the choice they make had no effect on the treatment given (Appendix 1, 2, 3 and 4). All patients/ parents willing to take part in this study gave informed written consent to collect and use extracted teeth for this project (Appendix 5 and 6). Each participant signed three copies of the consent form. One was filed in patient notes, a second one was given to the participant, and the last one was kept with project's supervisor. The flow diagram for patient recruitment is shown in figure 4.1 below.

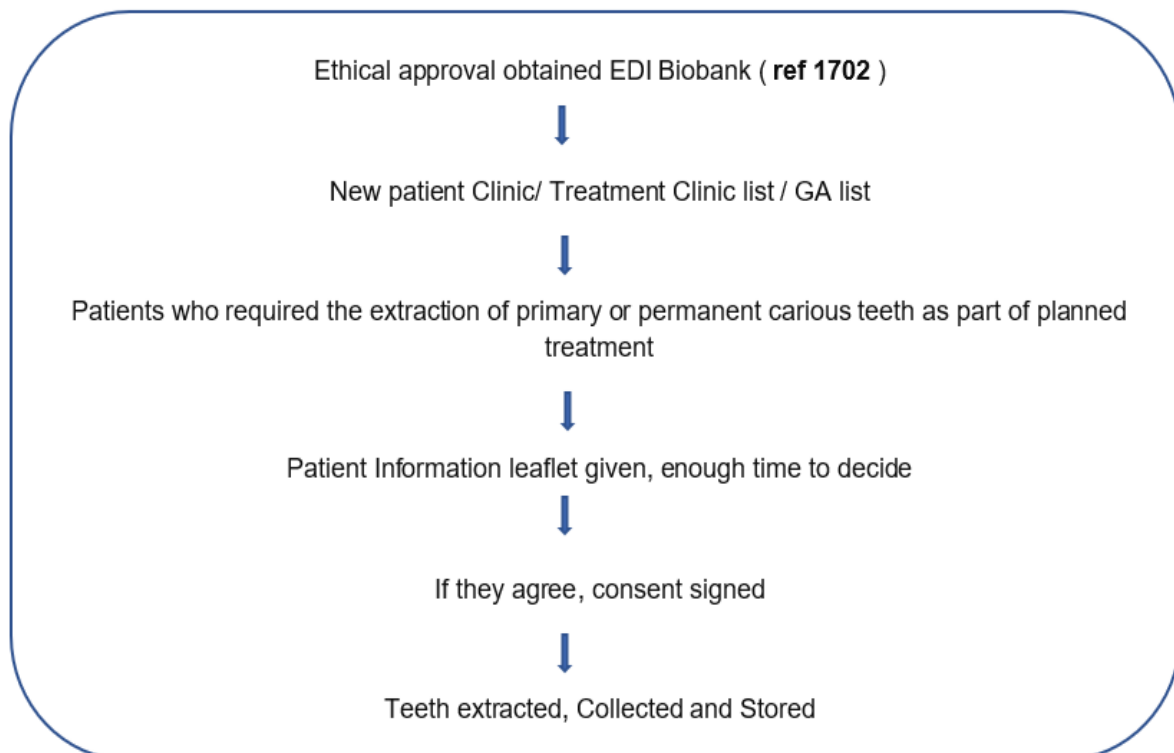


Figure 4.1: Schematic Diagram outlining how the sample teeth were collected

The Control group are paediatric patients in the Department of Paediatric Dentistry at the Eastman Dental Hospital, who required extractions of the teeth for orthodontic reasons or as part of planned treatment.

The inclusion criteria for this group included:

- Patient without any known illness or syndromes
- patients who required the extraction of primary or permanent sound teeth as part of planned treatment plan

The exclusion criteria included:

- Patients with any known relevant medical history
- Teeth with extensive caries
- Teeth that showed signs of enamel structure defects or any other dental anomalies
- Patients who did not speak and understand English sufficiently to consent for participation in the study

The second group was patients who required the extraction of primary or permanent carious teeth as part of planned treatment plan or exfoliated naturally.

The Inclusion criteria included;

- Patient without any known illness or syndromes
- Patients who required the extraction of primary or permanent carious teeth as part of planned treatment plan

The exclusion criteria included:

- Patients with any known relevant medical history
- Teeth with extensive caries
- Heavily restored or broken-down teeth
- Teeth that showed signs of enamel structure defects or any other dental anomalies
- Patients who did not speak and understand English sufficiently to consent for participation in the study

Those who decided to enrol in the study were given three copies of the consent to sign. A copy of each form was kept in a filing cabinet in the locked office of the primary supervisor, the other copy was given to the patient/parent for his/ her reference and the last one was filed in the patient's clinical records.

4.3 Samples collection and storage

In accordance with Human Tissue Act 2004 in Eastman Dental Institute, 256 Grays Inn Road, London, protocols of teeth storage and disinfection were applied. The patients were identified from patient's clinical list, and the general anaesthesia theatre list. After each extraction, samples were collected in a plastic pot with patient ID stickers and number of teeth and type obtained. The pots were filled with normal saline solution, until taken to the Eastman Dental Institute laboratory, the same day. Disinfection was made by removing any soft tissue remnants surrounding the extracted teeth, and teeth were washed thoroughly with the use of micro-brushes under running water. A scalpel blade was used to debride the tooth from any intact clots, gingival or periodontal tissues. The samples were then placed in 70% concentration ethanol at room temperature for 3-5 days to be disinfected. After, the teeth were removed, and were stored individually in 0.1% concentration Thymol solution in a locked refrigerator at 4°C at the Eastman Biomaterial and Tissue Engineering Laboratory, the storage policy was according to the department's policy, until imaged. The benefit of sample storage is to prevent the microorganisms to grow within the samples as. All collected samples were given an anonymised number rather than patients name or hospital number to ensure patient confidentiality and to comply with data protection Act, and copies of patient consents were kept with the project primary supervisor L.B and N.G from biobank ethical approval committee at EDH. Patient details including age the type of the tooth and reason for extraction were recorded.

CHAPTER 5

The Assessment of the Samples Using Conventional Methods in Diagnosing Caries

5 The assessment of the samples using conventional methods in diagnosing caries

In this section, the assessment of all samples using the conventional methods of diagnosing caries in clinical set-up are going to be described. These are visual caries diagnostic tool (ICDAS) scoring system and radiographic methods.

5.1 Rationale of this section

To examine the samples using the gold standard caries diagnostic technique (ICDAS) and radiographs

5.2 Materials and methods

5.2.1 Materials and methods for clinical visual assessment using ICDAS

The International Caries Detection and Assessment System (ICDAS) was used to characterise the carious lesion stage of the selected samples. The author completed an e-learning training course (<https://www.icdas.org/icdas-e-learningcourse>) to use the ICDAS scoring system. This e-learning course is a 90-minute programme that has been developed to support training in ICDAS, demonstrating the ICDAS examination protocol and providing a full explanation of the scoring system. At the end of the course, the author was assessed by a test on a range of clinical photographs of different stages of dental caries, and completed the course successfully.

The samples were removed from 0.1% Thymol solution and washed under running water. Then, each sample was tested under dental chair light before and after prolonged drying for 5 seconds using the three in one air- water syringe. Scores were recorded for each sample. Photographs of the samples were taken using Canon™ camera (DS6041) with Canon™ macro Ring lite flash (MR-14EX) for a uniform flash light. Each sample was photographed against a dark background to enhance the contrast between the sample and the background. The tooth surfaces were wiped off excess moisture before imaging but were not fully dried. When a photograph was taken, the camera was fixed to a stand about 15 cm away from the tooth, as this was shown to be the best diameter to view the tooth with good clarity. Regarding the lighting, the room light was dimmed and used natural sun light to reflect the image without the use of a flash. The photographs were close recordings of the teeth. Each photograph was checked for clarity and if the photograph was not clear or if the lesion was not clearly visible, the photograph was repeated until the appearance on the photograph matched the clinical

view. The photographs were uploaded immediately to a computer where all data were saved, after each tooth was imaged and labelled according to tooth code with the tooth surface, and the samples were placed back in the container until the next experiment. The photographs were then printed, and the hard copies served as a mean for characterising the carious lesions by two different examiners.

5.2.2 Materials and methods for Radiographic assessments

Radiographic assessment of teeth is an essential part of diagnosing dental diseases such as dental caries and periodontal disease. In carious teeth, radiographs are used to investigate the extent of the lesions and its proximity to the pulp. This is especially important when planning the management of these teeth and possible extraction.

After taking the clinical photograph, excess moisture was wiped off the sample, using a cotton roll, and then the tooth was positioned against an intra-oral film on a flat table. Radiographic images for control (Figure 5.1) and carious teeth were taken at the same session using the same x-ray machine for all samples, using the same settings, type of film and exposure time to ensure no confounding was present. The x-ray machine used was model x-mind by Toshiba, with type F intra-oral film and the exposure time used was pre-set for permanent or primary anteriors/molars, maxillary or mandibular, as noted on the x-ray machine. Radiographic films were developed after all images were taken. Each radiographic film was coded according to the corresponding tooth code. The images were then scanned and uploaded with their corresponding clinical photographs.

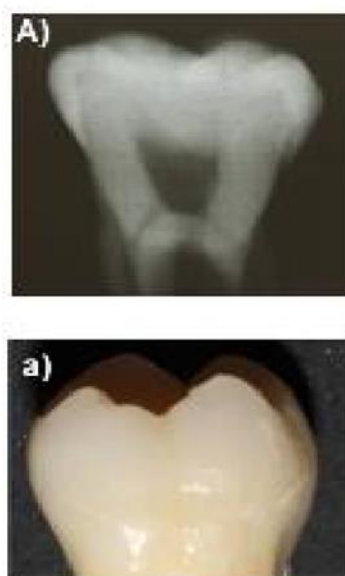


Figure 5.1: A) Radiographic image of a control tooth shown in the a) clinical photograph

5.3 Results

5.3.1 Results of clinical visual assessment using ICDAS

A total of 180 teeth (126 primary and 54 permanent) were visually examined and scored according to the ICDAS (Table 5.1), from 0 to 6. Score 0 means that after proper drying of the tooth surface by air for 5 seconds, there is no evidence of visual changes on the surface and it is completely sound. Score 1 means that after proper drying of tooth surface; a white spot lesion can be detected visually. Score 2 means that without proper drying of the sample surface, the white spot lesion can be seen even though the tooth is still in a wet medium. The main difference in the characteristic features between score 1 and 2 relied on whether the lesion was visible before drying or not. Score 3 means once prolonged air drying is applied to the tooth, enamel structure loss can be viewed within or at the margins of pits or fissures and a localized breakdown of enamel structure is evident without visible dentine in the carious cavity. Score 4 means that the lesion shows an intact enamel surface or localized enamel cavity or breakdown but with a shadow of underlying discoloured dentine. The colour of the intrinsic shadow might appear as brown, blue, or grey discolouration which is visible through the intact enamel surface. The shadow can be detected when the tooth is wet. Score 5 means that a distinct cavity on dental enamel is detected with visible dentine showing underneath enamel cavity and when the surface is examined wet, the dark dentine will appear through dental enamel. Score 6 means a deep cavity with extensive loss of dental structure with dentine evidently visible at the wall and base of the cavity and the cavity may extend to involve half of tooth surface with an increased possibility to reach the dental pulp.

ICDAS Lay Terms	Sound	Early Stage Decay		Established Decay		Severe Decay	
ICDAS Dental Terms	Sound	First visual change in enamel	Distinct visual change in enamel	Localised enamel breakdown	Underlying dentine shadow	Distinct cavity with visible dentine	Extensive cavity within visible dentine
ICDAS Detection	0	1	2	3	4	5	6
ICDAS Activity	ICDAS Activity +/-						

Table 5.1: Table demonstrates ICDAS scoring system
Image taken from <https://www.icdas.org>

Ten control mixture of sound teeth were collected from six different patients (table 5.2). The number of control teeth was small, because sound teeth were rarely indicated for extraction, unless they were deemed to have poor prognosis, or required for balancing or compensating extractions of teeth for orthodontic reasons, or as part of planned treatment.

Dentition	Control teeth N=10 mixture
Primary	4
Permanent	6

Table 5.2: Table demonstrates data of sound teeth samples used in the study

A hundred and seventy carious teeth were collected from thirty patients, as part of their treatment plan (Table 5.3), 122 were primary and 48 permanent teeth. The low number of Score 1 and 2 ICDAS was because incipient caries lesions are not considered an indication for teeth extraction, which made the collection of samples limited. ICDAS score 5 and 6 samples were the largest number collected, as most children have extractions for poor long-term prognosis teeth. This gave a total number of 180 teeth surfaces which were evaluated including sound teeth samples.

Dentition	ICDAS Score 1	ICDAS Score 2	ICDAS Score 3	ICDAS Score 4	ICDAS Score 5	ICDAS Score 6
Primary	1	-	3	16	32	70
Permanent	2	4	7	9	14	12
Total	3	4	10	25	46	82

Table 5.3: Table demonstrates data of carious teeth samples used in the study

5.3.2 Results of Radiographic assessment

From the radiographic images of control teeth, there is a clear contrast between enamel and dentine, with enamel being more radiopaque than dentine; and apparent continuity of the EDJ between them as shown in Figure 5.1.

The radiographic features of the carious teeth depended on the severity of the lesion, as well as the size and depth. If the caries is in the early demineralisation stage (score 1 and 2), the radiographic features would resemble that of normal enamel as shown in Figure 5.2. However, in the case of score 3 and 4 lesions as shown in Figure 5.3, the radiographic image showed a contrast between enamel and dentine, and the lesions were clearly defined.

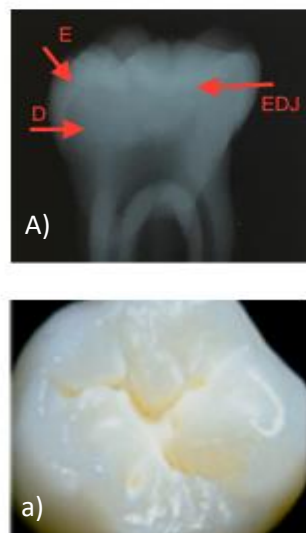


Figure 5.2: A) Radiographic image of a score 2 ICDAS tooth shown in the a) clinical photograph



Figure 5.3: A) Radiographic image of a score 3 ICDAS tooth shown in the a) clinical photograph

The most severe score is the lesion that involves the dental pulp as in score 6 ICDAS. The tooth structure in this score is already compromised due to the loss of enamel structure. Radiographically, this results in radiolucency in the enamel and dentine encroaching to the dental pulp, as shown in Figure 5.4.

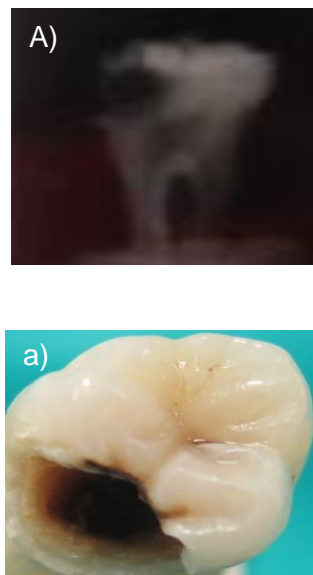


Figure 5.4: A) Radiographic image of a score 6 ICDAS tooth shown in the a) clinical photograph

5.4 Discussion

Dental caries is a complex disease, and several caries detecting tools have been produced to help in identifying and detecting the presence of carious lesions. ICDAS is considered the gold standard in caries lesions assessment and detection. The scores correspond to six stages of carious lesions, starting from early changes on enamel surface that can be visible clinically, to established and extensive caries. ICDAS is a simple, practical and evidence-based system that can be used in clinical setting, public health programmes and dental research. However, this system is unable to detect the depth of early white spot lesion before it become established caries. The other method to assess the depth of the lesion is radiographs. However, in clinical situation, radiographs are not indicated to detect caries white spot lesions. Also, radiographs use ionising radiation that has a potential to cause health risks.

5.4.1 Clinical visual assessment using ICDAS

With the ICDAS scoring system, the higher the score, the more severely affected the tooth. However, it does not explain what is happening to the tooth's ultrastructure; how severe or deep the lesion is, to predict its prognosis and treatment plan. Clinicians can vary in their ability to diagnose dental caries according to the scoring system, as this can differ from one clinician to another. This may explain why there is a wide range of prevalence of dental caries worldwide. With very early lesions, for example score one and two, where there is only a slight white opacity, the lesion can be easily missed, especially if, the tooth is wet, or there is suboptimal lighting. There is a need for new systems that can allow the clinicians to determine the advancement of carious lesions, so better treatment modalities can be provided.

5.4.2 Radiographic assessment

Clinicians usually undertake radiographic assessment of oral and dental tissues to assess the degree and severity of a related condition. They always comply with the ALARA principle which stands for "As Low As Reasonably Achievable", which is a safety principle specifically designed to reduce radiation doses and releases of radioactive materials and it is a regulatory requirement for all radiation safety programs (International Commission on Radiological Protection, 2008). To comply with this patient should be exposed to a minimal dose of X-ray radiation which produces a good quality image and minimizes the chance for any further exposures (International Commission on Radiological Protection, 2008). This is due to the ionizing effect of the radiation on the patient.

When comparing carious teeth to sound, different aspects were noticed; control teeth showed clear contrast between enamel and dentine due to the different degree of X-ray absorption and scattering of both structures, as enamel is highly radiopaque compared to dentine. This

is because enamel is a well organised structure and highly mineralised in comparison to dentine. Between them we can see a homogenous continuity of the EDJ. If the structure of enamel or dentine is altered, the degree of radiographic contrast between these structures is also affected. However, when there has been a change in the density, or a breakdown in the homogenous EDJ, this reflects a lesion.

In caries, radiographic imaging has a role in investigating the extent of the lesion into the tooth structure (Vandenberghe et al., 2010). Unfortunately, for ICDAS score 1 and 2, the radiographic features were not very distinctive on x-ray images, the enamel structure appeared similar to that of control enamel, making it difficult to detect early enamel lesions from dental radiographs. However, in the more severe lesions, we can start to see some radiographic changes appearing for example radiolucent areas. The degree of enamel radiolucency depends on the severity of the carious lesion. In score three, four, five and six, the enamel is more radiolucent and as the lesion progresses through dentine, radiolucency is more apparent but the exact proximity to the dental pulp cannot always be determined. Lesions where the tooth surfaces are broken down, show radiolucent changes in enamel and in dentine, and if very severe they show loss in tooth structure, which is seen as breakage in the homogenous continuity of the outline.

Radiographic imaging has potential risks associated with it due to increased patient's radiation exposure. Radiation as explained earlier can have carcinogenic effects, and other side effects, which were explained previously. In addition, radiographs cannot distinguish active from inactive disease, for example periodontal disease is not identified until significant bone loss has occurred. Besides this, radiographs usually give an underestimated picture about any given lesion. They are also 2 Dimensions images of 3 Dimensions objects such as teeth. In addition, lesions shown on x-rays tend to be underestimated, as the actual lesion is usually deeper than what is seen on an x-ray and is usually not seen radiographically until it is 30% into enamel (Woodward et. al., 1996).

It would be helpful for the dentist to have a baseline guide to assess the severity and long-term prognosis of the lesion before deciding on the best management approach. However, limitations were found in the conventional methods of diagnosing carious lesions; therefore, this study aims in overcoming these limitations and bring OCT to the clinical settings as a diagnostic tool to show the extent of the lesion and predict its prognosis. Moreover, it is important to investigate novel diagnostic techniques that avoid the use of radiation to the patient.

CHAPTER 6

OCT as a Diagnostic Imaging Tool

6 OCT as a diagnostic imaging tool

6.1 Optical Coherence Tomography Scanner

The OCT (Figure 6.1) was used to image the samples after mounting the teeth in an artificial upper and lower jaw with the use of an adjustable phantom head to replicate the clinical scenario. The instrument used was the VivoSight™ OCT scanner, manufactured by Michelson Diagnostics, United Kingdom, which has a multi-beam Swept-source frequency Domain scanner. The light used in the OCT instrument was near infrared with 1305 nm wavelength, which is considered a class one eye safe laser. In tissues, it has less than 7.5 μm of optical resolution laterally and 5 μm optical resolution axially. The depth of focus is 1 mm and can scan an area of up to 6 mm (width) X 6 mm (length) with depth of about 1.2 mm to 2.0 mm of the scanned tissue. It can scan 35 frames in one second with 10 kHz scan rate. The image obtained can be presented as a vertical B scan (figure 6.1 5), En-face image or 3D in TIFF (Tagged Image File Format) stack or DICOM (Digital Imaging and Communications in Medicine) formats.

The OCT instrument consists of light source, Santec HSL-2000-12-MDL, the processing system- Dell Precision T3600, image display, and mounted OCT scanning probe. The scanning probe was mounted on adjustable arm, which gave more stability for the probe. The phantom head allowed modification in the distance between the teeth and OCT probe to obtain the best image quality.

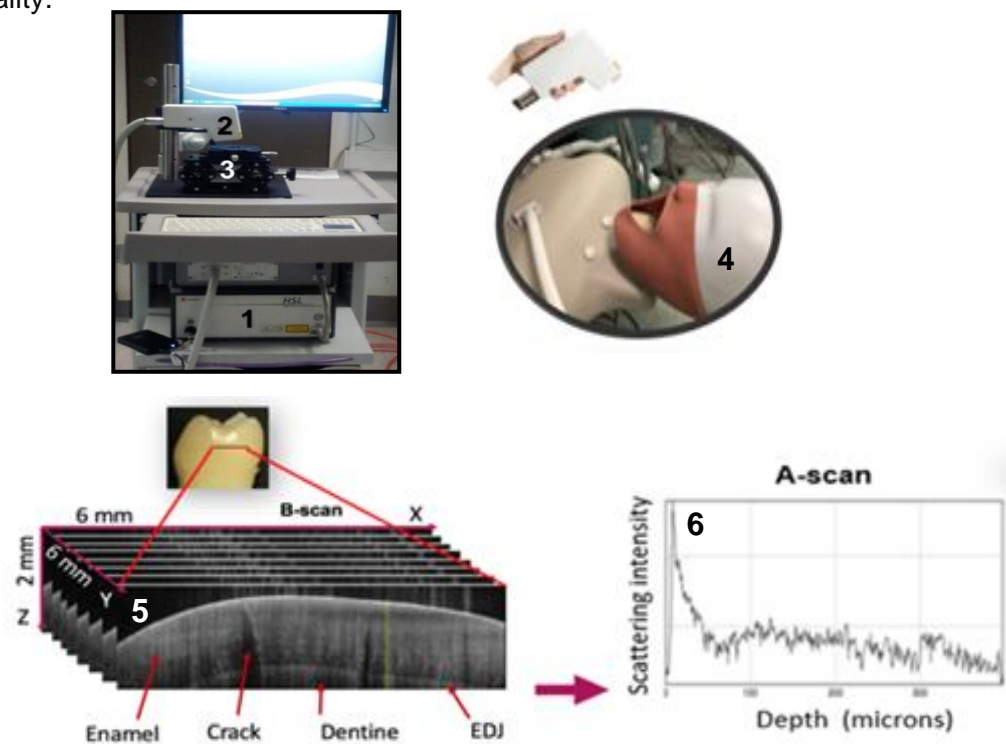


Figure 6.1: Image shows the different parts of OCT machine; 1) 10 Santec light source, 2) OCT scanning probe, 3) Adjustable platform, 4) Phantom head, 5) B-scan, 6) A-scan

6.2 The assessment of samples using OCT scanner

6.2.1 Method

OCT imaging was conducted in the Division of Biomaterial and Tissue engineering lab at Eastman Dental Institute, University College London.

The next step after taking clinical and radiographic images, was the OCT imaging of the samples. Multiple B scans were taken, depending on the number of lesions which were presented per tooth, imaging each lesion separately, but using the exact same settings for each. The samples were removed from the storage solution (0.1% Thymol) and excess Thymol was wiped off using paper tissues. To simulate the oral cavity a phantom head model with a pink modelling wax rims at the maxilla and mandibular region were used to maximise the representation of the clinical setting. Samples were mounted on the artificial upper and lower jaws, to stabilize the sample in a perpendicular position to the OCT scanning probe, and then positioned on adjustable phantom head below the OCT scanning laser.

The size of the imaged area, the number of frames taken and the distance between individual frames were the same for all tooth samples imaged. The maximum width of the OCT frame that can be scanned was 6mm, therefore this width was selected for all scans. These frames were possible to be collected along a maximum distance of 6mm in an occlusal direction. Each lesion was scanned several times, until the best image was chosen, saved and exported with the other data. Each sample was saved in a separate file named with the ID code, and the file consists of the clinical photo, x-ray and OCT B and A scans.

There were two methods of OCT imaging acquisition in the OCT scanner software. Free run acquisition where a single image could be captured at one time. The second method was taking multiple frames of an area. Multiple frames can be captured using either the manufacturer's pre-set system or can be accustomed by the operator. The pre-set system can be either multi-one (captures 60 consecutive b-scan images with 100 μ m distance between them and a scanning widow of 6mm x 6mm) or multi-two (captures 500 consecutive b-scan images with 4 μ m distance between them and a scanning widow of 2mm x 2mm). In this study multiple frames were taken for each sample using the multi-one pre-setting. The scan started at or close to the cemento-enamel junction (CEJ) cervically and ended at the cusps coronally. The scans were then exported from OCT software as 16-bit TIFF images and saved to the database.

OCT images (B-scans) were analysed using ImageJ software, which is a Java based processing programme developed by Wayne Rasband at the National Institute of Health in Maryland in USA (Schneider et al., 2012). It was designed with an open architecture that provides extensibility via Java plugins and recordable macros. It helps in analysing and extracting the information needed from three dimensional live images. In addition to that, it helps in analysing the data by creating density histograms and corresponding scattering profile plots. The latest version of Image J when was used in the analysis, which was Image J 1.47 with 64bit Java, 2013.

There are two approaches to OCT data analysis, the first is qualitative analysis (B-scans) by investigating the changes in enamel structure in caries and control samples. The second approach is quantitative analysis by measuring the back scattered signals intensity when the laser travels into the depth of enamel structure (A-scans). Both approaches were performed to analyse the obtained OCT images of all samples.

The images were uploaded to ImageJ to be analysed quantitatively and qualitatively by studying the degrees of scatter and reflection experienced by the scanning spot comparing between control and carious teeth via plotting the scattering intensity profile (A-scans). The distance measurement on ImageJ was changed to micrometres (μm). Then a rectangular region of interest was selected with a $40.5 \mu\text{m}$ width on the a-scan (10 pixels wide). Additionally, scattering profiles were extracted from single frames and plotted as a function of the sample's depth using Origin Pro 9.0TM (OriginLab Corporation, Northampton, MA 01060, USA).

From the B-Scans, the region of interest was chosen randomly and then a signal intensity profile is plotted (A-Scan). For the qualitative analysis, the images were studied and any abnormalities in the enamel structure was documented, described and compared to sound enamel (B-scans).

6.2.2 Results of Optical Coherence Tomography (OCT)

All one hundred and eighty teeth collected in the previous chapter were scanned using OCT. The number of scans per surface was based on the number of lesions present; some had only one while others had more. A total of 180 lesions were scanned separately. Scanning area was 6mm X 6mm with depths of 2mm, and the setting for the OCT machine was the same for all the lesions. Each lesion was scored using the ICDAS scoring system post completion of online training course as described in previous chapter. The acquisition used was pre-set multi-one system for all samples. The total scan time for each image was approximately 45 seconds. The number of frames of images captured were 600 frames with $10 \mu\text{m}$ distance between each frame. Each of the frames measured 1482 pixels X 460 pixels analogous to

6000 μm (6 mm) X 1840 μm (1.84 mm) with each 1 pixel corresponding to about 4 μm . Because of these consecutive frames, a 3-Dimensional image can be presented.

The images were then exported from OCT software as 16-bit TIFF/TM images to Image J to interpret the A-scans. The signal intensity profiles of both control and carious teeth showed a sharp peak in the beginning of the intensity profile as the light hits the tooth surface, displaying a change in refractive index between air and tooth structure. The profile plots provide a direct vision of the scattering of light photons as they travel through the tooth and any disruption in the enamel structure results in altered scattering, which could be measured in the profile.

6.2.2.1 Results of control sample

An example of a control tooth surface scanned by OCT is shown in Figure 6.2. Both the clinical photograph and OCT B-scan are demonstrated here. A solid black line (figure 6.2a) indicates the position of the area of interest across the enamel surface. From the clinical photograph, the enamel surface is sound and free from any enamel defects, with no caries lesions.

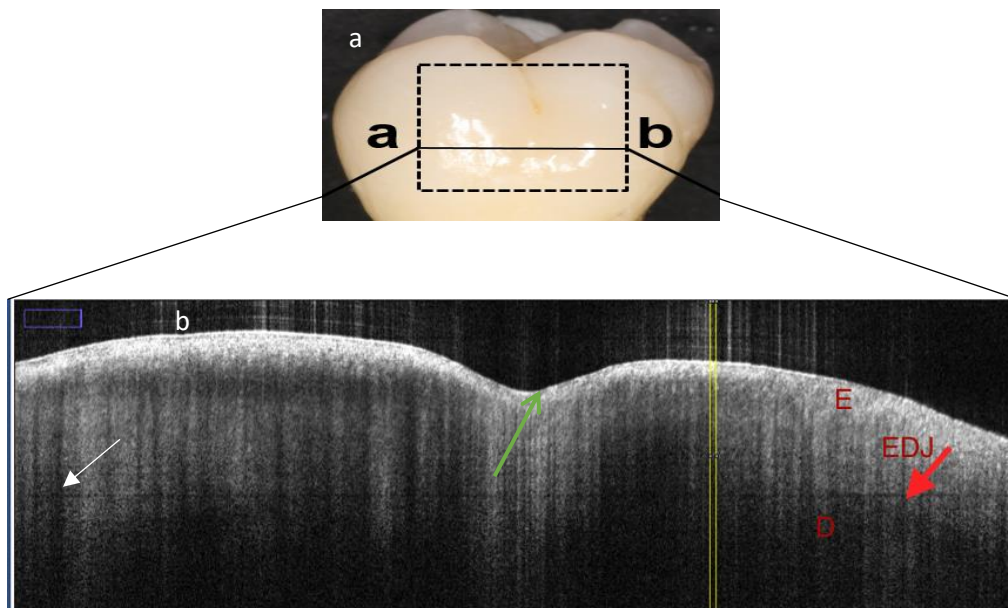


Figure 6.2: a) Control sample clinical photo and b) OCT B-scan. The position at which the image was taken is marked on the tooth surface by the solid dark line (ab). It clearly shows Enamel structure (E), dentine (D) and Enamel Dentine Junction (EDJ)

In the obtained OCT B-scan (figure 6.2b), basic layers of the crown are demonstrated. Enamel and dentine can be seen clearly. The enamel dentine junction is clearly visible, and the structure of enamel shows uniform scattering. The structure of dentine is distinct from enamel. There is also a small crack (white arrow in Figure 6.2b) and interestingly the area below the crack is dark. The dimensions of the image are 1500 X 460 pixels corresponding to 6000 μm X 1840 μm .

A homogenous and uniform scattering in enamel structure can be recognised from the OCT scan. From the clinical photograph, the OCT image is located just above the middle of the surface where it is bulbous, and the enamel is thick. At the enamel surface, there is an increase in surface brightness related to the buccal side of the OCT image when compared to the rest of B-scan (indicated by the green arrow) and the areas underneath these regions look darker than the rest of the enamel structure. This is because of the increased scattering of the incident light and decreased light arriving there anyway because of scatter by more superficial layers.

6.2.2.2 Results of ICDAS score 1 sample

The OCT scan of the ICDAS score 1 sample is demonstrated in Figure 6.3. The clinical picture of the sample shows clearly the white spot lesion on the distal side of the tooth after prolonged drying time with the black box indicating the position of the scan (figure 6.3a). In the OCT scan obtained (figure 6.3b), only the enamel is visible, due to the increased in the enamel thickness at the region where the OCT scan was taken. The position of the scan taken was located on the maximum interproximal curvature at the contact point of the distal surface of first permanent molar (FPM) as shown from the clinical photograph in Figure 6.3a.

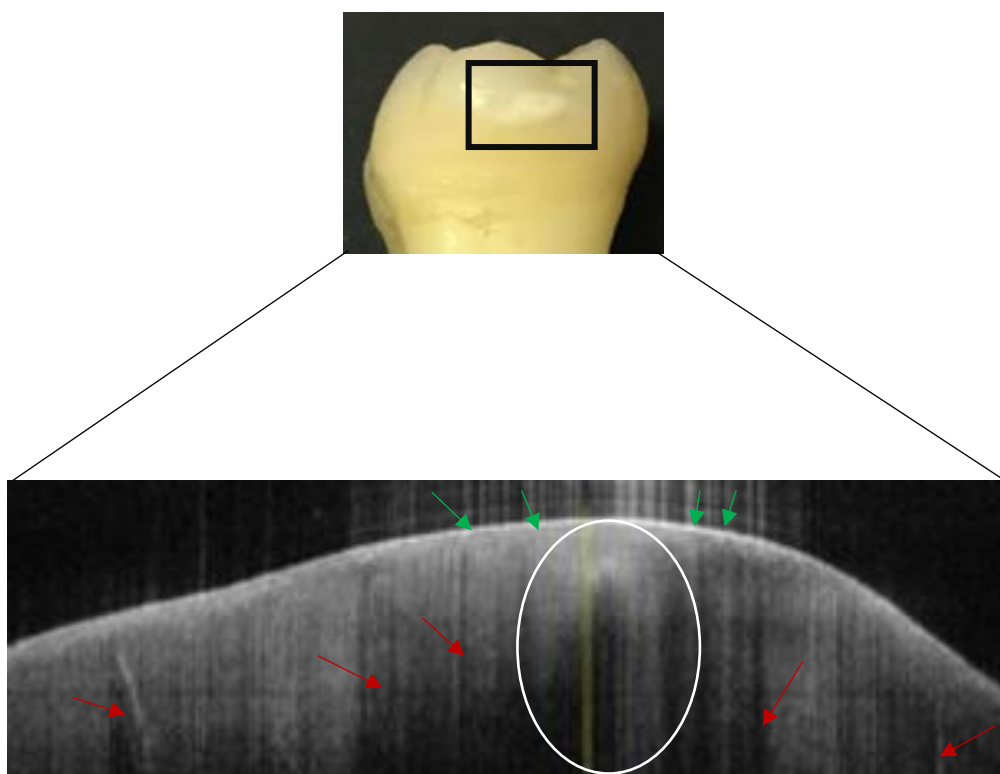


Figure 6.3: a) ICDAS score 1 sample clinical photo and b) OCT b-scan. In this image only, the structure of enamel is shown which looks homogenous in the outer surface, however beneath the intact enamel variations can be seen in scattering pattern which is indicated by white circle. Red arrows indicate the cracks and dark shadows can be seen below the cracks and green arrows indicate the increase scattering at enamel surface

The selected region highlighted in yellow on the OCT B-scan (figure 6.3b), illustrating a homogenous enamel in the outer surface of the tooth, however beneath the intact enamel we can see variations in scattering pattern showing that there is something subsurface that is abnormal (indicated by white circle). The white spot lesion in the clinical photograph looks non cavitated. However, from OCT scan, there is a change in enamel structure, which is correlated to the white spot lesion on the clinical photograph. There are a subsurface crack can be identified in the buccal side of the scan (indicated by red arrows). As it shown from the OCT scan, the brightest colour due to the highest scattering pattern is present at the surface of the enamel (indicated by green arrows).

6.2.2.3 Results of ICDAS score 2 sample

An example of ICDAS score 2 sample is illustrated in Figure 6.4. The clinical picture of the sample shows clearly the white spot lesion on the occlusal surface of the tooth with the black box that indicate the position of the scan (figure 6.4a). In this OCT B-scan (figure 6.4b), only the enamel is visible. The enamel structure looks heterogenous with variations in scattering pattern (indicated by white circle). The white spot lesion in the clinical photograph looks non-cavitated. However, from OCT scan, there is a change in enamel structure, which is corresponding to the white spot lesion on the clinical photograph. Also, there are subsurface cracks can be identified along the scan (indicated by red arrows) and the area below the crack is dark. The enamel in the middle of the OCT B-scan is carious enamel where there is an increased brightness along the depth of enamel in comparison with the adjacent enamel (indicated by green arrows). The enamel surface shows early signs of decay.

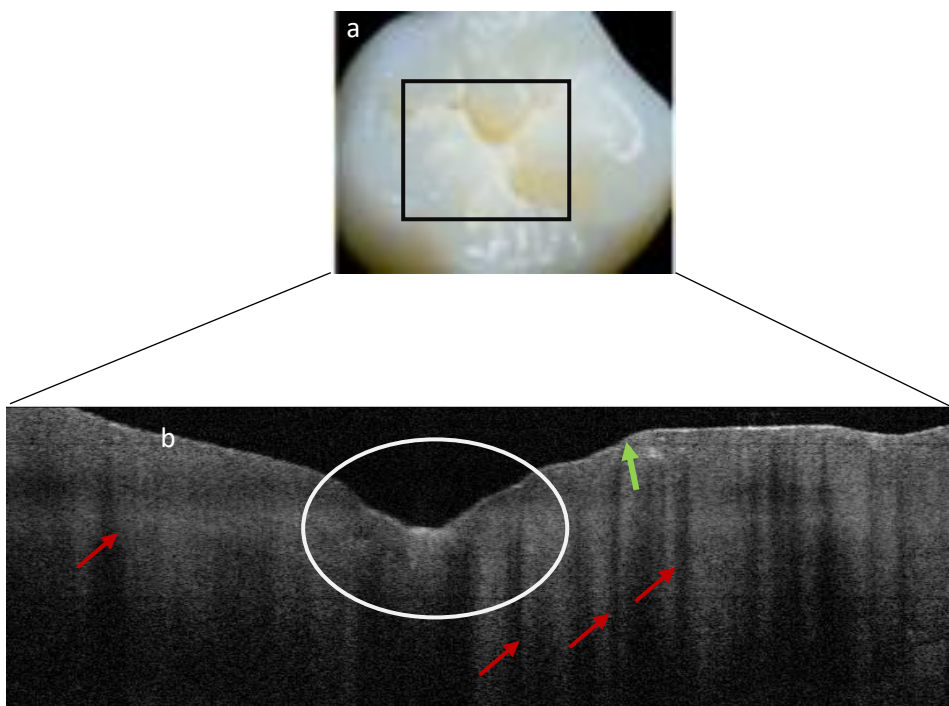


Figure 6.4: a) ICDAS score 2 sample clinical photo and b) OCT b-scan. In this image only, the structure of enamel is shown which looks non-homogenous which is indicated by white circle. Red arrows indicate the cracks and green arrows indicate the increase scattering at enamel surface, the enamel in the middle of the OCT B-scan is carious enamel where there is an increased brightness along the depth of enamel in comparison with the adjacent enamel

6.2.2.4 Results of ICDAS score 3 sample

Figure 6.5 shows the OCT B-scan for the ICDAS score 3 sample. The clinical picture of the sample (figure 6.5a), shows the cavitated enamel lesion on the occlusal surface of the tooth, with the black box that indicate the position of the scan. In OCT scan (figure 6.5b), the enamel and dentine can be seen in the distal part of the scan. The enamel dentine junction (EDJ) is visible, and the enamel structure looks non-homogenous with variations in scattering pattern (indicated by white circle). The enamel in the middle of the OCT scan is carious, which correlates with the cavitated lesion on the clinical photograph. The OCT scan also shows an increased brightness along the fissure pattern in comparison with the adjacent enamel as the enamel surface shows early signs of cavitation (indicated by green arrows). Also, there are numerous small opaque structures related to the EDJ, resembling enamel spindles in histological sections (figure 6.6).

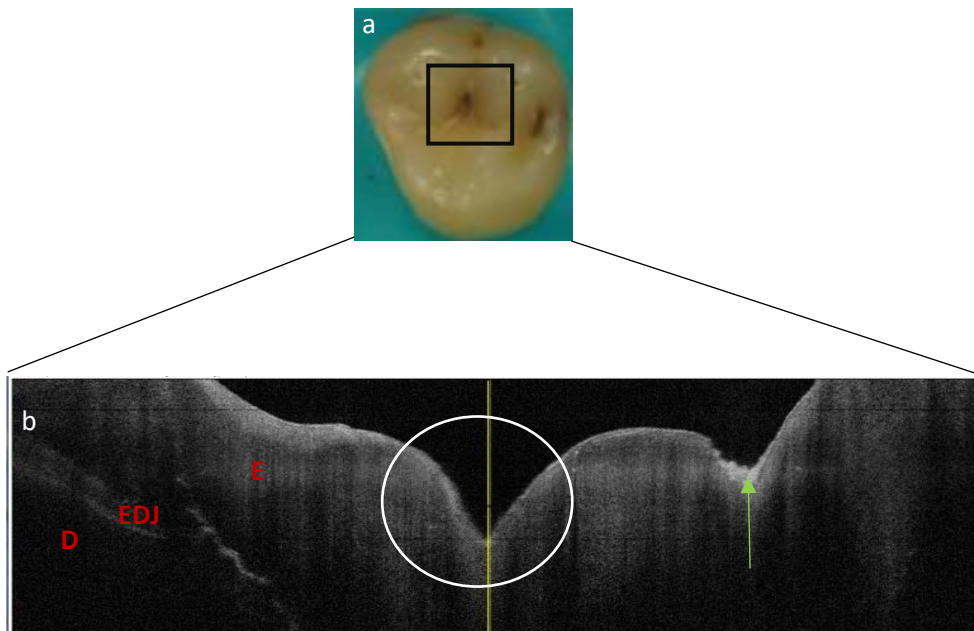


Figure 6.5: a) ICDAS score 3 sample clinical photo and b) OCT b-scan. In this image only, the structure of enamel is shown which looks non-homogenous. The green arrow indicates areas of surface enamel cavitation, the white circle indicates cavity lesion

6.2.2.5 Results of ICDAS score 4 sample

An OCT B-scan of the ICDAS score 4 sample is demonstrated in Figure 6.6. The clinical picture of the sample (figure 6.6a) shows clearly the occlusal lesion scanned within the black box. The lesion shows a localised enamel surface cavity or breakdown but with a shadow of underlying discoloured dentine. The colour of the intrinsic shadow appeared as a dark brown discolouration that is visible through the intact enamel surface. This cavitated lesion can be detected when the tooth is wet. The most prominent feature in this OCT B-scan (figure 6.6b) is the distinctive enamel lesion towards the mesial side of the scan. The enamel structure looks heterogenous with variations in scattering pattern correlating to the clinical cavity (indicated by white circle). There is a subsurface crack can be identified in the scan (indicated by red arrow) and interestingly the area below the crack is dark. As it shown from the OCT scan, where the surface of the enamel is smooth it can be recognised by the bright line spanning the length of the section due to the highest scattering pattern that is present at the surface of the enamel (indicated by green arrows).

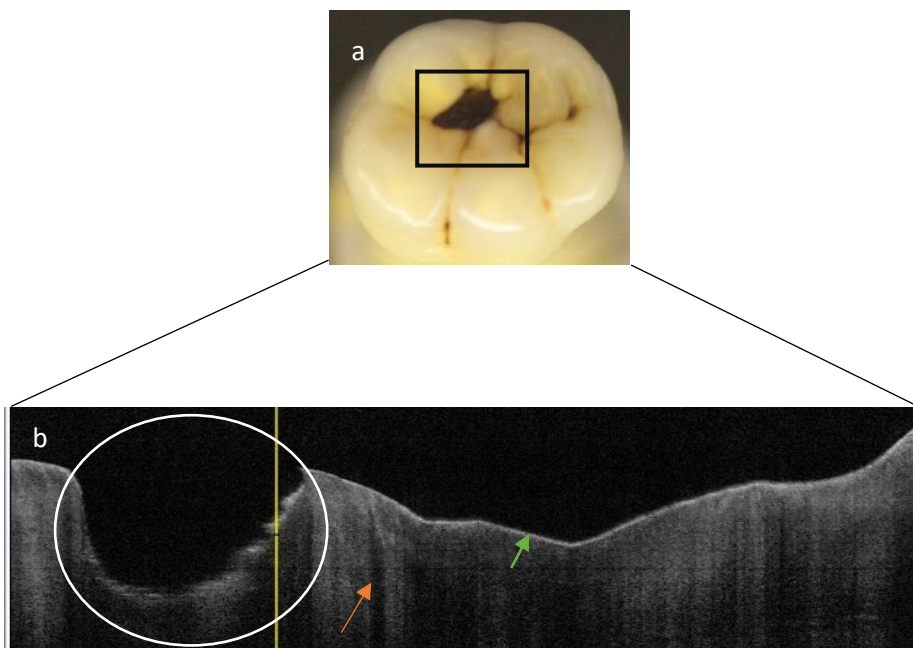


Figure 6.6: a) ICDAS score 4 sample clinical photo and b) OCT b-scan. The OCT image demonstrates the occlusal surface of a first permanent molar tooth with a cavitated carious lesion (ICDAS 4). The brightest colour is due to the highest scattering pattern that is present at the surface of the enamel which is indicated by green arrow. The white circle illustrates carious lesion. A subsurface crack can be identified in the scan which is indicated by red arrow

6.2.2.6 Results of ICDAS score 5 sample

The OCT scan of the ICDAS score 5 sample is demonstrated in Figure 6.7. The clinical picture (figure 6.7a) shows clearly the cavitated occlusal lesion with the black box that indicate the position of the scan. The lesion has a distinct cavity on dental enamel and is detected with visible dentine showing underneath enamel cavitation. When the surface is examined wet, the dark dentine showed through dental enamel. But when air is applied for 5 second, a frank cavity was visually detected with evidence of carious enamel demineralisation, which is presented as dark brown on cavity walls especially in the pits and fissures. In the OCT scan (figure 6.7b), enamel and dentine are visible at the region where the OCT scan was taken. The enamel and dentine structures look non-homogenous with variations in scattering pattern (indicated by white circle). The cavity is extensive clinically. OCT scan shows dramatic changes in enamel and dentine structures, which is correlated to the occlusal cavity on the clinical photograph. The white circle shows the extent of the carious lesion beyond EDJ. On the B-scan, where the surface of the enamel is smooth it can be recognised by the bright line spanning the length of the section due to the highest scattering pattern at the surface of the enamel (indicated by green arrows).

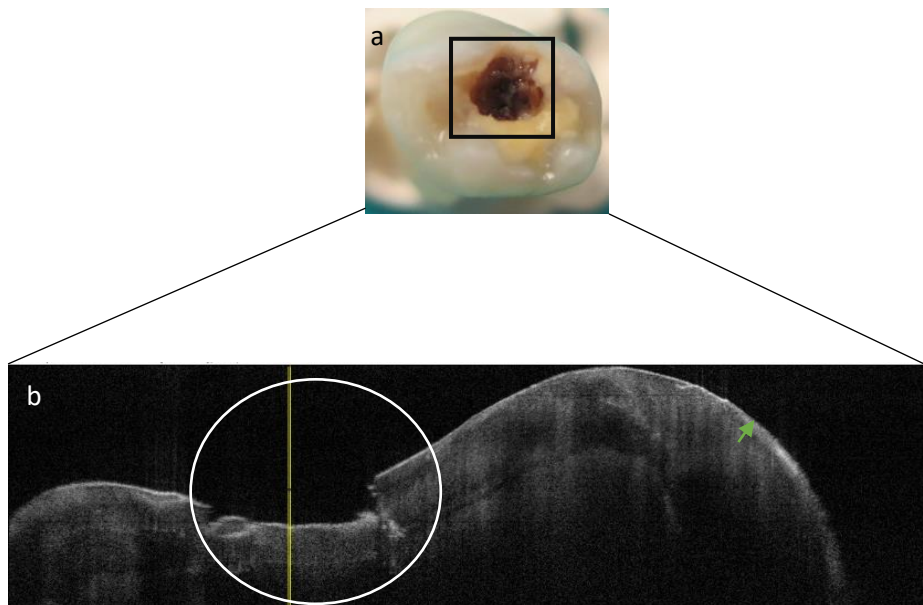


Figure 6.7: a) ICDAS score 5 sample clinical photo and b) OCT b-scan. The OCT image demonstrates the occlusal surface of a first permanent molar tooth with an extensive cavitated carious lesion (ICDAS 5). The brightest colour is due to the highest scattering pattern that is present at the surface of the enamel which is indicated by green arrow. The white circle illustrates carious lesion

6.2.2.7 Results of ICDAS score 6 sample

Figure 6.8 demonstrates the OCT B-scan of the ICDAS score 6 sample. The clinical picture of the sample (figure 6.8a) shows the extensive mesio-occlusal lesion with extensive loss of dental structure with dentine evidently visible at the wall and base of the cavity. The cavity extends to involve half of tooth surface with an increased likelihood to reach the dental pulp. The black box indicates the position of the scan. In the OCT B-scan (figure 6.8b), enamel and dentine are visible at the region where the OCT scan was taken. The enamel and dentine structures look heterogenous with extensive variations in scattering pattern due to the carious lesion and the loss of dental hard tissues (indicated by white circle). The cavity is extensive clinically. OCT scan shows dramatic changes in enamel and dentine structures, which is correlated to the occlusal caries on the clinical photograph. The brightest colour on the smooth enamel surface is due to the highest scattering pattern (indicated by green arrows).

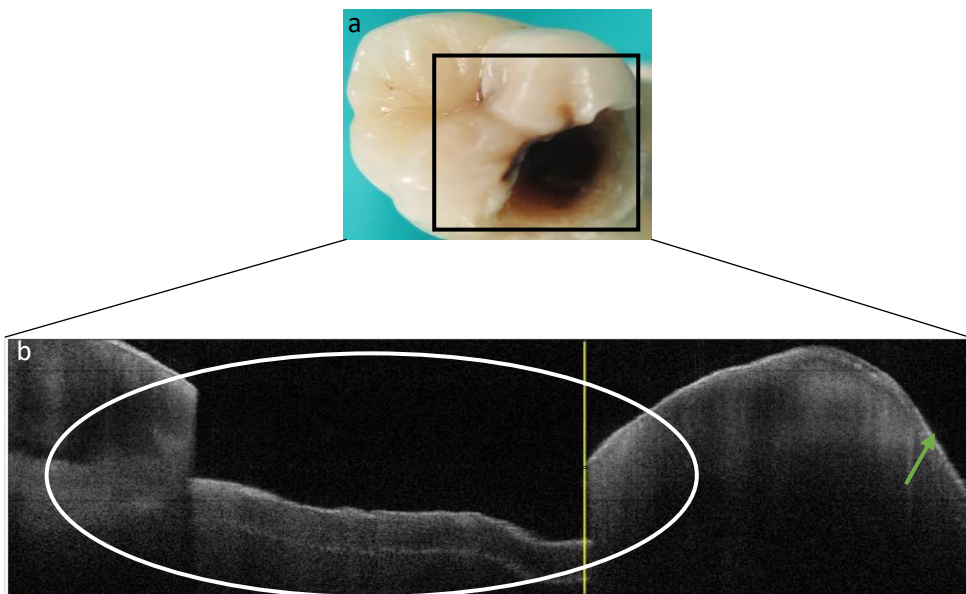


Figure 6.8: a) ICDAS score 6 sample clinical photo and b) OCT b-scan. The OCT image demonstrates the occlusal surface of a first permanent molar tooth with an extensive cavitated carious lesion (ICDAS 6). The green arrow indicates the area where the highest scattering pattern is present at the surface of the enamel where cusp inclination and complex enamel is and difficult incident angle to account for. The white circle illustrates carious lesion extending beyond EDJ deep into dentine

6.3 Advanced Diagnostics Using OCT Signal Intensity Profiles

6.3.1 Method

Scattering intensity profiles were measured from the B-scans of the samples as a function of depth (figure 6.9). The width of selected area on the B-scans was ten pixels, which corresponds to 40.5 μm for all samples.

The OCT B-scans were transferred to Image J software to obtain the signal intensity profiles (A-scan). The width was 6000 μm , corresponding to 1500 pixels, this means that one pixel is equal to 4 μm . Consequently, the selected rectangular area of interest has a width of 40 μm . Next, the data from the scattering intensity profiles were extracted and plotted as a function of depth using Origin lab pro 2018.

6.3.2 Application of signal intensity profile

All the samples were investigated using this approach. All the selected regions on the B-scan were taken in areas with no subsurface cracks whenever possible as it might affect the scattering pattern of enamel structure. In all types of enamel, the signal intensity profiles showed sharp increase (spike-like) in the intensity profile as the light hits the tooth surface. As the laser travelled through the depth of enamel, any changes in enamel structure will result in changes in scattering pattern. These profiles provide a direct representation of the scattering of light photons as they travel through the enamel layer. These changes can be detected and measure from the A-scan (figure 6.9c) .

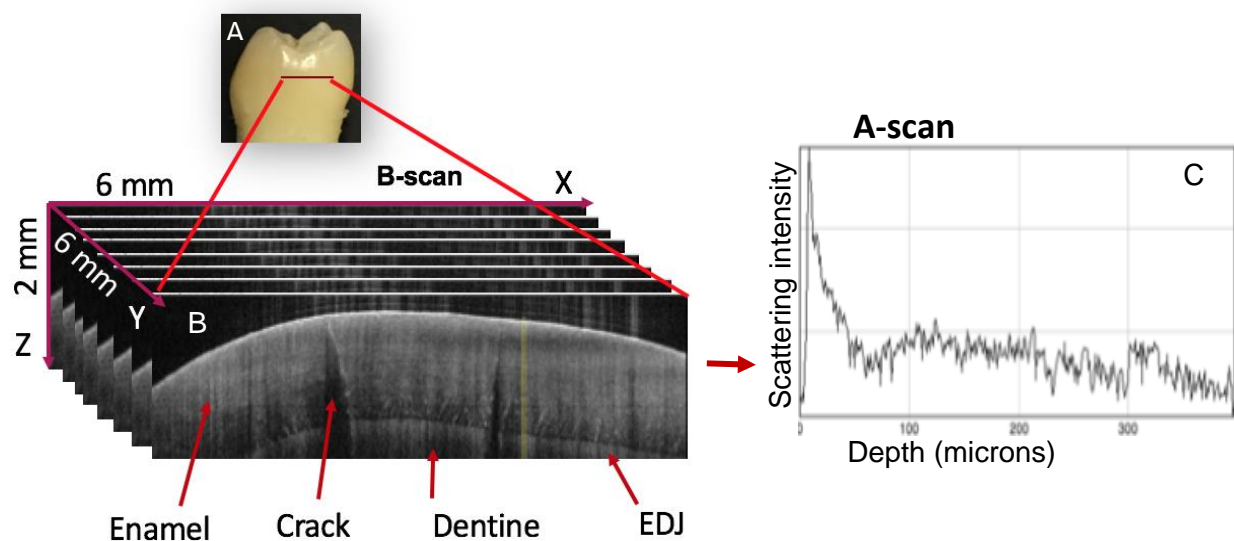


Figure 6.9: A) Control tooth B) OCT B-scan C) OCT A-scan
In this image the scattered intensity was plotted against depth in enamel

6.3.2.1 Signal Intensity Profile of Control Sample

An example of control sample signal intensity profile is shown in figure 6.10, showing the clinical photograph of the tooth (figure 6.10a), with the red box indicating where the OCT frame was taken. The selected region is highlighted in yellow on the B-scan OCT frame (figure 6.10 b and c). It can be seen from the B-scan image that the enamel structure is uniformly scattered. The signal intensity profile in 6.10d shows initially a non-scattering phase where light travels in air. However, at the air/surface interface a sharp scattering peak (X) is observed as photons encounter a medium with a greater refractive index i.e. enamel ($n \sim 1.63$) compared to air ($n=1$). Following the strong air/surface scattering peak, the profile presents an exponential decay (**) profile as photons travel through the enamel. From this intensity profile the total distance travelled by photons in enamel and dentine was about $1800\mu\text{m}$. The green arrows in figure 6.11b, c and d indicate the position of the EDJ. In figure 6.11d, there is a slight increase in back scattered light intensity as light photons hit the EDJ.

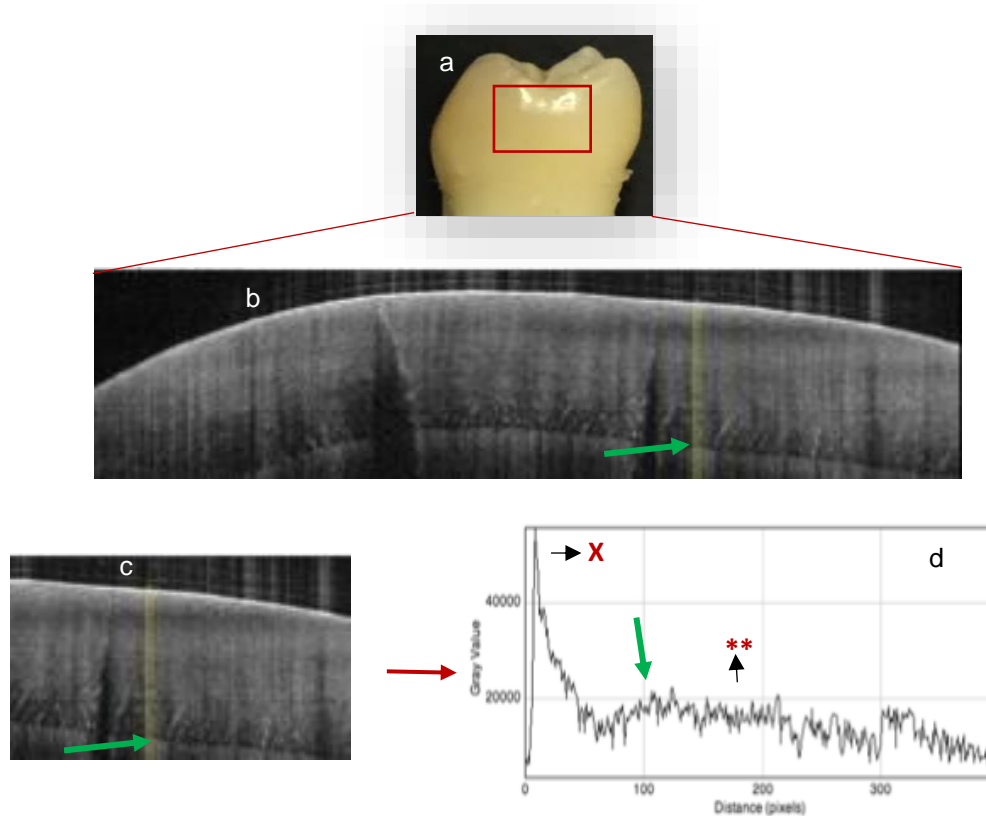


Figure 6.10 Signal intensity profile of a control healthy enamel. a) mesial surface of a control First permanent molar; b) OCT B-scan image taken from the same surface, the selected region is highlighted with yellow vertical lines; c) a magnification of the selected region; d) the signal intensity profile of the selected region in b and c; the green arrows in b, c and d indicate the position of the EDJ.

Figure 6.11 shows scattering intensity profile plot taken from different regions on a single OCT image of one control sample which illustrates similar findings despite changing the extraction region. This confirmed our observations of control samples markers on A-scans i.e.; sharp initial peak followed by gradual smooth decay. The decay of the scattering profiles in healthy enamel (figure 6.11) may present some small variations which are due to localised interruptions in the enamel structural and chemical homogeneity. It is also necessary to consider that the non-scattering phase prior to the enamel-air scattering peak will vary from one profile to another as one needs to consider the curvature of the enamel surface whilst recording the profiles.

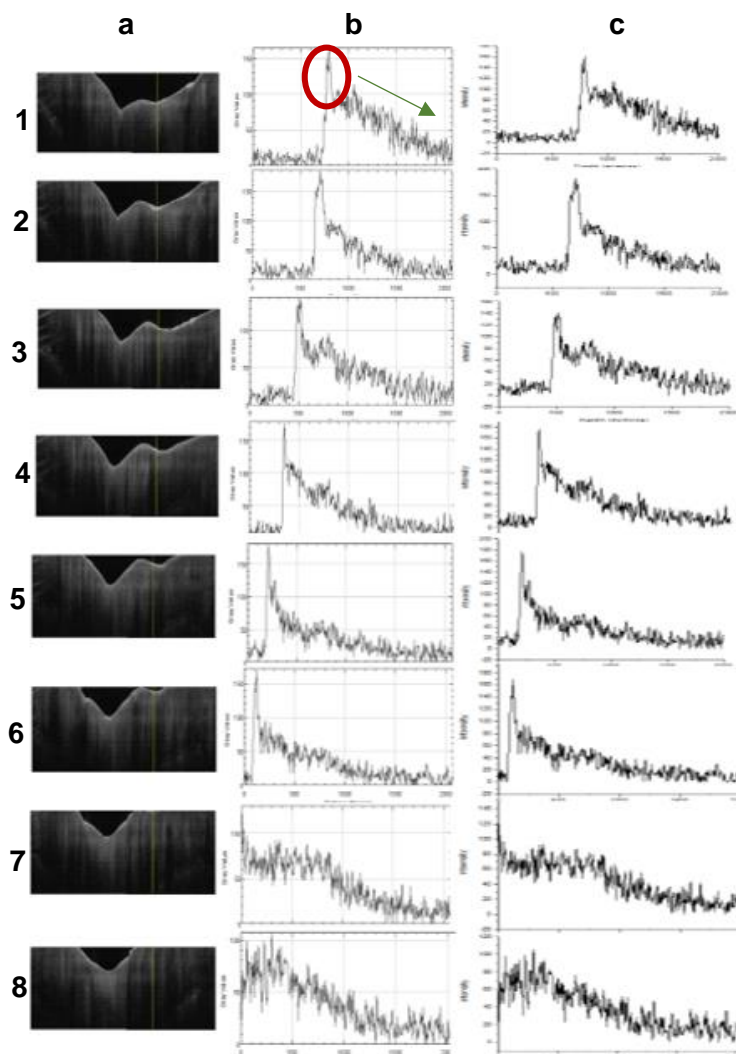


Figure 6.11 Back scattered light intensity profiles extracted from eight different selected regions in an OCT image of a control sample healthy enamel; (a) 10 pixels wide selected regions (1-8); (b) the intensity profile plots in function of depth of scan.; (c) values graphs of B-scans at different intervals. The red circle illustrates the initial sharp peak followed by gradual smooth decay as indicated from the green arrow

6.3.2.2 Signal Intensity Profile of ICDAS score 1 Sample

An example of ICDAS score 1 sample signal intensity profile is shown in figure 6.12 which shows a clinical photo of the tooth (figure 6.12a) as well with a box indicating where the OCT frame has been taken. The selected region is highlighted in yellow on the b-scan OCT frame (figure 6.12 b and c). It can be seen from the b-scan image that the enamel structure appears homogenous but there is an increase in brightness at the surface of the enamel. Cracks can be identified as well. In the a-scan, an area of no-scattering intensity can be seen at the beginning of the profile (figure 6.12d). From the obtained A-scan a delay is observed before a wide peak is formed at the interface between air and enamel due to the high curvature. The wide peak persisted for about 100 μm then the scattering intensity decays associated with high noise is formed when the photon travels through the depth of the enamel.

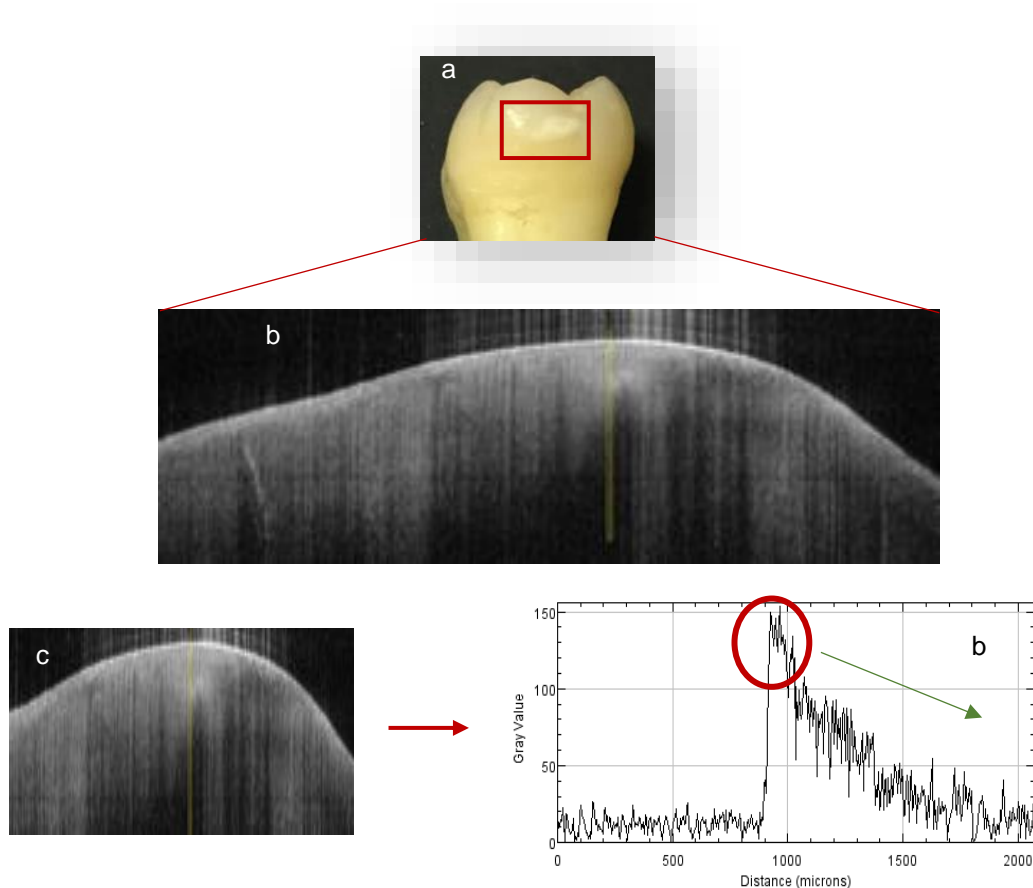


Figure 6.12 Signal intensity profile of ICDAS score 1. a) mesial surface of a First permanent molar; b) OCT b-scan image taken from the same surface, the selected region is highlighted with yellow vertical lines; c) a magnification of the selected region; d) the signal intensity profile of the selected region in b and c. The red circle illustrates the wide initial peak and the green arrow shows the delayed decay which is associated with wide noise

Figure 6.13 shows scattering intensity profile plot taken from different regions on a single OCT image of one tooth of ICDAS score 1 sample which illustrates similar findings despite changing the extraction region, confirming our observations of ICDAS score 1 samples marker on A-scans i.e.; wide initial peak followed by delayed decay that is associated with high noise. The decay of the scattering profiles in healthy enamel (figure 6.13) may present some small variations which are due to localised interruptions in the enamel structural and chemical homogeneity. It is also necessary to consider that the non-scattering phase prior to the enamel-air scattering peak will vary from one profile to another as one needs to consider the curvature of the enamel surface whilst recording the profiles.

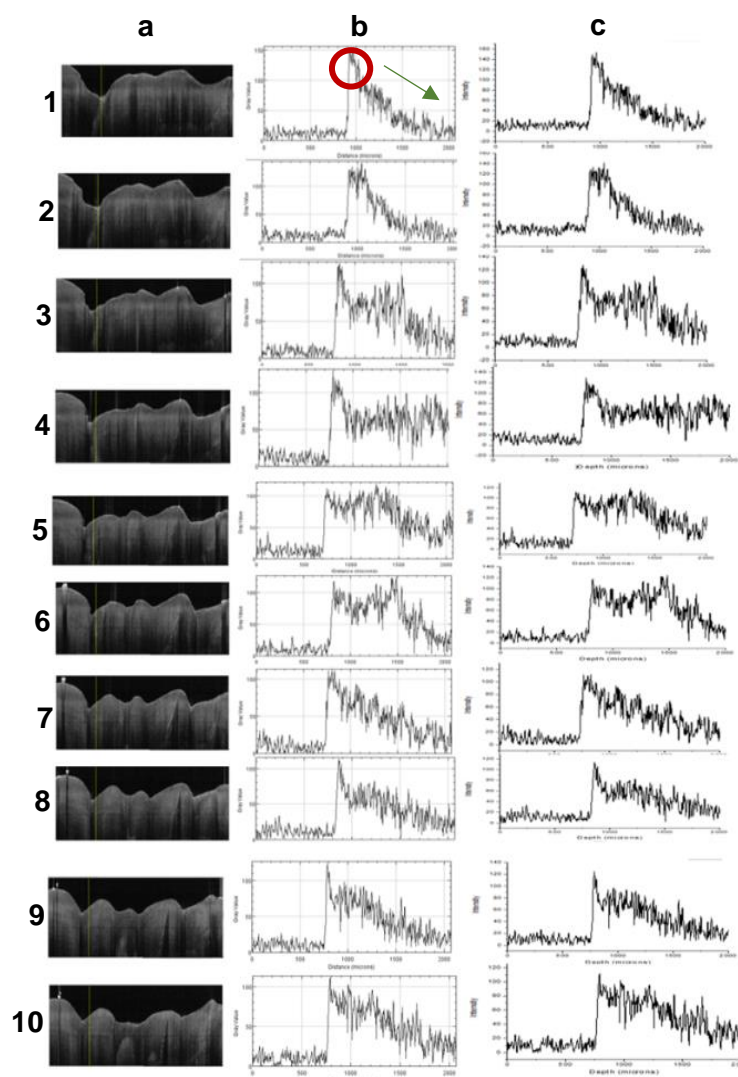


Figure 6.13 Back scattered light intensity profiles extracted from ten different selected regions in an OCT image of ICDAS score 1 sample; (a) 10 pixels wide selected regions (1-10); (b) the intensity profile plots in function of depth of scan.; (c) values graphs of B-scans at different intervals. The red circle illustrates the wide initial peak and the green arrow shows the delayed decay which is associated with high noise

6.3.2.3 Signal Intensity Profile of ICDAS score 2 Sample

Figure 6.14 shows an example of ICDAS score 2 sample signal intensity profile and a clinical photo of the tooth as well with a box indicating where the OCT frame was taken (figure 6.14a). The selected region is highlighted in yellow on the B-scan OCT frame (figure 6.14 b and c). It can be seen from the B-scan image the heterogeneous appearance of the enamel, with areas displaying the natural grey scale contrast reminiscent of control sample, and other areas displaying subsurface lesions. There is an increase in brightness at the surface of the enamel. In the A-scan, an area of no-scattering intensity can be seen at the beginning of the profile (figure 6.15d) due to increased curvature of occlusal fissures. A very sharp peak is developed at interface between the air and the enamel, which persisted for a very short period and then the scattering intensity decayed when the photon travelled through the depth of the enamel come to broadline fast.

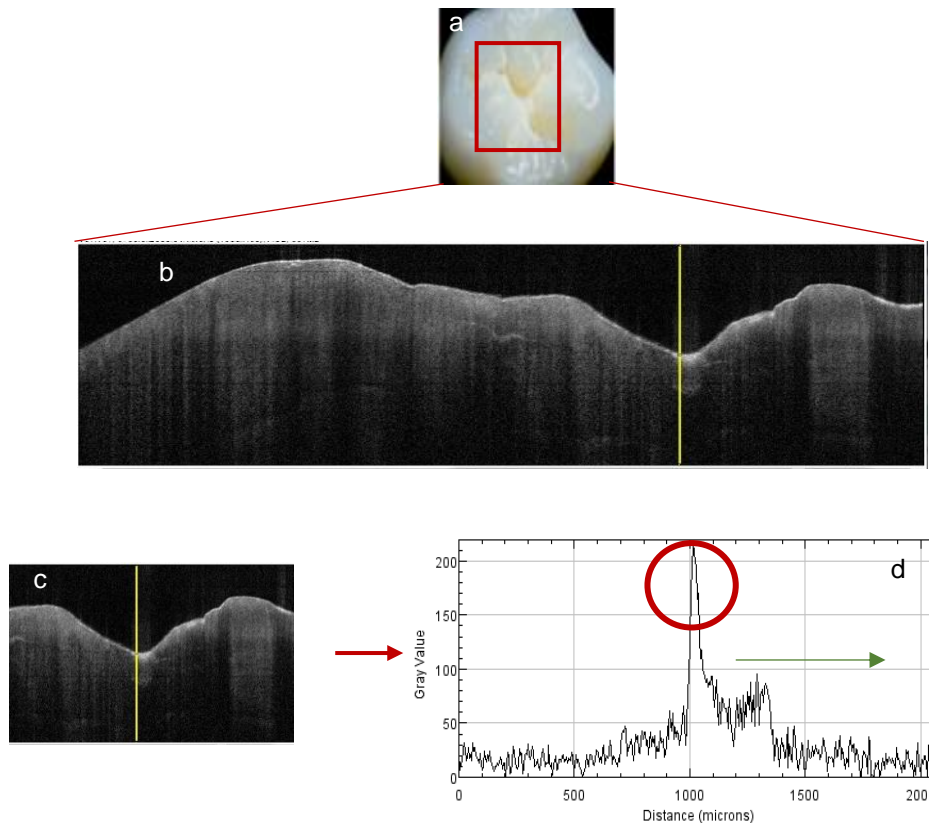


Figure 6.14 Signal intensity profile of ICDAS score 2. a) occlusal surface of a First permanent molar fissures; b) OCT b-scan image taken from the same surface, the selected region is highlighted with yellow vertical lines; c) a magnification of the selected region; d) the signal intensity profile of the selected region in b and c. The red circle illustrates the very sharp initial peak and the green arrow shows how decay comes to broadline very fast

Scattering intensity profile plot of ICDAS score 2 sample taken from different regions on a single OCT image is illustrated in figure 6.15. The decay of the scattering profiles in various enamel (figure 6.15) shows some small variations which are due to localised interruptions in the enamel structural and chemical homogeneity as caries penetrates. The prominent feature in these A-scans is the very sharp initial peak in each scan that is come to baseline very fast despite changing the extraction region, which confirm our observations of ICDAS score 2 samples marker on A-scan. It is also necessary to consider that the non-scattering phase prior to the enamel-air scattering peak will vary from one profile to another as one needs to consider the curvature of the enamel fissures whilst recording the profiles.

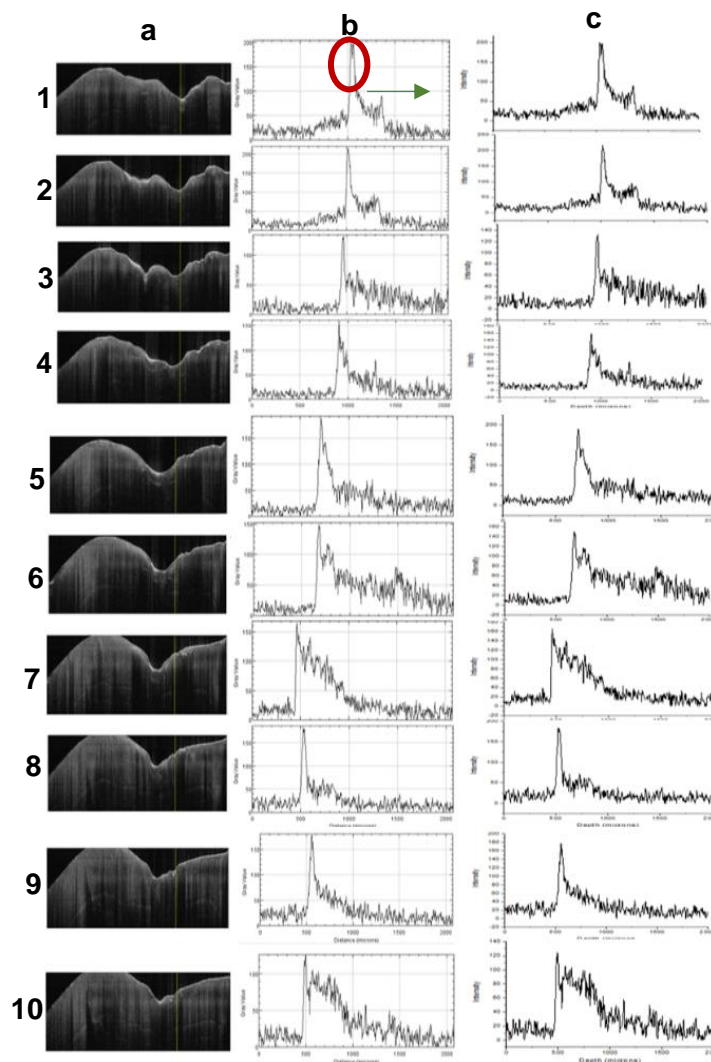


Figure 6.15 Back scattered light intensity profiles extracted from ten different selected regions in an OCT image of ICDAS score 2 sample; (a) 10 pixels wide selected regions (1-10); (b) the intensity profile plots in function of depth of scan.; (c) values graphs of B-scans at different intervals. The red circle illustrates the very sharp initial peak and the green arrow shows how decay comes to baseline very fast

6.3.2.4 Signal Intensity Profile of ICDAS score 3 Sample

ICDAS score 3 sample signal intensity profile is shown in figure 6.16 and a clinical photo of the tooth as well with a red box indicating where the OCT frame was taken (figure 6.16a). The selected region is highlighted in yellow on the b-scan OCT frame (figure 6.16 b and c). It can be seen from the B-scan image the heterogeneous appearance of the enamel. There is an increase in brightness at the surface of the enamel as well. In the A-scan, an area of no-scattering intensity can be seen at the beginning of the profile due to the increase of fissure curvature (figure 6.16d). A very wide delayed steady peak is developed at interface between the air and the enamel which shows that there are some changes subsurface, that persisted for a short period and then the scattering intensity decayed when the photon travelled through the depth of the enamel come to broadline fast.

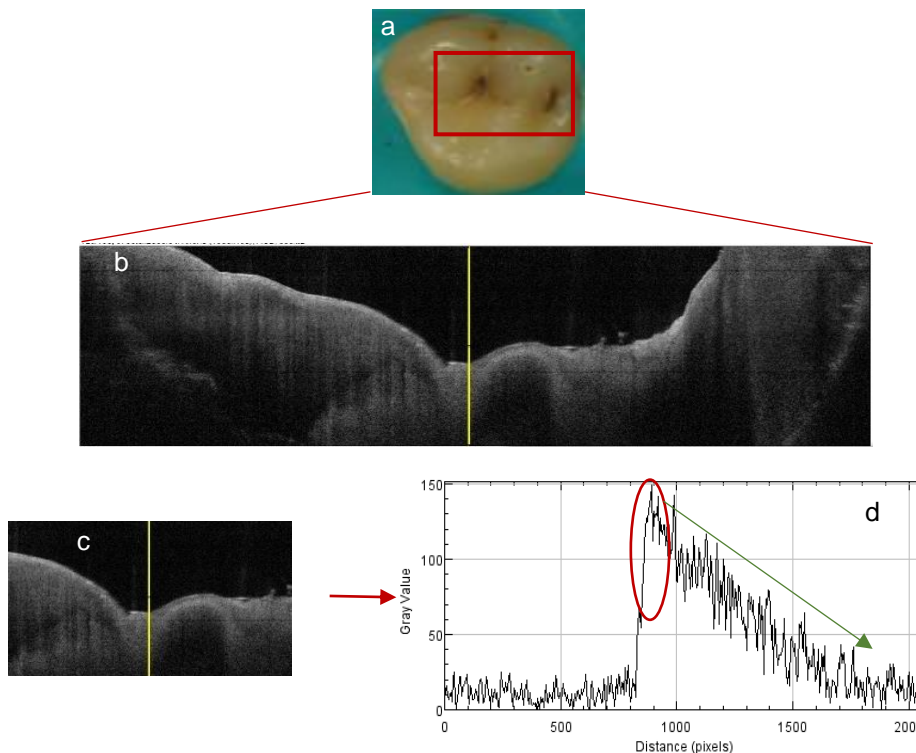


Figure 6.16 Signal intensity profile of ICDAS score 3. a) occlusal surface of a First permanent molar fissures; b) OCT b-scan image taken from the same surface, the selected region is highlighted with yellow vertical lines; c) a magnification of the selected region; d) the signal intensity profile of the selected region in b and c. The red circle illustrates the very wide delayed initial peak and the green arrow shows how decay comes to broadline

Figure 6.17 shows scattering intensity profile plot of ICDAS score 3 sample taken from different regions on a single OCT image. The decay of the scattering profiles of carious enamel (figure 6.17) presents some variations which are due to localised interruptions of caries in the enamel structural and chemical homogeneity. The scattering intensity profile, which was extracted from the highlighted yellow line on the B-scan (figure 6.17c), show a wide scattering area which is followed by a wide peak at the surface of the enamel. The peak persisted for about 30 μm then the scattering decreased by depth. It is also necessary to consider that the non-scattering phase prior to the enamel-air scattering peak will vary from one profile to another as one needs to consider the curvature of the enamel fissures whilst recording the profiles.

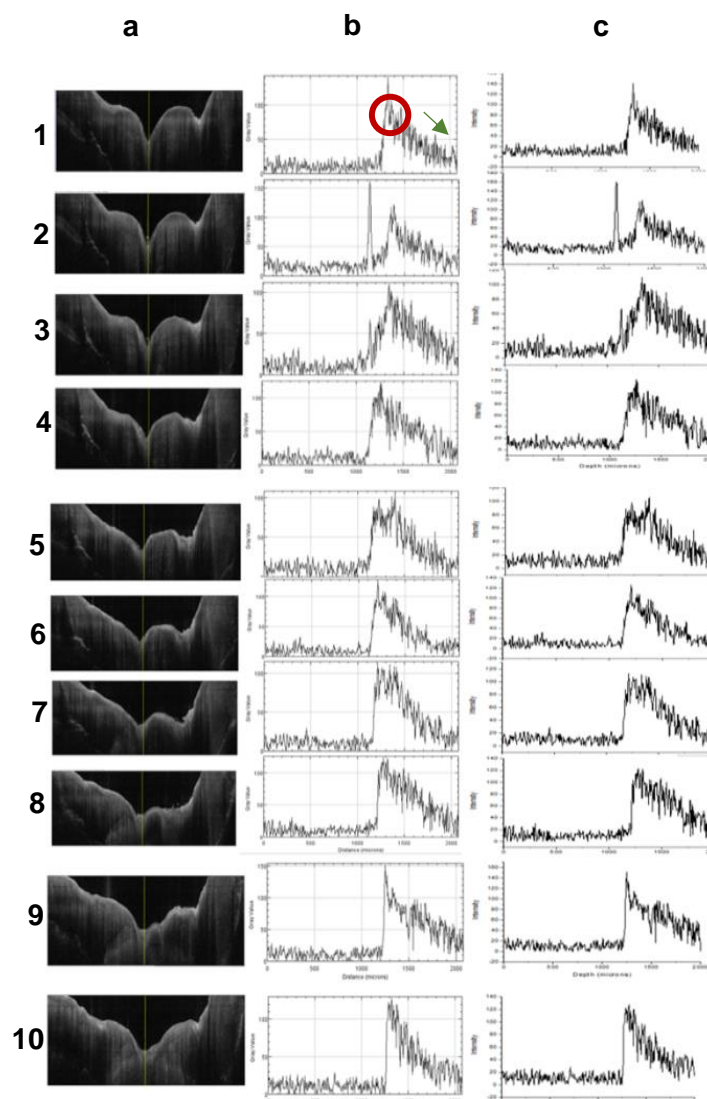


Figure 6.17 Back scattered light intensity profiles extracted from ten different selected regions in an OCT image of ICDAS score 3 sample; (a) 10 pixels wide selected regions (1-10); (b) the intensity profile plots in function of depth of scan.; (c) values graphs of B-scans at different intervals. The red circle illustrates the very wide delayed initial peak and the green arrow shows how decay comes to baseline

6.3.2.5 Signal Intensity Profile of ICDAS score 4 Sample

Figure 6.18 demonstrates an example of ICDAS score 4 sample signal intensity profile and a clinical photo of the tooth as well with a box indicating where the OCT frame was taken (figure 6.18a). The selected region which is highlighted in yellow on the B-scan shows the region of interest where carious lesion can be seen (figure 6.18 b and c). It can be seen from the B-scan image the heterogeneous appearance of the enamel, with areas displaying the natural grey scale contrast reminiscent of sound enamel, and other areas displaying subsurface lesions showing signs of disrupted enamel conformation and the grey-scale gradient is not uniform in those areas. Cracks can be identified as well. There is an increase in brightness at the surface of the enamel. In the A-scan (figure 6.18d) the intensity profile does not show a single intensity peak as the case of sound enamel, instead several irregular waves are shown before it starts to decay which persisted for a short period and then the scattering intensity decayed when the photon travelled through the depth of the enamel come to broadline.

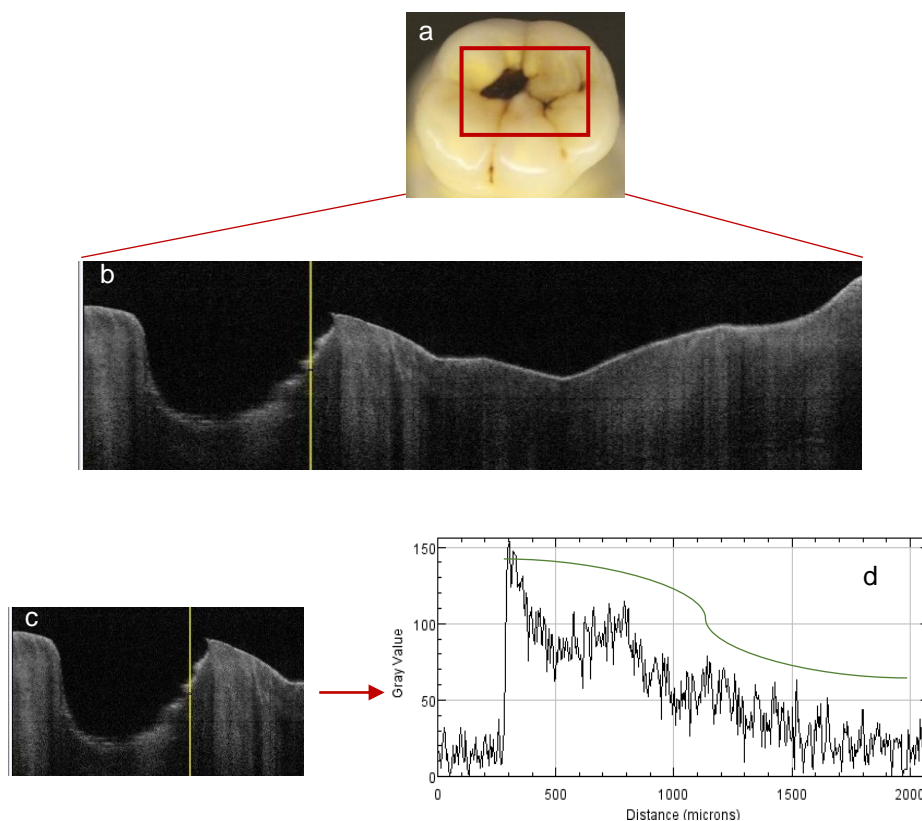


Figure 6.18 Signal intensity profile of ICDAS score 4. a) occlusal surface of a First permanent molar showing cavitated lesion; b) OCT b-scan image taken from the same surface, the selected region is highlighted with yellow vertical lines; c) a magnification of the selected region; d) the signal intensity profile of the selected region in b and c. The green curve illustrates the irregularity of multiple peaks across the carious lesion

Figure 6.19 shows scattering intensity profile plot taken from different regions on a single OCT image of ICDAS score 4 sample. The decay of the scattering profiles in figure 6.19 present variations across the scanned lesion which are due to localised interruptions in the enamel structural and chemical homogeneity because of caries progression. The scattering intensity profile, which was extracted from the highlighted yellow line on the B-scan, show a wide scattering area which is followed by multiple irregular waves at the surface of the enamel. The waves persisted for short period then the scattering decreased by depth. It is also necessary to consider that the non-scattering phase prior to the enamel-air scattering peak will vary from one profile to another.

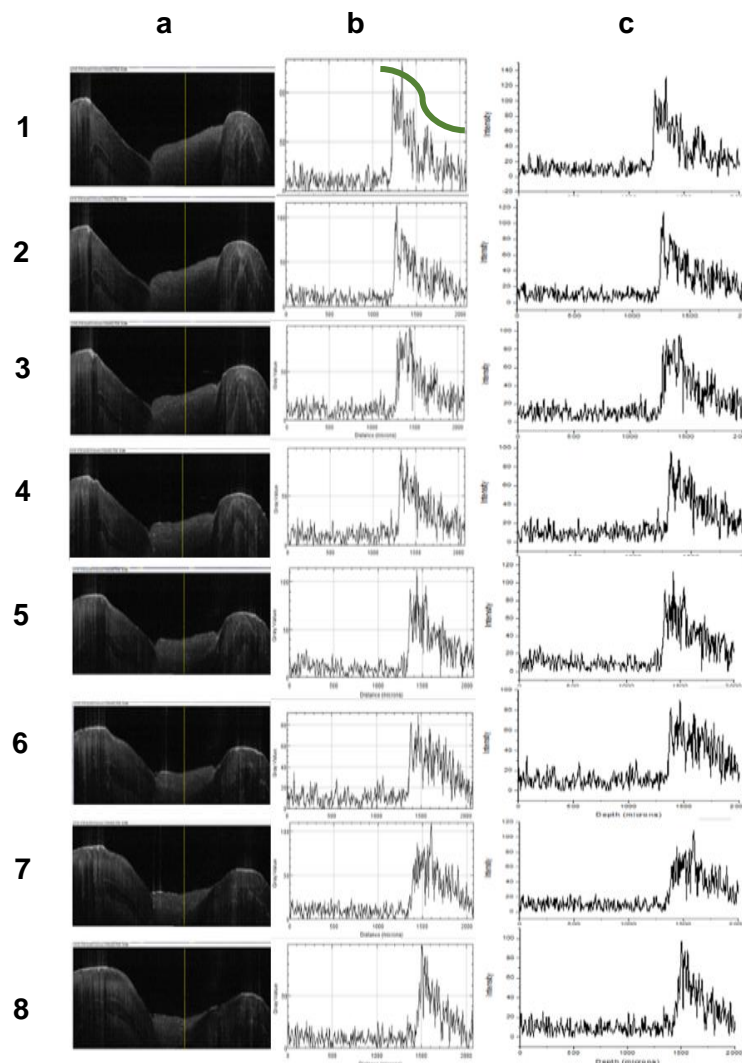


Figure 6.19 Back scattered light intensity profiles extracted from eight different selected regions in an OCT image of ICDAS score 4 sample; (a) 10 pixels wide selected regions (1-8); (b) the intensity profile plots in function of depth of scan.; c) values graphs of B-scans at different intervals. The green curve illustrates the irregularity of multiple peaks across the carious lesion

6.3.2.6 Signal Intensity Profile of ICDAS score 5 Sample

An example of ICDAS score 5 sample signal intensity profile is illustrated in figure 6.20 which shows a clinical photo of the tooth with a box indicating where the OCT frame was taken (figure 6.20a). The selected region is highlighted in yellow on the B-scan OCT frame (figure 6.20 b and c). It can be seen from the B-scan image the heterogeneous appearance of the enamel, with areas displaying the natural grey scale contrast reminiscent of sound enamel, and other areas displaying subsurface lesions showing signs of extensive disruption in enamel conformation and the grey-scale gradient is not uniform in those areas. In the A-scan, an area of no-scattering intensity can be seen at the beginning of the profile as the photon penetrates caries lesion (figure 6.20 d). In addition to that the intensity profile does not show a single intensity peak as the case of ICDAS score 1 and 2, instead several irregular waves are shown indicating subsurface destruction before it starts to decay which persisted for a short period and then the scattering intensity decayed when the photon travelled through the depth of the enamel appear more jagged.

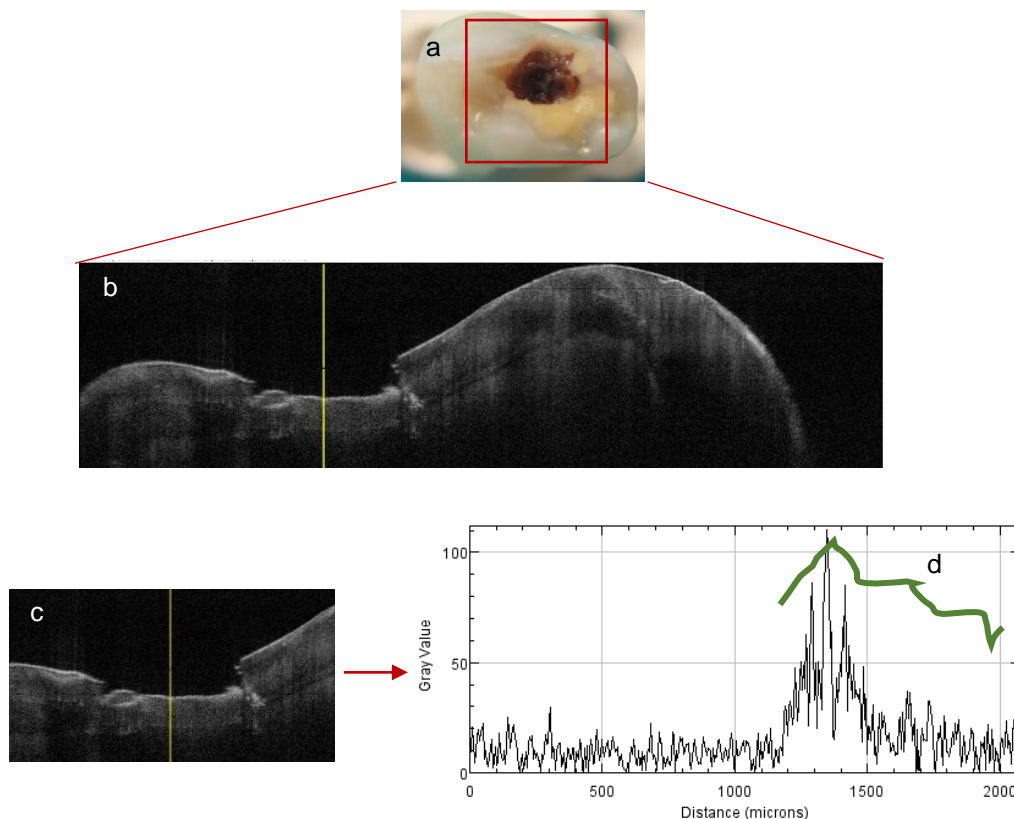


Figure 6.20 Signal intensity profile of ICDAS score 5. a) occlusal surface of a First permanent molar showing cavitated lesion; b) OCT b-scan image taken from the same surface, the selected region is highlighted with yellow vertical lines; c) a magnification of the selected region; d) the signal intensity profile of the selected region in b and c. The green line indicates jagged irregular waves

Figure 6.21 shows scattering intensity profile plot taken from different regions on a single OCT image of ICDAS score 5 sample. The decay of the scattering profiles in figure 6.21 may present variations which are due to extensive interruptions in the enamel structure because of caries. The scattering intensity profile, which was extracted from the highlighted yellow line on the B-scan, show a wide scattering area which is followed by multiple irregular waves at the surface of the enamel. The irregular waves produced at the surface are followed by rapid decay of scattering intensity and long vertical distance. The waves persisted for short period then the scattering decreased by depth. There is inconsistency across the lesion as the photon penetrates the extensive lesion the marker defers as a result of subsurface changes towards dentine. It is also necessary to consider that the non-scattering phase prior to the enamel-air scattering peak will vary from one profile to another as one needs to consider the loss of the enamel surface whilst recording the profiles.

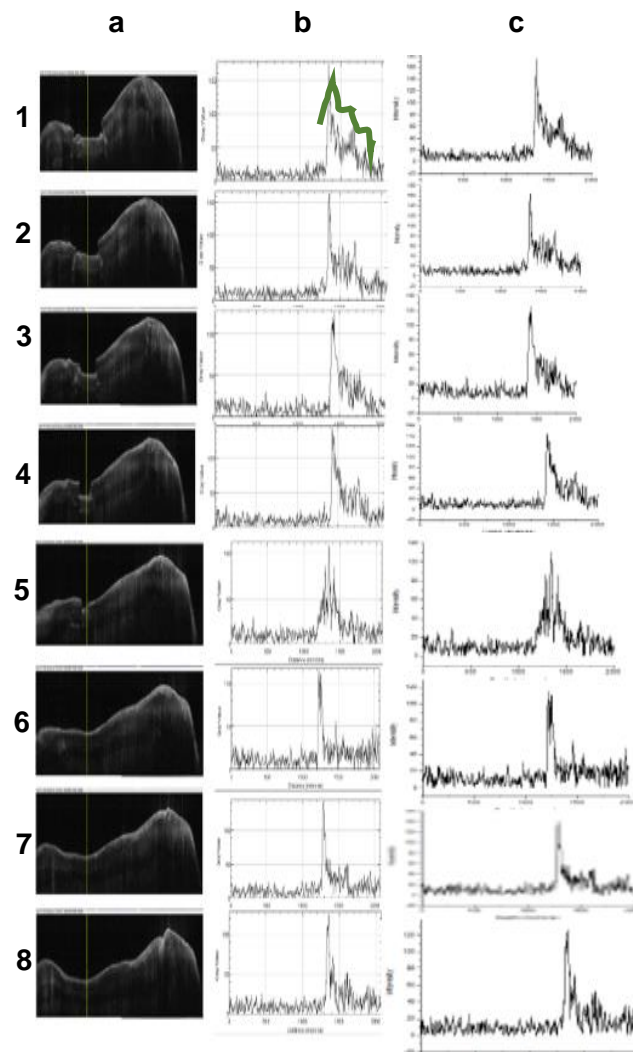


Figure 6.21 Back scattered light intensity profiles extracted from eight different selected regions in an OCT image of ICDAS score 5 sample; (a) 10 pixels wide selected regions (1-8); (b) the intensity profile plots in function of depth of scan.; (c) values graphs of B-scans at different intervals. The green line indicates jagged irregular waves

6.3.2.7 Signal Intensity Profile of ICDAS score 6 Sample

Figure 6.22 shows an example of ICDAS score 6 sample signal intensity profile as well as a clinical photo of the tooth with a red box indicating where the OCT frame was taken (figure 6.22a). The selected region is highlighted in yellow on the B-scan OCT frame (figure 6.22 b and c). It can be seen from the B-scan image the heterogeneous appearance of the enamel, displaying subsurface lesions because of extensive disruption in enamel conformation and loss of extensive hard tissue, and the grey-scale gradient is not uniform in those areas. There is an increase in brightness at the surface of the sound enamel. In the A-scan, an area of no-scattering intensity can be seen at the beginning of the profile as the photon penetrates destructive tissues (figure 6.22 d). In addition to that the intensity profile does not show a single intensity peak as the case of previous scores, instead several irregular peaks, with two or more initial peaks are shown indicating extensive subsurface destruction before it starts to decay which persisted for a short period before another sharp peaks can forms and then the scattering intensity decayed when the photon travelled through the depth of the enamel appear more irregular.

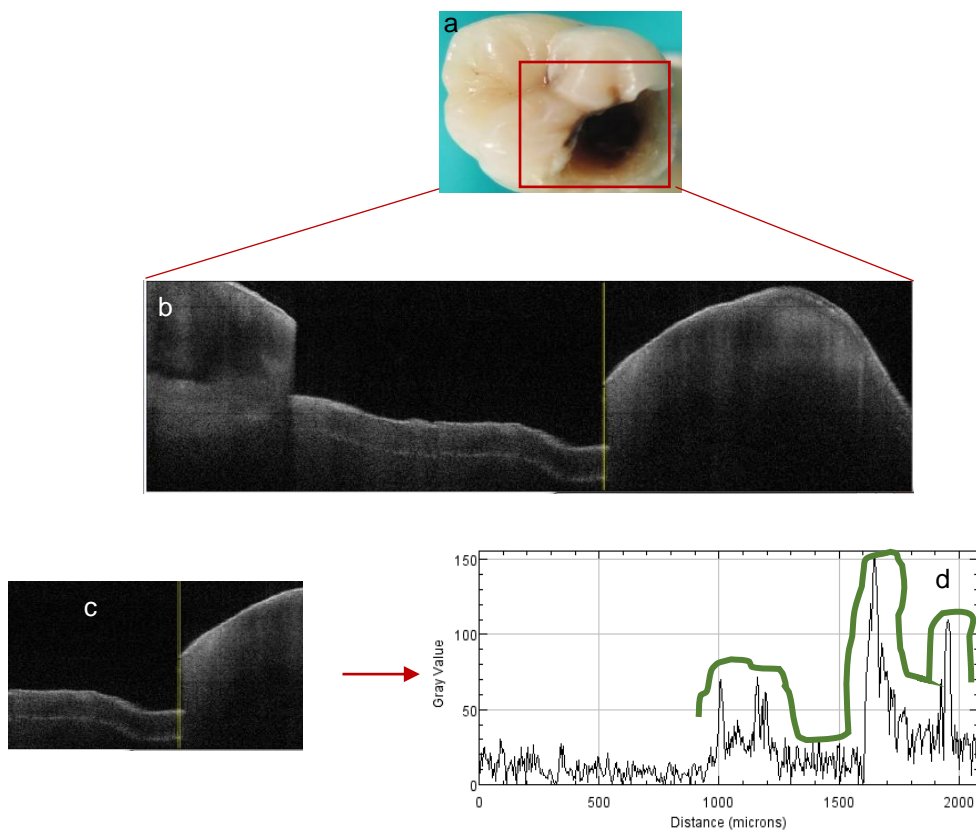


Figure 6.22 Signal intensity profile of ICDAS score 6. a) occlusal surface of a First permanent molar showing extensive disto-occlusal lesion; b) OCT b-scan image taken from the same surface, the selected region is highlighted with yellow vertical lines; c) a magnification of the selected region; d) the signal intensity profile of the selected region in b and c. The green line illustrates waves irregularities

Figure 6.23 shows scattering intensity profile plot taken from different regions on a single OCT image of ICDAS score 6 sample. The decay of the scattering profiles in figure 6.23 shows variations when the region of interest extracted from multiple location across the same lesion which is due to localised enamel and dentine structures loss. The scattering intensity profile, which was extracted from the highlighted yellow line on the B-scan, shows a wide scattering area which is followed by multiple irregular initial peaks at the surface of the enamel. The irregular peaks produced at the surface are followed by another peak and rapid decay of scattering intensity and irregular vertical distance. The scatter persists for short period then the scattering decreased by depth different markers appear due to loss of effect of penetration beyond dentine in such extensive lesions.

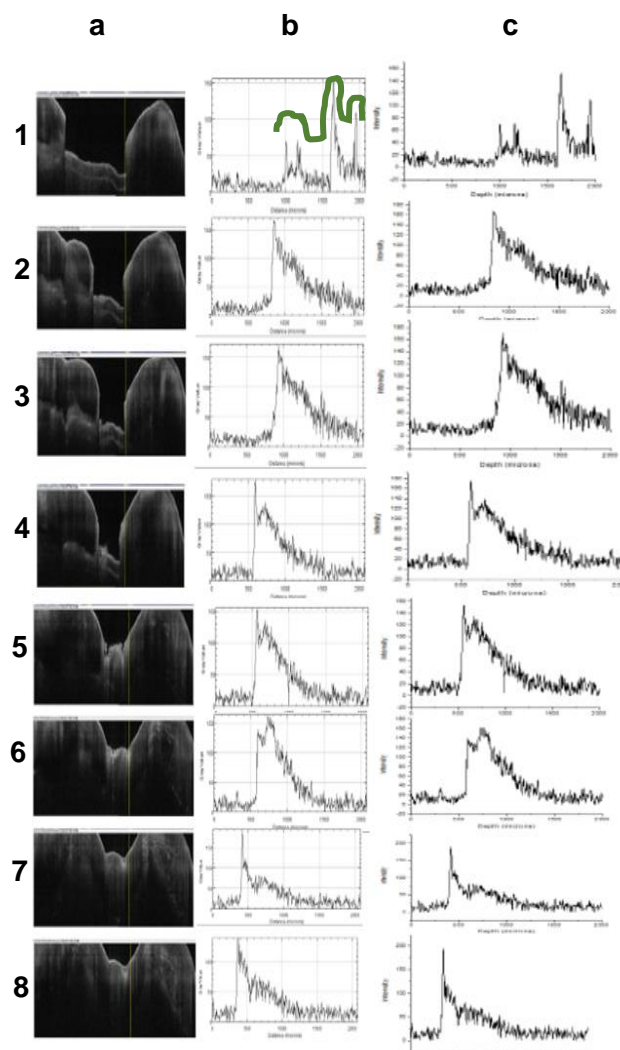


Figure 6.23 Back scattered light intensity profiles extracted from eight different selected regions in an OCT image of ICDAS score 6 sample; (a) 10 pixels wide selected regions (1-8); (b) the intensity profile plots in function of depth of scan.; c) values graphs of B-scans at different intervals. The green line illustrates waves irregularities

Summary of scattering intensity profile plots markers taken post observation of previously mentioned different control and Scores 1-6 ICDAS samples are illustrated below in figure 6.24.

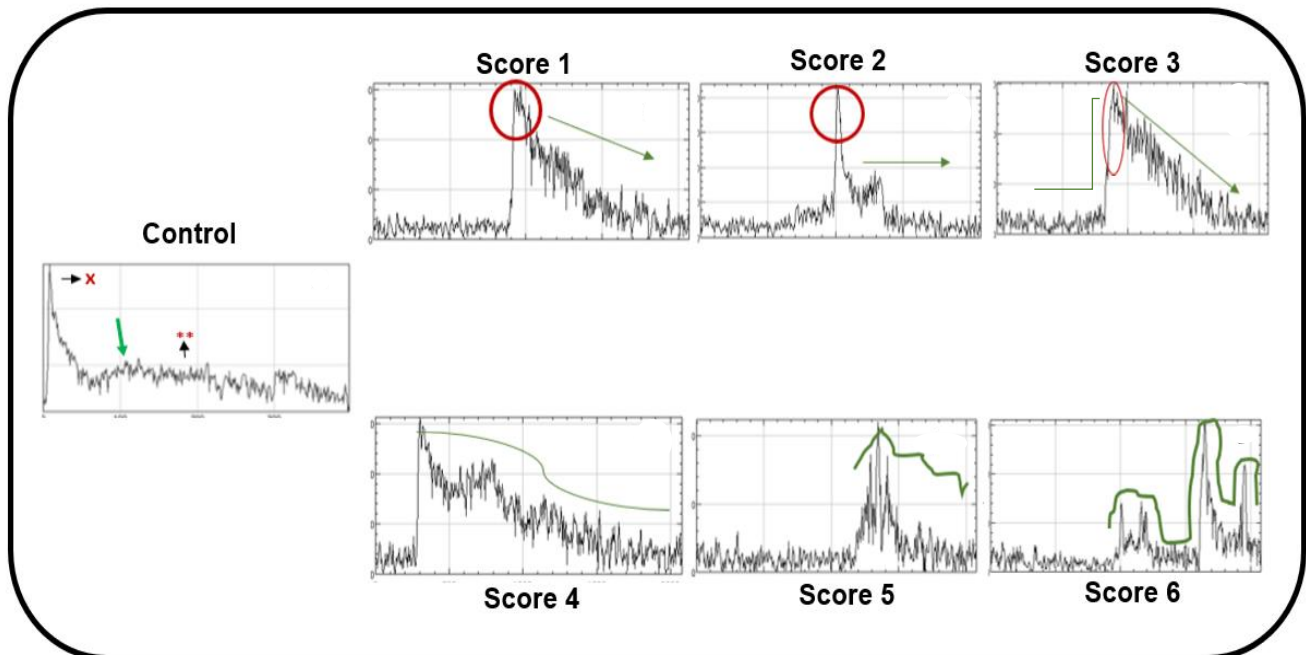


Figure 6.24: Summary of back scattered light intensity profiles of control and scores 1-6 ICDAS

6.4 Discussion

6.4.1 Optical coherence tomography scanning

OCT is a non-destructive imaging system which shows tooth structure up to a depth of nearly 2mm. In this project, the maximum image dimension that can be captured was used. The sections or frames obtained from OCT scanning were very thin (10 μ m) which are very difficult to be obtained by the physical cutting of a tooth. Also, in this study no cutting, slicing or preparation of tooth was needed prior to scanning it, as mentioned earlier the frames obtained are very thin. This enables the clinician to detect even the small abnormalities found in the ultra-structure of teeth. Also, with the use of OCT it was possible to view microscopic structures that could not be seen with the use of the conventional radiographs such as enamel fracture lines.

The total time needed for taking a full scan of 600 OCT frames of the lesion was about 45 seconds, therefore making the OCT scanner a handy, easy to use, and a time effective diagnostic tool. However, the difficulty that had encountered me while doing this project is the fact that it was hard to manoeuvre the current OCT scanning head around the posterior teeth in the jaw. In addition, the current scanner is large and difficult to manipulate in the clinical set-up. As a result, considering the size of the current OCT scanner it is difficult to scan posterior

teeth intra-orally especially in children with small mouths and high levels of interproximal caries; therefore, an appropriately sized dental scanning probe must be used to help scan posterior teeth. The design could be the same as that of a light curing machine used in curing composite filling material, oral wand prototype, or as that of an intra-oral camera or fibre-optic trans-illuminator, which can be easily carried and used inside the oral cavity.

Also, it does not involve ionising radiation hazard and this is an important merit of OCT over conventional radiographic imaging technique currently used clinically. The use of OCT has been reported in the literature for assessing restorations, dental anomalies such as MIH and fluorosis, demineralization and remineralization of dental hard tissues (Fried et al., 2002, Feldchtein et al., 1998).

There are important points to be considered when using OCT scanner on teeth in general and specifically when imaging carious affected teeth. The current OCT imaging scanner is a dermatological one and is intended for imaging skin and not the dental hard tissues. This has some implications. To begin with, it is difficult to be used intraorally in children when imaging first permanent molars as these teeth are situated further back in the mouth and the current scanning probe need to be modified to be used in this case. However, it can be easily used on the anterior teeth as they are more accessible.

Also, the wavelength of the laser used in the VivoSight scanner is 1305nm which might not be suitable for imaging teeth. Darling et al. in 2006 suggested that a near-infra red region of 780-1550nm results in an optimal imaging technique due to low scattering and absorption in enamel and dentine. Maia et.al used two types of OCT; TD-OCT and sFD-OCT with light source wavelengths of 1280 nm and 840 nm, respectively in evaluating caries in deciduous teeth (Maia et al., 2010). They found that there was a great potential for OCT to be used routinely in clinical practice for caries detection and monitoring lesion progression (Maia et al., 2010). The same conclusion was reached by Amaechi et.al that looked at root caries using PS-OCT and correlated it with TMR (Amaechi et al., 2004). They demonstrated that the technique could replace conventional dental radiographs and avoid the hazards of ionising radiation directed to patients (Amaechi et al., 2004).

6.4.2 Diagnostic potential of OCT

OCT B-scans and A-scans have demonstrated the changes in enamel structure. When the gold standard clinical diagnostic tool (ICDAS) was compared with OCT results, OCT provided more description of lesion depth either by B-scans or A- scans. A common finding in healthy and caries affected teeth in this study was the presence of enamel cracks which propagated and extended up to the full thickness of enamel. The irregular appearance of the enamel

cracks in carious teeth may be due to the subsurface changes affected by caries progression which facilitate the propagation of such cracks.

Also, protocol of handling teeth likely to have made many more cracks and artefacts as all the samples were stored in 0.1% Thymol as per the Department policy. However, the use of thymol as a storage medium can influence the optical properties of the samples. Shi et al conducted a study to test the influence of the storage medium on the reading of DIAGNOdent. They found that the teeth that were stored in thymol showed a decrease in the fluorescence when compared to teeth stored in formalin (Shi et al., 2001). Furthermore, Francescut et al., conducted a study to evaluate the influence of the commonly used storage medium in dental research on the infrared laser fluorescence response. They concluded that teeth stored in formaline, chloramine and thymol showed a statistically significant reduction in light fluorescence intensity over 2 years (Francescut et al., 2006).

The behaviour of the scattering of light photons when travelled in the depth of dental enamel is complex and depends on the structure of the enamel. This was manifested when the quality of OCT images was looked . The appearance of healthy enamel OCT images was different from those of caries affected enamel; and those of the different ICDAS scores appeared also different from each other. This is a significant diagnostic finding of OCT imaging. Clinicians can use this technique to differentiate between the different ICDAS scores. However, the disadvantage of OCT is that the increased scattering of enamel shown by the bright areas in OCT images cause shadowing underneath these areas. This could make further assessment of the enamel below these areas difficult.

The en-face reconstruction of the images is a promising advancement of this imaging technique and aids in visualising the enamel structure and subsurface changes in an enhanced way. The ability to clearly visualise and locate caries gives the potential for OCT to be used in a 3D visualisation and reconstruction of the enamel lesions and to highlight areas of disruption within the enamel. This would be an important development in both diagnostic and prognostic evaluation of enamel conditions as it enables non-destructive subsurface imaging of teeth. Volumetric assessment of the enamel defect could be permitted in future by this method of reconstruction.

The intensity of the back scattered light as light photons travel along the depth of the enamel was also investigated by several researchers (Jones et al., 2006, Manesh et al., 2009) to highlight the effect of certain procedures such as demineralisation and remineralisation on dental hard tissues. The change in the enamel ultrastructure due to these processes causes

a change in the scattering of light. In this study A-scan signals of OCT were extracted from the B-scan images to observe the behaviour of light as it travels through the depth of normal and carious enamel, which may lead towards a more systematic diagnostic dental application of the technique using the intensity of back scattered light. The width of the selected regions was taken to be 40.5µm. This was done to get an average measurement representative of the area under investigation, instead of a line selection which was done by other researchers before (Jones et al., 2006).

Different intensity profiles were taken from several regions in a single OCT B-scan image in this research. Each profile showed distinctive behaviour of light scattering which resulted from the enamel being heterogeneously disrupted. Though, the decay of the scattering profiles in healthy enamel presented some small variations which could be due to localised interruptions in the enamel structural and chemical homogeneity. An example of scattering variations which was small is the one seen at the EDJ. This slight increase in scattering intensity could be due to change in refractive index between enamel ($n=1.63$) and dentine ($n=1.54$) or because of their different ultrastructure.

Signal intensity profiles of caries affected enamel showed that there was more than one peak of intensity instead of only one air-enamel peak that is normally seen in healthy enamel. The presence of these different appearance i.e.; sharp, very sharp, wide, and irregular scattering peaks indicates that the structure of the enamel is grossly disrupted. Diagnostically, these scattering peaks can be used as indicators of enamel lesions progression as different scores of ICDAS appeared different from each other. The depth at which these peaks are located below the air-enamel layer is also significant as this will provide information to clinicians about the extent of the lesion. This investigation of the scattering profiles may lead to future construction of intensity profile markers which can act as a reference in aiding clinicians to diagnose caries (figure 6.24).

The use of signal intensity profiles in comparing the reflectivity of enamel has been investigated before and was correlated with the ultrastructure of enamel. The main drawback of these studies is the fact that no one has validated these studies of OCT and dental caries against the gold standard of ICDAS. It is well established in the literature that the ultrastructure of carious enamel is different from that Jones et.al suggested that the porosity of the carious enamel controls the reflectivity of the lesion (Jones et al., 2006). Therefore, this technique could be possibly used in distinguishing the different types of carious lesions investigated.

When conventional diagnostic techniques were compared with OCT imaging, the latter technique gave a better description of caries lesions either qualitatively or using the intensity pro-

files of back scattered light. Conventional techniques either gave account of the clinical appearance of caries or showed images with low resolution of these lesions as in radiographic images compared to OCT resolution. Also, it was possible to measure the dimensions of certain lesions from OCT images with the aid of image J software directly to detect the extent of the lesions into the depth of enamel.

6.4.3 Conclusion

From other studies, the OCT findings in this project showed to agree with the literature findings. In a study which compared between conventional OCT and Polarisation sensitive OCT in investigating tooth structure as well as caries lesions, the conclusion was that both OCT techniques can provide adequate information on caries depth and location, as well as investigation of tooth structure (Baumgartner et al., 2000). Though, Hariri et.al used the signal intensity profiles in investigating the optical properties of enamel and dentine (Hariri et al., 2012). Nevertheless, due to the different patterns of interaction of light photons with enamel structure when the various scores of carious enamels were imaged, an attempt to understand the behaviour of light in these circumstances is important.

Also, the current preventative trend in dentistry is sealing caries and arresting the development of demineralisation. Sealant materials are typically employed in dentistry to prevent the development of cavities on the teeth as they prevent bacterial adhesion to enamel, thus arresting the development of demineralization and of caries. Oancea et al., in a study that was done in 2014 , assessed the interface between different sealant materials using swept source OCT (Oancea et al., 2014). Optical inspection and X-ray investigation revealed no defects, while SS-OCT proved capable to asses exactly the position, the nature, and the dimensions of each type of these defects (Oancea et al., 2014). Different failures were targeted into the structure of pit and fissure sealants, such as; bubbles, internal cracks, structural defects of sealant material, and structural defects of enamel, with marginal integrity and marginal adaptation of dental sealant (Oancea et al., 2014).

OCT is a non-ionising and safe method; thus, this is an advantage over radiographs, with higher resolution images. One of the drawbacks of OCT is the limited depth penetration, which is only 2-3mm and the insufficient scanning range, which is around 6x6mm maximum. In addition, when the surface is smooth, like in sound enamel, the scattering is less thus showing higher resolution. Whereas when there is a lesion, the surface is not homogenous, thus the scattering is more, which leads to lower contrast and penetration depth. Furthermore, when considering the size of the OCT scanner it is difficult to scan posterior teeth intra-orally especially in children with small mouths; therefore, an appropriately sized dental scanning probe must be used to help scan posterior teeth.

As already discussed, this technique is promising, and its merit is that it does not involve ionising radiation. The use of OCT to analyse demineralisation in dentine will provide practitioners with information of depth of lesion and proximity to dental pulp which they would be unable to obtain from direct vision or radiography. The knowledge of the depth of the caries and any subsurface abnormality related to the enamel or any restoration will enable dentists to develop an informed treatment plan i.e. whether to restore, root treat or extract the tooth. Saving patients, the expense and discomfort of unnecessary treatment and ensuring appropriate treatment.

Lastly, as mentioned earlier in this chapter, the scattering profile intensity plots between carious and healthy enamel were different. This gave rise to empirical markers, which were described earlier, to describe the A scan profile plots of both the control enamel, and different lesions of ICDAS scores. The emerging question here is whether these markers truly fit the stereotyping of the different lesions which will help clinicians in the future to differentiate between each score easily. This will be cover within chapter 7.

CHAPTER 7

Defining Markers in the OCT Scan and Scattering Profile Intensity Plots

7 Defining markers in the OCT scan and scattering profile intensity plots

As mentioned previously, the scattering profile intensity plots between carious and healthy enamel of primary and permanent teeth were different, with carious enamel showing several scattering peaks, instead of a single air-enamel peak. This assumption gave rise to empirical markers, which were described earlier, to describe the A scan profile plots of both the control enamel, and different lesions of ICDAS scores. It was decided to concentrate on 52 teeth only from the 180 collected which involves control and ICDAS score 1,2,3 and 4 samples, as scores 5 and 6 have extensive caries which is visible clinically, and not related to this study looking at white spot lesions. The aim here was to question whether the markers truly fit the stereotyping of the different lesions. This will help clinicians in the future to differentiate between each score easily.

7.1 Methods- multi-examiners evaluation of the markers

Three different lesions were randomly chosen of each group (control, score 1, score 2, score 3 and score 4 ICDAS), and their correlated A-scans were printed as hard copies. These were then given to two different examiners (examiners B and C) to study and describe what was seen based on their subjectivity. Both examiners then sat with the main author (examiner A), who had scanned the lesions, and different characteristics were then generated by comparing, removing the outliers and keeping the similarities, which lead to the extraction of similar characteristics. These were then used to extract empirical markers to stereotype each type of lesions differently. The different empirical markers are demonstrated in table 7.1.

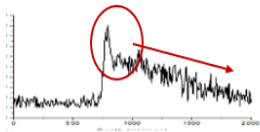
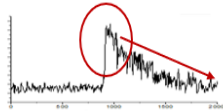
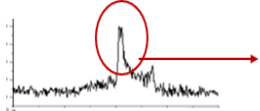
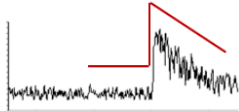
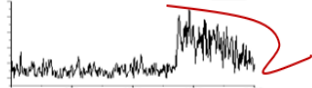
ICDAS score	OCT markers	
ICDAS Control	OCT Control <ul style="list-style-type: none"> • Sharp peak • Gradual smooth decay 	
Score 1	OCT Type 1 <ul style="list-style-type: none"> • Wide peak • Delayed decay associated with high noise 	
Score 2	OCT Type 2 <ul style="list-style-type: none"> • Very sharp peak • Come to broadline fast 	
Score 3	OCT Type 3 <ul style="list-style-type: none"> • Wide delayed steady peak 	
Score 4	OCT Type 4 <ul style="list-style-type: none"> • Irregular multiple waves 	

Table 7.1 illustrates different empirical markers of control and ICDAS 1-4 sample

7.1.1 Exercise 1: Intra-examiner reliability

Cycle 1

Consequently, the main author (examiner A) studied all 52 different A scans, and described them according to the characteristic features above, to see if they fit the criteria the examiner had to describe each lesion, without knowing which type it was, whether it had a sharp, very sharp/wide peak, delayed/fast decayed and if the scatter was more of a wave-like or jagged appearance. Later, the scans were de-blinded, and the markers were assessed to see if they did resemble lesion of interest.

Cycle 2

Examiner A repeated the exercise again a month later for the same 52 lesions, to assess intra-examiner reliability. The agreement was measured by the Cohen's Kappa index using stata15.

Kappa score

For data of population studies to be considered of good quality, it should be repeatable and reliable, which means clinical examiners should have the ability to apply the diagnostic criteria and have consistent results when repeated (intra-examiner reliability), therefore two different examiners were asked to repeat the exercise twice more than a week apart, to test their individual intra-reliability. In addition, inter-examiner reliability is needed, which means consistency between different examiners, thus the 10 different examiners. In addition, calibration and training is needed to ensure that all examiners have understood the exercise properly, and to yield good results and to thus get a good kappa score, which shows good agreement between examiners. Kappa score is defined as "a measure of true agreement. It indicates the proportion of agreement beyond that expected by chance" (Daly and Bourke 2000). It is calculated using the following formula, illustrated in figure 7.1.

$$\frac{(\text{observed agreement} - \text{expected treatment})}{(1 - \text{expected agreement})}$$

Figure 7.1 illustrates formula used to generate Cohen's Kappa

The value generated can then be used to analyse the strength of agreement between examiners. The values along with their strength of agreement are illustrated in table 7.2.

Kappa Statistic	Strength of Agreement
<0.00	Poor
0.00-0.20	Slight
0.21-0.40	Fair
0.41-0.60	Moderate
0.61-0.80	Substantial
0.81-1.00	Almost Perfect

Table 7.2 illustrates interpretation of Cohen’s Kappa values (McHugh, M.L., 2012.)

7.1.2 Exercise 2: Inter-examiner reliability

Fifty-two different A scans of all selected scores were randomly chosen, and hard copies were given to three different examiners, two of who were the same mentioned previously (examiners B and C), plus a third examiner (examiner D) who had not seen the scans before. Each examiner had to study the scan and fill in the table (table 7.3) according to the markers visible.

Sample number	Control	Score 1	Score 2	Score 3	Score 4

Table 7.3 Showing different types of scoring markers and each examiner filled in a table with presented sample number based on what they see in the a-scans

7.1.3 Exercise 3- Populating the Empirical Markers:

A calibration exercise was done with 10 different examiners all of them were dentists, 4 dentists with previous experience with OCT and 6 with no previous exposure to OCT, to make the sample more diverse. A presentation explaining the clinical features of caries with the ICDAS scoring categories, OCT, and A-scans of ICDAS scores 1-4 plus control A-scan was shown and then the different markers were explained with illustrations as demonstrated in table 7.1. A total of 52 different A-scans of the selected scores were randomly mixed and were then shown on a screen. Each examiner was then asked to fill in the boxes of the table 7.3 to assess inter-reliability. A week later, two of the 10 examiners were asked to repeat the exercise to check intra-reliability using Cohen’s kappa index.

7.2 Results

7.2.1 Exercise 1:intra-rater repeatability

- **Cycle 1**

35/52 scans correctly fitted the criteria which means that 67% of the scans showed that the markers accurately reflect the ICDAS score. ICDAS score 2 showed the most accurate results (75%) followed by ICDAS score 4 (72%), ICDAS score 1 (67%), and Control and ICDAS score 3 (60%) respectively, illustrated in table 7.4.

Type	Control	ICDAS Score 1	ICDAS Score 2	ICDAS Score 3	ICDAS Score 4
Number of lesions scanned	10	3	4	10	25
Fit criteria	6	2	3	6	18
Does not fit criteria	4	1	1	4	7
Percentage	60%	67%	75%	60%	72%

Table 7.4: Illustrates summary of results of first cycle

Cycle 2

A month later when examiner A repeated the exercise 29/52 scans correctly fitted the criteria which means 56% of the scans showed that the markers truly resemble the type. ICDAS score 1 showed the most accurate results (67%) followed by ICDAS score 4 (60%), ICDAS score 2, ICDAS score 3 and Control (50%) respectively, illustrated in table 7.5 in the next page. Also, bar charts summary of results of cycle 1 and 2 are illustrated in figure 7.2.

Type	Control	ICDAS Score 1	ICDAS Score 2	ICDAS Score 3	ICDAS Score 4
Number of lesions scanned	10	3	4	10	25
Fit criteria	5	2	2	5	15
Don't fit criteria	5	1	2	5	10
Percentage	50%	67%	50%	50%	60%

Table 7.5: Illustrates summary of results of second cycle

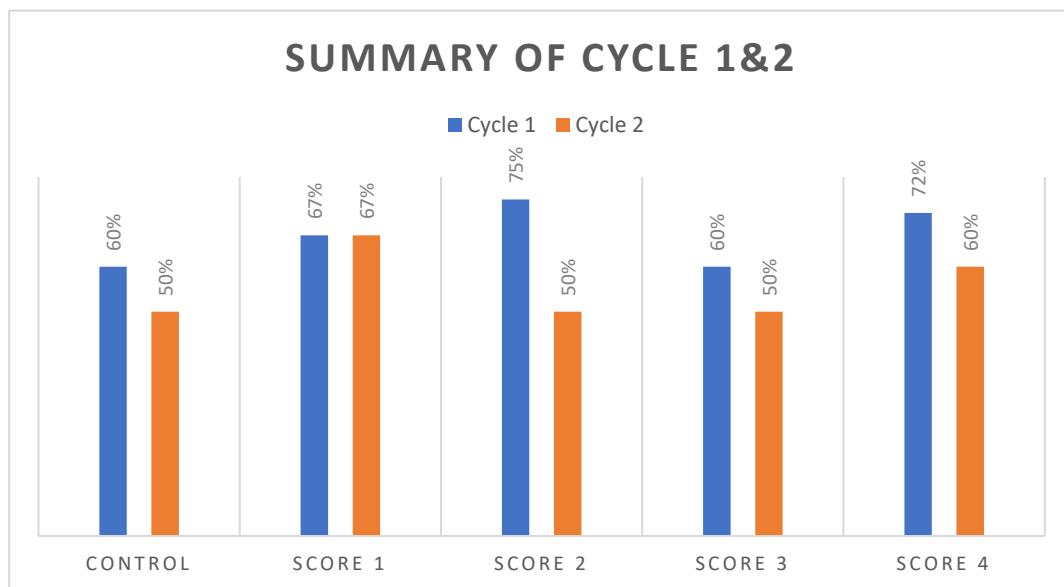


Figure 7.2: Bar charts summary of cycle 1 and 2 results

Statistical analysis was then performed, using stata 15 software, to assess the intra-rater reliability of examiner A between the two cycles using kappa analysis which is illustrated in table 7.6. The intra-rater reliability is defined as the degree of agreement among repeated administrations of a diagnostic test performed by a single rater. According to table 7.2 which shows interpretation of Cohen Kappa values the result in table 7.6 demonstrated next is of moderate agreement.

Agreement	Expected Agreement	Kappa	Standard Error	Z	Prob > Z
77.88%	59.21%	0.4578	0.0976	4.69	0.0000

Table 7.6: Illustrates intra-rater reliability in match of type to specified pattern of markers for examiner A over cycle 1 and 2, measured by Kappa index (Single rater, 52 lesions), Kappa score shows moderate strength of agreement

7.2.2 Exercise 2:

The combined result of the three examiners showed that 48/52 scans correctly fitted the criteria which means 92% of the scans showed that the markers truly resemble the type. ICDAS score 1,2 and 4 showed the most accurate results (100%) followed by ICDAS score 3 and Control (80%) respectively, illustrated in table 7.7.

Type	Control	ICDAS Score 1	ICDAS Score 2	ICDAS Score 3	ICDAS Score 4
Number of lesions scanned	10	3	4	10	25
Fit criteria	8	3	4	8	25
Don't fit criteria	2	0	0	2	0
Percentage	80%	100%	100%	80%	100%

Table 7.7: Illustrates summary of results of exercise 2

7.2.3 Exercise 3:

Table 7.8 below: Illustrates Cohen’s overall Kappa values of assessment of markers between 10 different examiners (inter-rater reliability). (10 different raters, 52 lesions), the overall Kappa is of moderate agreement as highlighted in red

Examiner	Kappa	Z	Prob > Z
Examiner 1	0.2906	4.77	0.0000
Examiner 2	0.8347	10.59	0.0000
Examiner 3	0.1765	2.74	0.0030
Examiner 4	0.4008	5.37	0.0000
Examiner 5	0.7793	10.13	0.0000
Examiner 6	0.2859	3.88	0.0001
Examiner 7	0.3101	4.50	0.0000
Examiner 8	0.7821	10.07	0.0000
Examiner 9	0.5037	6.76	0.0000
Examiner 10	0.2578	3.88	0.0001
Overall	0.4621	5.07	0.0000

Table 7.9 below: Illustrates Cohen’s Kappa values of intra-rater reliability of assessment of markers, Examiner 6 (single rater, 1 week apart; 52 lesions), the strength of agreement of examiner 6 in the second attempt is of substantial agreement in comparison to the first attempt as highlighted in table 7.8 in green as it was fair

Agreement	Expected Agreement	Kappa	Standard Error	Z	Prob > Z
71.15%	24.78%	0.6165	0.0768	8.03	0.0000

Table 7.10 below: Illustrates Cohen’s Kappa values of intra-rater reliability of assessment of markers, Examiner 9 (single rater, 1 week apart; 52 lesions), the strength of agreement of examiner 9 in the second attempt is of moderate agreement which is like the first attempt as highlighted in table 7.8 in blue as it was within moderate range

Agreement	Expected Agreement	Kappa	Standard Error	Z	Prob > Z
57.69%	27.66%	0.4151	0.0734	5.66	0.0000

7.3 Discussion

Dental caries continues to be one of the most prevalent diseases and a significant burden for health systems. Although the importance of management of non-cavitated caries lesions has been recognized since the early 1900s dental caries have been traditionally spotted at the cavitation stage, and their management has focused strongly on operative treatment (Gomez, 2015). Caries lesions pose a challenge to dentists in diagnosing the extent and proximity of the lesion to the dental pulp and thus predicting the long-term prognosis. Over the last 20 years methods of detection of early carious lesions have received significant research attention.

Visual-tactile is the most common method of caries detection. Also, other non-invasive techniques for detection of early caries have been developed and investigated such as QLF, DD, FOTI and Electrical Conductance EC (Cortes et al., 2003). Previous systematic reviews suggested that the diagnosis of early caries lesions might be more accurately achieved in combination of the visual method and the use of other methods such as electrical methods and QLF for monitoring purposes (Gimenez et al., 2013, Gomez et al., 2013). All caries detection methods are subject to errors with less than perfect reliability and validity (Baelum et al., 2012).

It has been stated that a good detection method should be valid and reliable (Nyvad et al., 2008). Within the past years quantitative methods for detecting and monitoring carious lesions have been introduced. Reasons for the development of these methods are to detect earlier carious lesions than conventional methods, quantitative methods more reliable than qualitative methods, and quantitative assessments can monitor the course of the disease (Ten Bosch and Angmar-Månsson, 2000). Radiographic methods have poor sensitivity for occlusal lesions and by the time the lesions are radiolucent they have typically progressed deep into the dentin (Simon et al., 2017). New more sensitive imaging methods are needed to detect occlusal lesions.

In this study A-scans of OCT were extracted from the B-scan images to observe the behaviour of light as it travels through the depth of normal and caries affected enamel. Shimada et al., used OCT for detection of the challenging clinical cases of occlusal caries and reported a superior sensitivity in detection of early caries on occlusal surfaces using OCT over the existing clinical modalities of x-ray imaging and visual/tactile inspection (Shimada et al., 2010). Also, in previous studies (Sarkhouh et al., 2017), and earlier in this study it was found that carious and sound enamel showed different A-scans, which was easily differentiated between. On the other hand, when looking at A-scans of different ICDAS carious lesions, each profile

showed a distinctive behaviour of light scattering, which elevated a question to my interest; “ Can one differentiate the type of caries lesion by only observing the A-scan? ”

7.3.1 Exercise 1

Three examiners studied the scans and empirical markers were extracted for each ICDAS score. Results proved that by using the intensity of back-scattered light, these markers may lead toward a more systematic diagnostic dental application of the technique and by that one can not only differentiate between healthy and affected enamel, but also make diagnosis of different caries lesions easier and less subjective.

The characteristics were as follow; Sound enamel shows a scattering plot with a sharp initial peak followed by gradual smooth decay. For score 1 ICDAS lesion, the scattering plot shows a wide initial peak with delayed decay associated with high noise. Score 2 ICDAS, shows a scattering plot with a very sharp initial peak which comes to baseline very fast. For score 3 ICDAS, the scattering plot shows a very wide delayed steady peak. However, in the case of score 4 ICDAS lesions, the scattering plot showed irregular multiple waves. As caries progress further into enamel and dentine irregular waves appearance predominates the scattering plot as in score 5 and 6 ICDAS. These are illustrated in table 7.1 above. However, these observations are only based on a minor number of lesions (52) and not considered as universal markers.

Statistical analysis using Kappa was then done to investigate the reliability of the OCT markers. The results showed that OCT can distinguish between sound enamel and caries lesions but, and can also distinguish between the different caries lesions by looking at the characteristics and markers. However, these markers are only empirical, which means that they are based on the examiner's observations and assumptions rather than theoretical logic and have never been studied before. Although empirical, the results showed a 77.88% agreement (table 7.6) , with moderate intra-reliability (within same examiner) when compared using Kappa analysis.

Also, based on the data observed in both cycles 1 and 2, results show that the markers truly fit their criteria with a chance of 67% and 56% of them being accurate, respectively. Furthermore, we can draw an assumption that ICDAS score 2 has the most accurate markers, followed by score 4, score 1 and score 3, respectively. Although the score in cycle 2 were lower, they both illustrated the same conclusion. The reduction in results can be explained either as inaccuracy of results or since there has been a month interval between both cycles, so a re-calibration should have been done before attempting the 2nd cycle.

According to the most prominent marker seen in the different scans, one can estimate the type of lesion based on the initial peak, so wide being score 1 and very sharp being score 2. Score 3 is wide peak as score 1 but the peak is steadily delayed. As score 4 is a mixture between score 1,2, and 3 combined. Additionally, score 4 is easily diagnosed clinically as there will be evident loss of tooth structure, however the confusion is usually between score 1,2, and 3 lesions; so, for lesions other than score 4,5 and 6, even if we just look at the initial peak and describe its appearance (sharp/Wide/very sharp), one can diagnose the lesion accurately. Therefore, this can be further studied using a larger sample especially for ICDAS scores 1,2, and 3, to confirm these findings.

Moreover, based on the statistical analysis performed in exercise 1, it shows that the markers extracted, although empirical still show statistical significance in diagnosing the lesion, with high chances ranging from 59.21- 77.88%. The number shows a good prognosis for the sensitivity of this test, as the accuracy of dental diagnostics usually approximate around 40%. Therefore, this can be further studied using a larger sample, and by increasing the number of assessors to increase the sensitivity of these markers to confirm these findings.

7.3.2 Exercise 2

The intension of this exercise was to question the markers by assessing their inter-rater reliability, thus if it showed reliable results it would be taken further and populated into a larger exercise. The results of relating the profile to its lesion, showed that 92% of the scans showed that the markers truly resemble the type, with a total of 48 out of the 52 scans correctly fitting the criteria. ICDAS score 1,2 and 4 showed the most accurate results (100%) followed by ICDAS score 3 and Control (80%) respectively.

7.3.3 Exercise 3

The initial data showed that the markers can be promising in identifying the type of carious lesion based on A-scans, consequently populating these markers into a larger number of scans and examiners was performed to confirm the findings with a larger sample, as the larger the sample, the more accurate the results. To date, despite previous study looking at caries white spot lesions and OCT, this is the first study to consider extracting markers to analyse A-scans of different carious lesions. Moreover, as mentioned previously these markers are considered empirical as they were explored from studying different lesions and looking at different similarities between different examiners, thus these have not been proved or studied previously.

Based on Cohen's Kappa values (table 7.8), the inter-rater reliability results generated in this chapter show an overall moderate strength of agreement (0.41 – 0.60) between the 10 different examiners, and moderate to substantial agreement inter-rater reliability between the 10 different examiners when compared using kappa analysis. This demonstrates that examiners can easily characterise the lesion from observing the initial peak, with a moderate agreement of Kappa. Furthermore, when comparing the intra-rater reliability of assessment of markers for two different examiners (1 week apart), it was shown that rater 6 showed a 71.5% in consistency (table 7.9), while rater 9 scored 57.69% (table 7.10). Thus, again proving the strong agreement, and adding to the conclusion that these markers can be clinically significant.

CHAPTER 8

Progression of Lesion from 2D to 3D Diagnostics

8. Progression of lesion, from 2D to 3D diagnostics

The previous chapters of this thesis were used as building blocks to analyse a 3D image of the different carious lesions i.e. reconstruction of data. Following getting reliable markers from single A-scans of each ICDAS score lesion, it was thought to take this further and understand the lesion of each score by getting A-scans across the complete lesion instead of single one. Which will show the change of A-scans intensity across the carious lesion. This indicates that not just one A-scan can be used to quantify the extent to the lesions, but multiple A-scans can be used. Thus, the whole analysis in this project was based on a single A-scan which showed remarkable results but in fact we need to consider all the A-scans from the waterfall together to draw the bigger picture.

8.1 Methods

8.1.1 Mapping a-scans across the B-scan

In the previous chapter, an empirical A-scan was chosen from all the possible B-scan available. To overcome this restrictive analysis, it was feasible to extract more A-scans out of a single B-scan. To do so, the A-scan window was fixed to a 10-pixel width, and it was possible to effectively record up to 140 a-scans within a B-scan. A series of A-scans windows recorded across a given B scan are illustrated below (figure 8.1). Figure 8.2 illustrates consecutive regions of A-scans taken throughout a B-scan, with their corresponding A-scans .



Figure 8.1: Demonstrating schematic description of the distribution of the regions chosen throughout a B-scan of sample 13 ICDAS score 1, with the yellow boxes resembling a 10-pixel width of scan

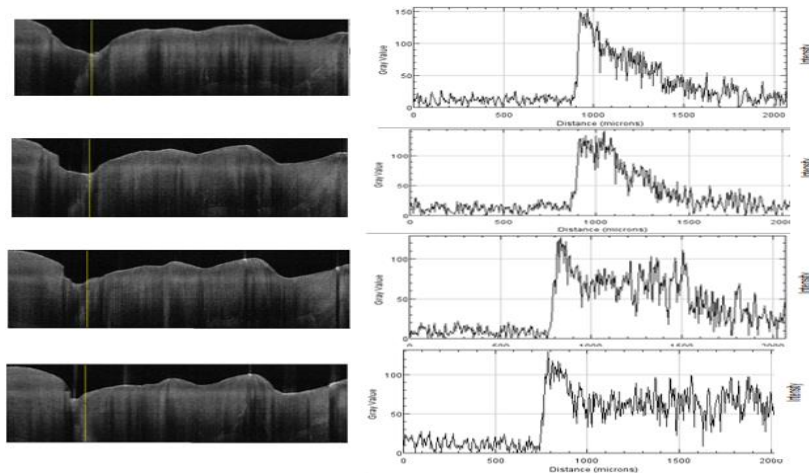


Figure 8.2: Illustrating consecutive regions of A-scans taken throughout a B-scan of sample 13 ICDAS score 1, with their corresponding A-scans

8.1.2 Mapping A-scans across the C-scan

To analyse the evolution of A-scans across a given lesion for ICDAS scores 0 to 4, an example of an A-scan at the centre of ICDAS score 3 lesions was selected. To do so, an A-scan at the centre of lesion was selected in a similar fashion as done in the previous chapter. The location of this A-scan, within its original B-scan (called reference B-scan), was fixed for this approach. Following on this, a series of A-scans were recorded in B-scans, before and after the reference B-scan. Intervals of 10 frames were selected between each B-scan. This allowed us to plot a waterfall series of A-scan using Origin Pro 9.0TM (Origin Lab Corporation, Northampton, MA 01060, USA) as illustrated below in figures 8.4 from the data series displayed below in figure 8.3.

1	X	Y	Y	Y	Y	Y	Y	Y	Y	Y	Y	Y
2	0	9.333	15	6	6.667	10	23.667	6.667	24	18	17	
3	4.53	9.333	20.333	11.667	14.333	19	19.667	4.333	23.333	16	21.333	
4	9.06	5.333	15.333	0	25	20	20	15.333	6.667	17	22	
5	13.59	9.333	17.667	11.333	12.667	12.667	4.667	19.333	19	24	14.667	
6	18.12	10	25.667	9	7.333	13.667	7	17.333	26.333	18.333	10.333	
7	22.65	4.333	20.667	10.333	9.667	9.667	14	18	18.333	16.333	15.333	
8	27.18	6	22.333	13.333	11.667	0	15.667	6	7.667	5.333	13.333	
9	31.71	17.667	21	21.333	14.333	14	6.667	3.667	5.667	7	20.333	
10	36.24	23.333	18	19.333	6	2.667	8.667	10.667	0.667	13.333	16.667	
11	40.77	22.333	38.667	10.667	8.667	2.333	11.333	1.667	16.333	19	1.333	
12	45.3	13.667	40.333	3.333	15.333	5.667	12	3.333	21.667	27.333	4.667	
13	49.83	9.667	12.333	19.333	11.333	13	12.667	0	22.333	11	22	
14	54.36	12	11	9.667	7	8.333	12.333	2.667	26	7	12.333	
15	58.89	15.667	31	14.667	17.333	10.667	7.667	6.667	24	11.333	5.333	
16	63.42	17	27.667	16	19.667	5.333	8.333	10.333	19.667	12.667	9	
17	67.95	17.333	27.667	0	17	8.667	18.333	2.333	0	3.333	10	
18	72.48	14.333	22.333	7.667	17.667	23.667	11.667	16.333	7.667	10.333	7	
19	77.01	11	28	4	3.333	13.667	0	15.667	5.333	6.333	15.333	
20	81.54	7	16	2	14	3	1.333	13	14.667	2.333	9.667	

Figure 8.3: showing how the data was fed to excel origin, with the a-axis being as a constant, and consequently adding the y-axis data for ICDAS score 3 sample

8.2 Results

Figure 8.4 illustrates stacks of A-scans across a selected lesion of ICDAS score 3 sample where regions of interests were extracted from the initial B-scan of the lesion with intervals of 10 frames each time. When the data were fed into Origin lab software a waterfall plot was formed within 20 seconds which represented the observed marker which was described earlier in the previous chapters when score 3 A-scan was studied. The waterfall plot confirms the characteristic of score 3 as in wide delayed steady peaks as if we extract any line from A-scan stacks we will see the exact representation of marker.

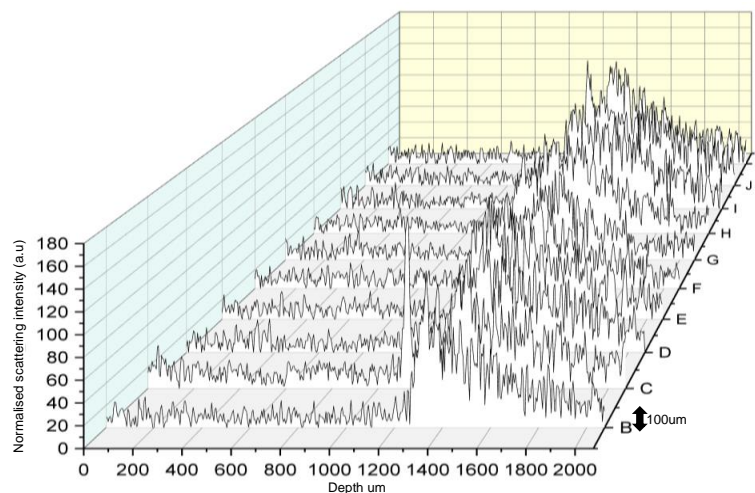


Figure 8.4: Illustrating A-scan waterfall plot (stacks of A-scans) across an ICDAS score 3 sample

8.3 Discussion

8.3.1 From building blocks to a whole image – cross-sectional analysis

Reconstruction of scans from a 2-Dimension perspective to a 3-Dimension facilitated interpretation of data, to understand exactly what is going on in a lesion instead of studying a single A-scan, from an arbitrary region. Data from the waterfall graph demonstrated previously was more accessible, illustrating more structural details and has made reading more sophisticated.

A waterfall plots illustrated in figure 8.4 is a three-dimensional plot in which multiple curves of data are displayed at the same time. Characteristically, the curves are staggered both across the screen and vertically, with 'nearer' curves masking the ones behind. The result is a series of mountain shapes that appear to be side by side. It is often used to show how 2-Dimensional information changes, or how lesions progress into structures; it is useful in comparing several two-Dimensional plots.

When composing waterfalls in general, the horizontal axis is considered a baseline measure (depth in enamel), and the bars may go either above or below the baseline, depending on the depth. On the other hand, the y-axis is the backscattering of light from the tooth structure; therefore, if there is a change in refractive index, the more it scatters thus the higher the peak, while if a loss of tooth structure is evident it will have less backscattering thus lower multiple irregular peaks of waves.

In the beginning of the project, a random region of interest from different B-scans of ICDAS scores 1-6 were chosen to represent the lesion. Despite ensuring that the region chosen was free from any cracks/fractures or an increased reflectivity, some bias can be found. Hence, when examining a lesion in a whole, all areas which are relevant, i.e. tooth structure and lesion of interest, and irrelevant, such as; air, curvature of tooth, can be scanned and compared to remove any sources of confounding. The single A-scans (1D) were used as building blocks to build a larger picture, like the concept of magnetic resonance imaging (MRI).

Therefore, we are trying to reinforce the point that one A-scan may not be able to represent a whole lesion, so consecutively we have moved to scanning across a lesion, and then with every 10-pixel width= 45um, we move and plot a new a-scan, to observe how the A-scan varies as we move across the lesion. From that we can noticed that as we go further across the lesion it shows as it is much more affected confirming the observed markers of each score. In addition, in some lesions, different ICDAS scores markers can be found as going deeper into a lesion, which cannot be diagnosed clinically or using plain 2-Dimension radiographs, hence we are not getting total information of the lesion or can be looked in a different way as this can be the source of subjectivity as a clinician might diagnose a lesion as a score 3 ICDAS while another might see it as a score 4, leading to difference in diagnosis.

To take this further and look at all A-scans present in a single B-scan, is not feasible by an individual. For example, when looking at a single B-scan of 6mm x 6mm, it is composed of 600 frames, and from each frame an A-scan can be produced. Also, a single A-scan is composed of 1400 pixels, so we can generate 140 different A-scans of 10-pixel width each. Hence, a single lesion can give us $600 \times 140 = 84,000$ a-scans.

Therefore, looking at a single scan, from a random region of interest to study a whole lesion will not give us a full description of the lesion, and we can miss areas of interest. However, when considering studying all lesions in a full view, considering we have 180 lesions, this equals to $600 \times 140 \times 180 = 15,120,000$; which is a very large number of scans, and is not feasible to study by hand. Consequently, this can be a starting step for further research, to populate the markers, program the generation of scans and thus put them together to have the diagnosis done in an automated way, moving towards reconstruction of volumetric data.

8.3.2 Clinical need for 3-Dimension volumetric data

Optical coherence tomography is a promising non-invasive optical imaging modality capable of providing 3-dimensional sub-surface morphology of biological tissue microstructure with micron-scale resolution (Hsieh et al., 2013). In OCT, the distance between optical reflections from different layers of tissue is measured through interferometry by retrieving the time delay of the light reflected from optical interfaces A-scan through Fourier transformation. A series of A-scans along a line on sample surface creates cross-sectional or B-scan images, while scanning the sample surface in two dimensions provides volumetric data. The 3-Dimensional volumetric data (figure 8.5) generate clinically accurate and immediately available images from the full data set without editing. Also, it allows the clinician to address specific concerns or questions that a patient have by interactively exploring different aspect of the data set. Moreover, it facilitates incorporation of the patients with their treatment plan, as a 3-Dimension image is often easier for patients to understand the picture, as its generated by integrating a series of sections into a form that is often easier to interpret than the sections alone. Carious lesions have been studied before in a 3-Dimension, showing good results.

In 1981 Lujik , mentioned the idea of diagnosing dental caries using MRI. Van Lujik suggested that using 3-D will help in the future to enable detecting caries below a restoration that cannot be easily seen on a conventional dental radiograph (Van Lujik, J.A., 1981). Also, Dhillon et al. used cross polarization optical coherence tomography (CP-OCT) to assess the initial depth of root caries lesions before removal and the volume of sound and demineralized tissue removed by the laser, where they have achieved highly selective lesion removal and minimal damage to surrounding sound tissues (Dhillon et al., 2019). Volumetric data for caries diagnosis advantages are; 3-Dimension of carious lesion visualisation and quantification. Therefore, determination and monitoring proximity of the lesion in relation to the pulp, also proximity and efficiency of restorations margins (Tymofiyeva, O., et al., 2009).

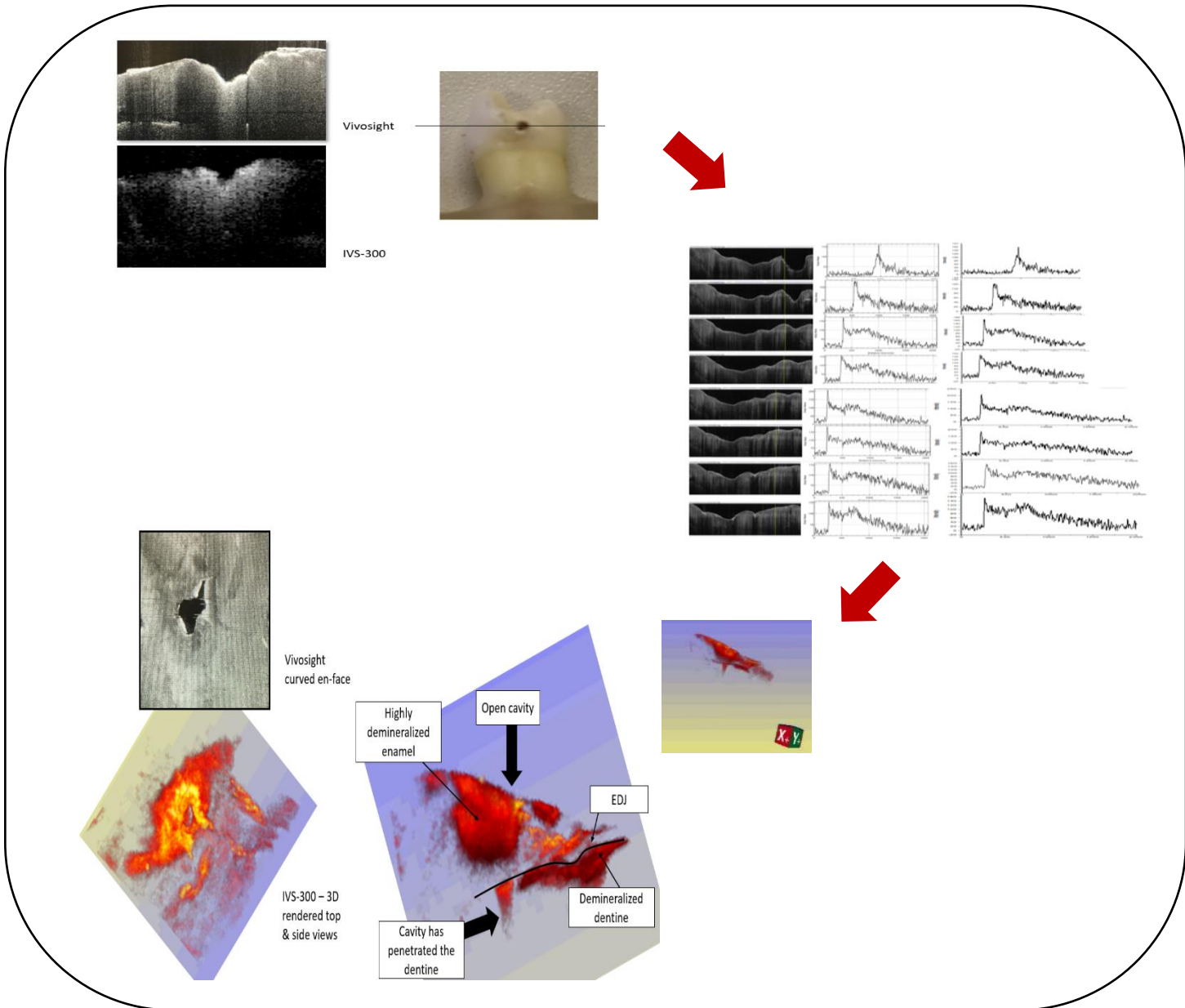


Figure 8.5: Demonstrate presentation of carious lesion from building block to a whole 3D volumetric image via IVS-300, 3D image courtesy of Dr Bozec; <https://www.santec.com/en/products/oct/ivs-300>

CHAPTER 9

Clinical Relevance

9 Clinical Relevance

9.1 Clinical relevance of caries and OCT

Dental caries is considered one of the most common oral diseases, affecting 60 – 90% of school children worldwide (Petersen, 2003). Early detection and treatment of incipient caries is important to prevent pain and further enamel destruction. Currently there is no universal diagnostic tool that can be used to detect carious lesions at the very early stages. In this project, the aim was to evaluate Optical Coherence tomography and to understand its light response to enamel changes so a better clinical diagnostic tool can be developed to identify early changes in enamel structure when it is affected by caries.

The use of OCT in clinical medicine has shown that the device is a helpful technique in clinical diagnostics. OCT is currently used widely in many medical fields since the 1990s; dermatology, endoscopy and ophthalmology. In dentistry the main use of OCT has been in dental research such as; in vitro demineralisation, remineralisation, and erosion (Jones et al., 2006, Manesh et al., 2009) is to highlight the effect of these processes on dental hard tissues. OCT has not been investigated for its potential clinical use especially for clinically diagnosing dental diseases. Owing to the ability of OCT in providing high-resolution 3-dimensional images, OCT has recently gained popularity in Dentistry research for diagnosis and screening of dental diseases and oral cancer (Fried et al., 2002).

None of the previous studies done on OCT have evaluated markers to each carious lesion, to help diagnose and monitor caries progression. OCT is proven to be safe as it is considered as a non-ionising, nor destructing technique as teeth will be examined without exposing the patient to radiation hazard. It is a simple technique that does not consume a long time to investigate enamel structure and it can be used at the chair side with real time imaging of the teeth. Though, this can only be applicable if further researches are done to compose a compatible device that can be used intra-orally, as this research is considered as a building block to build a bigger picture.

Employing OCT in clinical setting will aid in early diagnosis of dental conditions at the same time as conventional clinical examination, which would draw full information about the lesion, with minimal time. Consequently, this will help in early intervention and reversing demineralisation process. Also, having a 3-D real time image on a screen in front of the patient, helps in making more comprehensive and thorough treatment plan. The prognosis of the affected teeth can also be detected at the same time. OCT does not require a large space in the dental unit and it can fit into the dental practice easily.

Also, OCT might have a great relevance in monitoring the remineralisation and demineralisation process in vivo. In addition, it can be used to assess the efficiency of restorations and margins. Our findings in this project are important in that they open the door for such technique to be implemented into the dental field for better diagnosis and treatment.

9.2 Limitations

The sample size was one of the limitations in this project. This is because of the difficulty in obtaining score 1,2 and 3 ICDAS as these lesions are not considered an indication for teeth extraction, which means that the collection of samples was also limited. In the future, increasing the number of samples is required to confirm the observed findings and to confirm that OCT can diagnose and monitor the changes in mineral density that occurs in carious lesions.

Moreover, it is important to highlight that OCT has its limitations, thus it may not totally replace the current diagnostic tools but be added as an adjunct. The size of the current OCT probe used in this project is too big and not convenient and was not made to be used for intra-oral examination. There has been a dermatological probe implemented, which could be used on the anterior teeth only, however it is too bulky thus would be difficult to be used posteriorly, especially in small mouths like children consequently developing a smaller movable OCT probe is important to be used in the clinical set-up.

Also, OCT scan can only penetrate 2mm in depth, thus it cannot scan deeper than 2mm into the tooth structure, limiting it to enamel. Another limitation is the fact that intra-orally, the buccal and lingual/palatal surfaces are accessible for imaging whereas the mesial and distal interproximal surfaces are difficult to access. This fact is important to consider and if these surfaces are involved the use of radiographic image is inevitable. Though, imaging the occlusal surfaces is complicated by its topography. Lastly, the cost of the device, as it is considered expensive compared to other current diagnostic tools, with an average 100,000 pounds.

CHAPTER 10

Future work

10. Future work

With the current results from OCT, the next step of this project will be to continue to understand caries by studying more lesions clinically, radiographically and with OCT in a large population study. In addition, investigating the ultra-structure of enamel and compare it to carious enamel to understand the observed signal intensity profiles described in previous chapters, and why they behave differently. Consequently, using the markers extracted and studying these markers in a larger sample, with more calibration to examiners and implementing more statistics to prove these markers as diagnostic.

Moreover, batch process the data analysis to minimise and remove the human bias in selecting a specific scan region, by comparing more markers and computerising it. Also, automating waterfalls A-scans which will show the change of A-scans intensity across the carious lesion. Accordingly, indicates that not just one A-scan can be used to quantify the extent to the lesions, but multiple A-scans can be used. Thus, the whole analysis in my thesis was based on a single A-scan which was good but in fact we need to consider ALL the A-scans from the waterfall together.

Going one step further in the use of OCT in clinical field of dentistry by designing an intra-oral OCT scanning probe in a suitable size which is convenient for both the patient and the clinician. The design could be the same as that of a light curing machine used in curing composite filling material, or as that of an intra-oral camera or fibre-optic trans-illuminator, which can be easily carried and used inside the oral cavity. This step will lead to another important one, which is the use of this technique in clinical trials.

Until an intra-oral probe is available, caries in the anterior teeth could be investigated which are accessible to be scanned by the current probe. However, this scanner is large and difficult to manipulate in the clinical set-up. This advancement in OCT would help diagnose caries affected teeth at the chairside in an objective, non-ionising, real time scan, with a 3-D demonstration of the tooth and lesion, which can be easily interpreted by patients.

The future potential use of OCT is to monitor dental restorations such as; fillings, veneers and implants. In addition, it can be used as an adjunct in diagnosing dental anomalies such as MIH. Also, it can be used in monitoring dental plaque level on tooth surfaces as well as erosion which have been looked at previously by researchers using OCT. As OCT scanner is used to diagnose and monitor inflammatory and bulbous dermatological conditions, it can be used to diagnose these conditions in oral medicine. Oral cancerous and precancerous conditions can also be diagnosed using OCT.

CHAPTER 11

Conclusion

11. Conclusion

In conclusion, there is a need for new diagnostic imaging modalities which can give more information on the structure and extent of the dental caries, and does not involve ionising radiation. OCT was investigated in this research project, as it is a non-invasive diagnostic technique providing cross-sectional images of biologic structures based on the differences in tissue optical properties. OCT has several potential applications in dentistry. It has been proved to be safe and useful diagnostic tool when studying carious lesions, as it can detect the early changes that occur in the enamel structure at the early carious process.

Also, it is possible to obtain real-time images with excellent axial resolution. OCT was found to show a full understanding of the more advanced subsurface lesions as well with its depth and extent, in a 3-dimensional good clarity image that is not found in conventional methods. This helps in predicting the lesion's long-term prognosis; moreover, it helps in differentiating not only amongst carious and sound enamel of teeth, but also even between different ICDAS scores lesions, in a non-destructive, nor objective and real time method.

When caries affected teeth, surfaces were imaged using OCT, each lesion of the ICDAS scores interacted distinctively with the incident light. The variations observed in the back-scattered light in OCT experiment were because of mineral density variation within enamel structure as well as the changes in prismatic structures when caries progress. The definition of specific scattering markers for each ICDAS score of carious lesions that was carried will enable us to bring this technique one-step closer to the clinic. Also, the 3D visualization of lesions enables quantification of parameters such as lesion depth and volume which is highly desired in the field of Dentistry. The main limitations for clinical use of OCT in dentistry are high cost, probe size, and lack of commercial availability.

CHAPTER 12

Scientific Dissemination

12 Scientific Dissemination

12.1 Poster Presentations

12.1.1 Poster presentation at the International Association of Dental Research (IADR) in London, United Kingdom in July 2018 (Appendix 7)

Title: The Use of Optical Coherence Tomography as a Diagnostic Tool for Dental Caries

12.1.2 Poster presentation at the International Association of Paediatric Dentistry (IAPD) in Cancun, Mexico in July 2019 (Appendix 8)

Title: The Use of Optical Coherence Tomography as a Diagnostic Tool for Dental Caries

CHAPTER 13

References

13 References

Amaechi, B.T., Podoleanu, A.G., Komarov, G., Higham, S.M. and Jackson, D.A., 2004. Quantification of root caries using optical coherence tomography and microradiography: a correlational study. *Oral health & preventive dentistry*, 2(4).

Attrill, D. and Ashley, P., 2001. Occlusal caries detection in primary teeth: a comparison of DIAGNOdent with conventional methods. *British Dental Journal*, 190(8), p.440.

Azevedo, C.S.D., Trung, L.C.E., Simionato, M.R.L., Freitas, A.Z.D. and MATOS, A.B., 2011. Evaluation of caries-affected dentin with optical coherence tomography. *Brazilian oral research*, 25(5), pp.407-413.

Bader, J.D. and Shugars, D.A., 2004. A systematic review of the performance of a laser fluorescence device for detecting caries. *The Journal of the American Dental Association*, 135(10), pp.1413-1426.

Bader, J.D., Shugars, D.A. and Bonito, A.J., 2001. Systematic reviews of selected dental caries diagnostic and management methods. *Journal of Dental Education*, 65(10), pp.960-968.

Baelum V, Hintze H, Wenzel A, Danielsen B, Nyvad B. Implications of caries diagnostic strategies for clinical management decisions. *Community Dentistry and Oral Epidemiology*. 2012;40(3):257–266.

Banerjee, A., and Domejean S. (2013). *The contemporary approach to tooth preservation: minimum Intervention (MI) caries management in general dental practice*. *Primary Dental Journal*, 2(3), 30-37.

Baumgartner, A., Dichtll, S., Hitzenberger, C.K., Sattmann, H., Robl, B., Moritz, A., Fercher, A.F. and Sperr, W., 2000. Polarization-sensitive optical coherence tomography of dental structures. *Caries research*, 34(1),pp.59-69.

Beighton, D., Adamson, A., & Rugg-Gunn, A. (1996). Associations between dietary intake, dental caries experience and salivary bacterial levels in 12-year-old English schoolchildren. *Archives of Oral Biology*, 41(3), 271-280.

Besic, F. C. and Wiemann, M. R. 1972. DISPERSION STAINING, DISPERSION, AND REFRACTIVE INDEXES IN EARLY ENAMEL CARIES. *Journal of Dental Research*,51, 973-974.

Bjørndal L, Ricucci D. 2014. Pulp inflammation: from the reversible inflammation to pulp necrosis during caries progression. In: Goldberg Michel, editor. The dental pulp biology, pathology, and regenerative therapies. Berlin (Germany): Springer. p. 125–139.

Bourquin, S., Aguirre, A.D., Hartl, I., Hsiung, P., KO, T.H., Fujimoto, J.G., Birks, T.A., Wadsworth, W.J., Bunting, U. and Kopf, D., 2003. Ultrahigh resolution real time OCT imaging using a compact femtosecond Nd:Glass laser and nonlinear fiber. *Optics express*, 11(24), pp.3290-3297.

Caufield, P., Li, Y. and Bromage, T. (2012). Hypoplasia-associated Severe Early Childhood Caries – A Proposed Definition. *Journal of Dental Research*, 91(6), pp.544-550.

Child Dental Health Survey. 2013. Health and Social Care Information Centre for England, Wales, and Northern Ireland. Retrieved Online 12 August 2017 from: <http://content.digital.nhs.uk/catalogue/PUB17137>

Choma, M.A., Sarunic, M.V., Yang, C. and Izatt, J.A., 2003. Sensitivity advantage of swept source and Fourier domain optical coherence tomography. *Optics express*, 11(18), pp.2183-2189.

Cortes DF, Ellwood RP, Ekstrand KR. An in vitro comparison of a combined FOTI/visual examination of occlusal caries with other caries diagnostic methods and the effect of stain on their diagnostic performance. *Caries research*. 2003;37(1):8–16.

Daly, L. and Bourke, G.J., 2008. Interpretation and uses of medical statistics. John Wiley and Sons.

Darling, C. L., Huynh, G. D. and Fried, D. 2006. Light scattering properties of natural and artificially demineralized dental enamel at 1310nm. *Journal of biomedical optics*, 11.

Dhillon, N., Chan, K. H., Yang, V. B., & Fried, D. (2019). Image guided laser ablation of demineralization from root surfaces. *Proceedings of SPIE--the International Society for Optical Engineering*, 10857, 108570N.

Edgar, M., Dawes, C., O'Mullane, D. 2004. Saliva and Oral Health. 3rd ed. British Dental Association, London.

Ekstrand, K., Qvist, V. and Thylstrup, A. 1987. Light microscope study of the effect of probing in occlusal surfaces. *Caries research*, 21, 368-374.

Ekstrand, K., Ricketts, D. and Kidd, E. 1997. Reproducibility and accuracy of three methods for assessment of demineralization depth on the occlusal surface: an in vitro examination. *Caries research*, 31, 224-231.

FDI. (1992). A review of developmental defects of enamel (DDE) index. Commission on Oral Health, Research & Epidemiology. Report of a Federation Dentaire Internationale Working Group. *Int Dent J* 42:411-426.

Fejerskov, O., 1997. Concepts of dental caries and their consequences for understanding the disease. *Community dentistry and oral epidemiology*, 25(1), pp.5-12.

Fejerskov, O. and Thylstrup, A. Textbook of Clinical Cariology. Copenhagen: Munksgaard.(2nd ed) 1994:209–17.

Feldchtein, F.I., Gelikonov, G.V., Gelikonov, V.M., Iksanov, R.R., Kuranov, R.V., Sergeev, A.M., Gladkova, N.D., Ourutina, M.N., Warren, J.A. and Reitze, D.H., 1998. In vivo OCT imaging of hard and soft tissue of the oral cavity. *Optics express*, 3(6), pp.239-250.

Fercher, A.F., Hitzengerger, C. and Juchem, M., 1993. Measurement of intraocular optical distances using partially coherent laser light. *Journal of Modern Optics*, 38(7), pp.1327-1333.

Fercher, A. and Roth, E. 1986. Ophthalmic Laser Interferometry. *Proc SPIE*, 658, 48–51.

Fercher, A.F., 2010. Optical coherence tomography–development, principles, applications. *Zeitschrift für Medizinische Physik*, 20(4), pp.251-276.

Fercher, A. F., Drexler, W., Hitzengerger, C. K. and Lasser, T. 2003. Optical coherence tomography-principles and applications. *Reports on progress in physics*, 66, 239.

Francescut, P., Zimmerli, B. and Lussi, A. 2006. Influence of different storage methods on laser fluorescence values: a two-year study. *Caries research*, 40, 181-185.

Fried, D., Xie, J., Shafi, S., Featherstone, J.D., Breunig, T.M. and Le, C.,2002. Imaging caries lesions and lesion progression with polarization sensitive optical coherence tomography. *Journal of biomedical optics*, 7(4), pp.618-627.

Giannopoulou, C., Dudic, A. and Kiliaridis, S., 2006. Pain discomfort and crevicular fluid changes induced by orthodontic elastic separators in children. *The Journal of Pain*, 7(5), pp.367-376.

Gimenez T, Braga MM, Raggio DP, Deery C, Ricketts DN, Mendes FM. Fluorescence-based methods for detecting caries lesions: systematic review, meta-analysis and sources of heterogeneity. *PloS one*. 2013;8(4):e60421.

Gomez J. Detection and diagnosis of the early caries lesion. *BMC Oral Health*. 2015;Suppl 1:S3.

Gomez J, Tellez M, Pretty IA, Ellwood RP, Ismail AI. Non-cavitated carious lesions detection methods: a systematic review. *Community Dent Oral Epidemiol*. 2013;41:54–66.

Hariri, I., Sadr, A., Nakashima, S., Shimada, Y., Tagami, J. and Sumi, Y. 2012a. Estimation of the enamel and dentin mineral content from the refractive index. *Caries research*, 47, 18-26.

Hariri, I., Sadr, A., Shimada, Y., Tagami, J. and Sumi, Y. 2012b. Effects of structural orientation of enamel and dentine on light attenuation and local refractive index: an optical coherence tomography study. *Journal of dentistry*,40, 387-396.

Hartl, I., Li, X., Chudoba, C., Ghanta, R., Ko, T., Fujimoto, J., Ranka, J. and Windeler, R. 2001. Ultrahigh-resolution optical coherence tomography using continuum generation in an air–silica microstructure optical fiber. *Optics letters*, 26, 608-610.

Haruna, M., Ohmi, M., Mitsuyama, T., Tajiri, H., Maruyama, H. Hashimoto, M. 1998. Simultaneous measurement of the phase and group indices and the thickness of transparent plates by low-coherence interferometry. *Optics letters*, 23, 966-968.

Hee, M. R., Swanson, E. A., Fujimoto, J. G. and Huang, D. 1992. Polarizationsensitive low-coherence reflectometer for birefringence characterization and ranging. *JOSA B*, 9, 903-908.

Heinrich-Weltzien, R., Kuhnisch, J., Van der veen, M., De josselin D., Jong, E. and Stober, L., 2003. Quantitative light-induced fluorescence (QLF)--a potential method for the dental practitioner. *Quintessence international*, 34(3).

Hill, M. J. and Marsh, P. D. (1990). Factors controlling the Microflora of the Healthy Mouth. In M.J. Hill & P.D. Marsh (Eds.) *Human Microbial Ecology (1st Ed)* (pp. 2- 47). Boca Raton, Florida: CRC Press.

Hsieh, Y.-S., Ho, Y.-C., Lee, S.-Y., Lu, C.-W., Jiang, C.-P., Chuang, C.-C., Wang, C.-Y. and Sun, C.-W. 2011. Subgingival calculus imaging based on swept-source optical coherence tomography. *Journal of biomedical optics*, 16.

Hsieh, Y.-S. Y.-C. Ho, S.-Y. Lee, C.-C. Chuang, J. C. Tsai, K.-F. Lin, and C.-W. Sun, "Dental optical coherence tomography," *Sensors (Basel)* 13(7), 8928–8949 (2013).

Huang, D., Swanson, E. A., Lin, C. P., Schuman, J. S., Stinson, W. G., Chang, W., Hee, M. R., Flotte, T., Gregory, K. and Puliafito, C. A.1991. Optical coherence tomography. *Science (New York, NY)*, 254, 1178.

ICDAS Foundation: International Caries Detection and Assessment System.2014.Retrieved online from; www.icdas.org

International Commission on Radiological Protection. 2008. Radiological Protection in Medicine Annals of the ICRP 2008. Publication 105.

Ismail, A., Sohn, W., Tellez, M., Amaya, A., Sen, A., Hasson, H. and Pitts, N. 2007. The International Caries Detection and Assessment System (ICDAS): an integrated system for measuring dental caries. *Community dentistry and oral epidemiology*, 35, 170-178.

Jones, R., Darling, C., Featherstone, J. and Fried, D. 2006a. Imaging artificial caries on the occlusal surfaces with polarization-sensitive optical coherence tomography. *Caries research*, 40, 81-89

Jones, R.S., Darling, C.L., Featherstone, J.D. and Fried, D., 2006b. Remineralization of in vitro dental caries assessed with polarization-sensitive optical coherence tomography. *Journal of biomedical optics*, 11(1).

Kidd, E.A.M. and Fejerskov, O., 2004. What constitutes dental caries Histopathology of carious enamel and dentin related to the action of cariogenic biofilms. *Journal of dental research*, 83(1_suppl), pp.35-38.

Kienle, A., Michelsl, R. and Hibstl, R. 2006. Magnification—a new look at a long known optical property of dentin. *Journal of dental research*, 85, 955-959.

Knüttel, A., Bonev, S. and Knaak, W. 2004. New method for evaluation of in vivo scattering and refractive index properties obtained with optical coherence tomography. *Journal of Biomedical Optics*, 9, 265-273.

Koch, P., Huttmann, G., Schleiermacher, H., Eichholz, J. and Koch, E. 2004. Linear optical coherence tomography system with a down converted fringe pattern. *Optics letters*, 29, 1644-1646.

Kuhnisch, J., Iffland, S., Tranaeus, S., Hickel, R., Stosser, L. and Heinrich-weltzien, R. 2007. In vivo detection of non-cavitated caries lesions on occlusal surfaces by visual inspection and quantitative light-induced fluorescence. *Acta Odontologica Scandinavica*, 65, 183-188.

Loesche, W. J. (1976). *Chemotherapy of dental plaque infections*. *Oral Sci Rev*, 9: 65-107.

Maia, A., Fonseca, D. D., Kyotoku, B. B. and Gomes, A. S. 2010. Characterization of enamel in primary teeth by optical coherence tomography for assessment of dental caries. *International Journal of Paediatric Dentistry*, 20, 158-164.

Manesh, S. K., Darling, C. L. and Fried, D. 2009. Polarization-sensitive optical coherence tomography for the non-destructive assessment of the remineralization of dentin. *Journal of biomedical optics*, 14, 044002-044002-6.

Manji F, Fejerskov O, Nagelkerke NJ, Baelum V. Community Dent Oral Epidemiol. 1991 Dec;19(6):324-8.

Marsh, P. D. and Nyvad, P. D. B. (2008). The oral microflora and biofilms on teeth. In O. Fejerskov and E. Kidd (Eds.). *Dental Caries: The Disease and its Clinical Management* (2nd Ed). Oxford: Blackwell Munksgaard Ltd.

Marsh, P. D. and Martin, M. V. (1999). *Oral Microbiology* (4th Ed)(p.1-2). Woburn, Massachusetts, U.S.A.: Butterworth-Heinemann Medical.

Mccomb. 2000. Caries-detector dyes-how accurate and useful are they? *J Can Dent Assoc*, 66, 195-8.

McHugh, M.L., 2012. Interrater reliability: the kappa statistic. *Biochemia medica: Biochemia medica*, 22(3), pp.276-282.

Meng, Z., Yao, X.S., Yao, H., Liang, Y., Liu, T., Li, Y., Wang, G. and Lan, S.,2009. Measurement of the refractive index of human teeth by optical coherence tomography. *Journal of biomedical optics*, 14(3).

Moynihan, P. J., & Kelly, S. A. M. (2014). Effect on caries of restricting sugars intake: systematic review to inform WHO guidelines. *Journal of dental research*,93(1), 8-18.

Nokhbatolfoghahaie, H., Alikhasi, M., Chiniforush, N., Khoei, F., Safavi, N., and Zadeh B. Y.(2013). Evaluation of accuracy of DIAGNOdent in diagnosis of primary and secondary caries in comparison to conventional methods. *Journal of lasers in medical sciences*, 4(4), 159.

Nyvad, B and Fejerskov, O.1997. Assessing the stage of caries lesion activity on the basis of clinical and microbiological examination. *J Community Dent Oral Epidemiol*. 1997 Feb;25(1):69-75.

Nyvad B, Fejerskov O, Baelum V. In: Dental Caries: The disease and its clinical management. Fejerskov O, Kidd, E, editor. Blackwell Munksgaard; 2008. Visual-tactile caries diagnosis; pp. 49–69.

Oancea Roxana, Adrian Bradu, Cosmin Sinescu, Radu Marcel Negru, Meda Lavinia Negrutiu, Iulian Antoniac, Virgil-Florin Duma & Adrian Gh. Podoleanu (2015) Assessment of the seal-ant/tooth interface using optical coherence tomography, *Journal of Adhesion Science and Technology*, 29:1, 49-58.

Ohmi, M., Ohnishi, Y., Yoden, K. and Haruna, M. 2000. In vitro simultaneous measurement of refractive index and thickness of biological tissue by the low coherence interferometry. *IEEE transactions on biomedical engineering*, 47,1266-1270.

Otlis, L. L., Everett, M. J., Sathyam, U. S. Colston, B. W. 2000. Optical coherence tomography: A new imaging: Technology for dentistry. *The Journal of the American Dental Association*, 131, 511-514.

Petersen, P. E. 2003. The World Oral Health Report 2003: continuous improvement of oral health in the 21st century—the approach of the WHO Global Oral Health Programme. *Community Dentistry and oral epidemiology*, 31, 3-24.

Pitts, N.B. and Stamm, J.W., 2004. International Consensus Workshop on Caries Clinical Trials (ICW-CCT)—final consensus statements: agreeing where the evidence leads. *Journal of Dental Research*, 83(1_suppl), pp.125-128.

Povazay, B., Bizheva, K., Unterhuber, A., Hermann, B., Sattmann, H., Fercher, A. F., Drexler, W., Apolonski, A., Wadsworth, W. and Knight, J. 2002. Submicrometer axial resolution optical coherence tomography. *Optics letters*, 27, 1800-1802.

Pretty, I. A. 2006. Caries detection and diagnosis: novel technologies. *Journal of dentistry*, 34, 727-739.

Ribeiro, D. A. 2012. Cytogenetic biomonitoring in oral mucosa cells following dental X-ray. *Dento-maxillo-facial radiology*, 41, 181-4.

Public health epidemiology programme. 2013. Oral health survey of three-year-old children. Retrieved Online 12 August 2017 from; <http://www.nwph.net/dentalhealth/reports/DPHEP%20for%20England%20OH%20Survey%203yr%202013%20Report.pdf>

Public health epidemiology. 2015. National Dental Epidemiology Programme for England: oral health survey of five-year-old children 2015 A report on the prevalence and severity of dental decay. Retrieved Online 12 August 2017 from: http://www.nwph.net/dentalhealth/14_15_5yearold/14_15_16/DPHEP%20for%20England%20OH%20Survey%205yr%202015%20Report%20FINAL%20Gateway%20approved.pdf

Sabel, N, Johansson, C, Kuhnisch, J, Robertson, A, Steiniger, F, Noren, JG. (2008). Neonatal lines in the enamel of primary teeth—a morphological and scanning electron microscopic investigation. *Arch Oral Biol* 53:954-963.

Sarkhouh, S., Parekh, S. and Bozec, L., Investigating the ultrastructure of enamel white spot lesions (WSL) using Optical Coherence Tomography at different length scales. 2017; p 62-64.

Selwitz, R. H., Ismail, A. I., & Pitts, N. B. (2007). Dental caries. *The Lancet*, 369(9555), 51-59.

Schwendicke, F., Frencken, J., Bjørndal, L., Maltz, M., Manton, D., Ricketts, D., Van Landuyt, K., Banerjee, A., Campus, G., Doméjean, S., Fontana, M., Leal, S., Lo, E., Machiulskiene, V., Schulte, A., Splieth, C., Zandona, A. and Innes, N. (2016). Managing Carious Lesions. *Advances in Dental Research*, 28(2), pp.58-67.

Sergeev, A. M., Gelikonov, V. M., Gelikonov, G. V., Feldchtein, F. I., Kuranov, R.V., Gladkova, N. D., Shakhova, N. M., Snopova, L. B., Shakhov, A. V., Kuznetzova, I. A., Denisenko, A. N., Pochinko, V. V., Chumakov, Y. P. Streltzova, O. S. 1997. In vivo endoscopic OCT imaging of precancer and cancer states of human mucosa. *Optics Express*, 1, 432-440.

Seow, WK, Young, WG, Tsang, AK, Daley, T (2005). A study of primary dental Enamel from preterm and full-term children using light and scanning electron microscopy. *Pediatr Dent* 27:374-379.

Shi, X.-Q., Tranaeus, S. and Angmar-mansson, B. 2001. Validation of DIAGNOdent for quantification of smooth-surface caries: an in vitro study. *Acta Odontologica Scandinavica*, 59, 74-78.

Shimada, Y. A. Sadr, M. F. Burrow, J. Tagami, N. Ozawa, and Y. Sumi, "Validation of swept-source optical coherence tomography (SS-OCT) for the diagnosis of occlusal caries," *J. Dent.* 38(8), 655–665 (2010).

Simon J. C., H. Kang, M. Staninec, A. T. Jang, K. H. Chan, C. L. Darling, R. C. Lee, and D. Fried, "Near-IR and CP-OCT imaging of suspected occlusal caries lesions," *Lasers Surg. Med.* 49(3), 215–224 (2017).

Song, G., Wang, X., Ren, H., Zhang, W., Zhang, L. and Fang, Z. 2000. Simultaneous measurements of the thickness and refractive index of microstructures in obscure specimen by optical coherence tomography. *Optik*, 111, 541-543.

StataCorp. 2017. *Stata Statistical Software: Release 15*. College Station, TX: StataCorp LLC

Stephan R. M., Miller B. F. A quantitative method for evaluating physical and chemical agents which modify production of acids in bacterial plaques on human teeth. *J Dent Res* 1943;22:45–51.

Stookey, G.K., 2004. Optical methods—quantitative light fluorescence. *Journal of Dental Research*, 83(1_suppl), pp.84-88.

Sundstorm, F., Fredriksson, K., Montan, S., Haftstrom-bjorkman, U. and Strom, J. 1985. Laser-induced Fluorescence from Sound and Carious Tooth Substance-Spectroscopic Studies. *Swedish Dental Journal*, 9, 71-80.

Swanson, E. A., Izatt, J., Lin, C., Fujimoto, J., Schuman J., Hee, M., Huang, D. and Puliافت, C. 1993. In vivo retinal imaging by optical coherence tomography. *Optics letters*, 18, 1864-1866.

Takahashi, N. and Nyvad, B. (2008) Caries ecology revisited: Microbial dynamics and the caries process. *Caries Research*, 42, 409-418.

Takahashi, N. and Nyvad, B. The role of bacteria in the caries process: ecological perspectives. *J Dent Res*. 2011; 90:294–303.

Ten Bosch J, Angmar-Månsson B. Characterization and validation of diagnostic methods. *Monogr Oral Sci*. 2000;17:174–189.

The Ionising Radiation (Medical Exposure) Regulations . (2017) . Retrieved Online 12 October 2019, from; www.legislation.gov.uk/ukxi/2017/1322/contents/made

Tubiana, M. 2000. Radiation risks in perspective: radiation-induced cancer among cancer risks. *Radiation and Environmental Biophysics*, 39, 3-16.

Twetman, S., Axelsson, S., Dahlen, G., Espelid, I., Mejare, I., Norlund, A. and Tranaeus, S. 2013. Adjunct methods for caries detection: a systematic review of literature. *Acta Odontologica Scandinavica*, 71, 388-397.

Tymofiyeva, O., Boldt, J., Rottner, K., Schmid, F., Richter, E.J. and Jakob, P.M., 2009. High-resolution 3D magnetic resonance imaging and quantification of carious lesions and dental pulp in vivo. *Magnetic Resonance Materials in Physics, Biology and Medicine*, 22(6), p.365.

US NATIONAL RESEARCH COUNCIL. 2006. Health risks from exposure to low levels of ionizing radiation BEIR VII – Phase 2. *Washington DC: National Academies Press*.

Vandenbergh, B., Jacobs, R. and Bosmans, H. 2010. Modern dental imaging: an overview of the current technology and clinical applications in dental practice. *European radiology*, 20, 2637-55.

Van Luijk, J.A., 1981. NMR: dental imaging without x-rays?. *Oral Surgery, Oral Medicine, Oral Pathology*, 52(3), pp.321-324.

Wang, X., Shaffer, J., Weyant, R., Cuenco, K., DeSensi, R., Crout, R., McNeil, D. and Marazita, M. (2010). Genes and Their Effects on Dental Caries May Differ between Primary and Permanent Dentitions. *Caries Research*, 44(3), pp.201-208.

Werneck, R. I., Mira, M. T., and Trevilatto, P. C. (2010). A critical review: an overview of genetic influence on dental caries. *Oral diseases*, 16(7), 613-623.

Welzel, J. 2001. Optical coherence tomography in dermatology: a review. *Skin Research and Technology*, 7, 1-9.

What is the burden of oral disease? . (2017). Retrieved Online 20 August 2017, from; http://www.who.int/oral_health/disease_burden/global/en/.

White, S. and Mallya, S. M. 2012. Update on the biological effects of ionizing radiation, relative dose factors and radiation hygiene. *Australian Dental Journal*, 57 Suppl 1, 2-8.

WHO guideline: sugar consumption recommendation. (2015). Retrieved Online 14 August 2017, from; <http://www.who.int/mediacentre/news/releases/2015/sugar-guideline/en/>

Willmott, N. S., Bryan, R. A. E. and Duggal, M. S. 2008. Molar-incisor-hypomineralisation: a literature review. *European archives of paediatric dentistry : official journal of the European Academy of Paediatric Dentistry*, 9, 172-9.

Woodward, G.L. and Leake, J.L., 1996. The use of dental radiographs to estimate the probability of cavitation of carious interproximal lesions. Part I: Evidence from the literature. *Journal (Canadian Dental Association)*, 62(9), pp.731-736.

Yip, H., Stevenson, A. and Beeley, J. 1994. The specificity of caries detector dyes in cavity preparation. *British dental journal*, 176, 417-421.

CHAPTER 14

Appendices

Appendix 1 – Ethical Approval 1702



University College London Hospitals 
NHS Foundation Trust

UCL Eastman Biobank for Studying Health and Disease

13/10/2017

Dr. Laurent Bozec
UCL Eastman

Project Title: The Use of Optical Coherence Tomography and Ultrasound as a Diagnostic Tool for Dental Caries

Reference number: 1702

Dear Investigator

I am writing to inform you that your application to the UCL Eastman Biobank as detailed above was approved by the Committee on 10/10/2017.

All researchers must complete and comply with the regulatory and governance requirements and information requested on the Biobank application form. Further information is available on the UCL Eastman biobank website, or on the UCL-CI WICI (<http://www.ucl.ac.uk/eastman/research/departments/clinical-research/biobank>)

Please keep this copy of the ethics approval letter for the Biobank for your records. The current duration of the ethical approval is until 12th June 2023 in line with the duration of the Research Tissue Bank approval. This approval may be renewed for a further period in the future. We will be asking you to complete an annual return giving information on the number of patients consented and samples taken. We may at any time request to audit your project to ensure compliance with the necessary regulatory and governance requirements.

Thank you for your application to the Biobank and if you have any questions, please do not hesitate to contact Yuan-Ling Paula Ng (y.ng@ucl.ac.uk).

Yours Sincerely



Yuan-Ling Paula Ng

Chair, UCL Eastman Biobank



UCL Eastman Biobank for Studying Health and Disease

PARENT/GUARDIAN INFORMATION SHEET

Why have I been asked to read this document?

We are inviting potential donors to donate tissue and provide access to their clinical notes and imaging to the UCL Biobank for Studying Health and Disease.

Please read the following information carefully and discuss it with others if you and your child wish. Please ask us if there is anything that is not clear or if you and your child would like more information.

Why do we want to study your child's notes and imaging (x-rays and scans)?

Research will add to our overall understanding of human and dental diseases, and may help to design new ways to diagnose and treat disease.

What is the UCL Eastman Biobank for Studying Health and Disease?

The biobank is a collection of human material including saliva, plaque, blood, teeth and other normal and diseased tissue from potential adult and child donors attending the Eastman Dental Hospital. Samples from the biobank are used in ethically approved research.

What is the purpose of the UCL Biobank for Studying Health and Disease?

The purpose of the biobank is to have tissue available, now and in the future, for research projects investigating oral and human disease and the normal functioning of the human body. The biobank will primarily be for the use of scientists conducting research at the UCL Eastman Dental Institute, however potentially it could be used by scientists working in the UK or, in the public sector but not for commercial research. Only projects that fall under the described remit of the Biobank will be approved.

Does my child have to take part?

No. Whatever your child's decision, it will not affect any treatment or care your child receives in this or any other hospital, now or in the future.

What will it involve if I decide to permit my child take part?

On behalf of your child, you will be asked to sign a consent form:

- that allows clinical information to be extracted from your child's notes and imaging (x-rays and scans) from the Eastman Dental Hospital or University College London Hospital NHS trust (UCLH);
- that allows your child's data to be stored on a secure database in a coded/anonymised form;
- that allows storing a small piece of tissue eg a tooth, that is surplus to diagnostic requirements, for research projects including research on new therapies for managing dental disease;
- that allows collection of saliva, blood or plaque specimens for research projects including genetic research. Genetic analysis of your child's saliva often explains why certain diseases develop.

Additional tissue purely for research purposes is not removed at any time.

All these samples will be collected when your child visits his/her hospital. The saliva sample is taken by gently stroking the inside of your child's cheek with a cotton swab. The plaque sample is taken by rubbing a cotton swab over your child's gums and teeth.

Blood sample will be drawn your child's arm by a trained clinician or nurse. Firstly, we will examine and place a cuff on your child's arm to maintain a small amount of pressure. We will then find a suitable vein and clean it with an antiseptic sponge, and subsequently insert a needle in your child's arm which will collect your blood into a blood tube. Your child should not feel any discomfort or pain. This usually takes less than one minute. The needle will be removed and a sterile dressing applied to your child's arm.

We may ask for any of the above samples on more than one occasion but you can refuse at any time without giving a reason and without your child's medical care being affected.

What are the advantages and disadvantages of my child taking part?

There are potentially no advantages to your child if they participate in research but it may help others in the future. Your child will not receive a financial reward. Donated tissue is considered to be a 'gift' to the biobank.

Will my child's information be kept confidential?

Yes. All information about your child and his/her tissue samples will be treated with the strictest confidence. All information about your child would be coded so that it cannot be traced back to your child by the researcher. Results from genetic studies will be placed on a database to which only authorised individuals have access. Before having access to your child's clinical information and/or tissue samples, researchers must agree to conditions which safeguard your child's confidentiality.

Are my child and I going to receive feedback on the sample(s) my child donated?

We do not expect significant health-related findings from the studies which are approved by the UCL Eastman Biobank to use your donated teeth, plaque, saliva or blood. You and your child will therefore not be informed of the test results including genetic tests. Donating saliva, blood or plaque will have no impact on your medical insurance.

Family members

It is sometimes useful to have saliva, plaque or even blood samples from family members as this allows us to study the impact of genetic and environmental factors on the development of a disease. Therefore in some instances we may ask you to consent to allow us to contact your child's family members (parents/grandparents/cousins etc). You will also be given the Information Sheets to pass on to your child's relatives.

What if there is a problem or I require further information?

If you and your child would like further information or you have concerns about this research at any time you can:

- discuss it with your child's dentist or nurse
- email us on eastmanbiobank@ucl.ac.uk, we will try to answer your and your child's questions
- Normal NHS complaints procedures will apply.

What will happen if I do not want my child to carry on with the study?

You and your child are free to withdraw your consent at any time. This means that researchers will no longer be able to access any of your child's notes and images, and your child's tissue samples in the biobank will be destroyed. You and your child do not have to give a reason for changing your mind. However, if the data has already been used it is not always possible to recall it.

What will happen to any samples that my child gives?

Your child's samples will be used in a variety of studies and may include detailed analysis of your child's DNA to compare healthy DNA with the abnormal DNA found in patients with various diseases, or analysis of the bacteria and other organisms found in your mouth. Samples and data may be given for research purposes to other approved researchers in UK.

What will happen to the results of the study?

The results of our research will be published on our website <https://www.ucl.ac.uk/eastmanresearch/departments/clinical-research/biobank>, in dental or medical journals.

Who is organizing and funding UCL Biobank for Studying Health and Disease?

The biobank is overseen by the Research & Development Unit of UCL and UCLH. The cost of operating the biobank is funded by UCL Eastman Dental Institute.

Who has reviewed the project?

The UCL Biobank for Studying Health and Disease has been given a favourable ethics opinion for conduct in the NHS by the NRES Committee Yorkshire and the Humber – Leeds East.

Many thanks for taking the time to read this information.



UCL Eastman Biobank for Studying Health and Disease

Information Sheet for children aged 5 and under

(Parent/guardian to use this document as a guide to talk to your child in whichever way is best for them).

www.ucl.ac.uk/eastman/research/departments/clinical-research/biobank

Hello...

We would like to ask you and your family if we could keep your bad teeth that we have taken out and take some saliva when you see the dentists. We will keep these safely in our Tissue Bank and use them to try and find new ways to get children who have bad teeth and gum like you, better.

What do I have to do?

You don't have to do anything. If we need to make you feel better, by taking any bad teeth out, we might ask you if we can keep them. We might ask you to spit into a pot or rub some cotton wool onto your gums to see what kinds of bugs live there.

Will this help me?

We can't promise that this will help you but it could help other children who have mouth problems in the future.

Do I have to say yes?

No you don't. If you decide to say no, nobody will be cross with you. If you say yes, but decide to change your mind later then that's ok too, no one will be upset. You will still get the care you need.

What do I do now?

We know you may have some worries about doing this. Talk with your family and take time to think about what you are being asked to do. The dentists and nurses would also be happy to help you if there is anything you don't understand or you want to know.





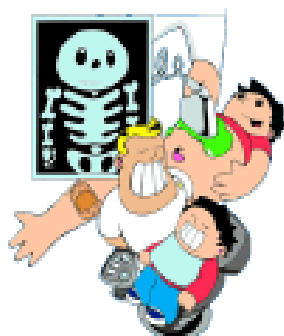
UCL Eastman Biobank for Studying Health and Disease

Information Sheet for Children 6-10 years old

Dentists at UCLH are doing a research study and would like to ask for your help. Research means finding out more about something. It is a way we try to find out the answers to questions.

Why is this project being done?

Some children have big problems with their teeth. Dentists don't always know why this happens or the best way to treat it. Sometimes as well tooth or gum problems can cause problems in other parts of the body. We would like you to help us find out more about this.



Why have I been chosen to take part?

We ask patients at this hospital having treatment to be in our research study, and are inviting you to take part too.

What do I have to do to take part?

You don't have to do anything. If you have any treatment, teeth or other tissue we remove will be kept. Normally we throw this away. If you agree to take part in our project, the signed consent form allows us to keep this tissue and researchers can study it to learn more about disease, and hopefully make better treatments in the future.

We might also like to take a small saliva or plaque sample. We might even ask if we can take some blood, but you can always say no if you are not happy with this.

Will joining in help me?

We cannot promise the study will help you but what we discover might help other children with tooth problems.

Do I have to take part?

You do not have to take part. You can say no and no one will be cross or upset. If you say yes, but later change your mind then that's ok as well. Just tell your parents, dentist or nurse. They will not be cross with you and you will still get the treatment you need.

Will anyone find out if I am on this study?

Your name and the things about you will be kept a secret - only the people who are doing the research will be able to see this information.

What do I do now?

Take time to decide whether or not you want to take part, and please ask us if there is anything that you do not understand.

If you have questions that the person who looks after you cannot answer, you can email us on eastmanbiobank@ucl.ac.uk, we will try to answer your question, or will speak to Dr. Yuan-Ling Ng (Telephone number [REDACTED]).





UCL Eastman Biobank for Studying Health and Disease

Information Sheet for Children 11-15 years old

We are asking if you would like to take part in a research project to help us understand more about dental diseases. Before you decide if you want to join in, it is important to understand why the research is being done and what it will involve for you. So please consider this leaflet carefully. Talk about it with your family, friends, dentist or nurse if you want to.

We are doing this research to gain a better understanding of the disease processes involved in dental and human disease and the normal functioning of the human body.

The UCL Eastman Biobank is a source of clinical information and tissue for a number of research projects that study dental and human disease and the normal functioning of the human body. The research we do could help develop new methods of detecting and managing disease.

Why have I been chosen?

You have been invited to join our study because you are being seen by dentists at Eastman Dental Hospital, University College London Hospital NHS Trust (UCLH).

Do I have to take part?

No, it is up to you to decide whether or not to take part. If at any time you don't want to do the research anymore, just tell a parent or guardian, or dentist or nurse. Nobody will be upset.

What will I be asked to do?

When you have any treatment, a little bit of your tissue (eg a tooth) is sometimes removed in order to manage your condition. If you allow us, we will keep some or all of that tissue that would have normally been thrown away, to use it for our research. There is no need to take any extra tissue from you during surgery, and only tissue that would otherwise be thrown away is kept for research. You would have exactly the same treatment as if you had decided not to take part in the study.

We may also ask for samples of saliva or plaque. Having saliva samples means spitting into a pot. Having plaque samples means letting us rub your gums with a cotton wool roll or swab. Finally we might ask if we can take some blood. You can say no if you are not happy with this.

Will joining in help me?

We cannot promise the study will help you but the information we get might help treat others with various diseases and conditions in the future.

Is there anything to be worried about if I take part?

No, there are no added risks to the treatment or investigation that you are having for your condition.

What if there is a problem or something goes wrong?

If there is a problem and you wish to complain, or have any worries about this study then you can talk to a parent or guardian, your dentist, or people that work in our hospital, who will help you with any problems you have.

Will anyone else know I am taking part in this study?

We will keep your information in confidence. This means we will only tell those who have a need or right to know. We will only send out information that has your name and address removed.

What will happen to the results of the study?

The results of our research will add to our overall understanding of dental and human disease and the normal functioning of the human body. This information may help design new ways to diagnose or treat diseases and other conditions in the future. You will be able to read about our studies on the internet <https://www.ucl.ac.uk/eastman/research/departments/clinical-research/biobank>.

Please ask any questions if you need to.

If you have any questions that the person who looks after you cannot answer, you can email us on eastmanbiobank@ucl.ac.uk, we will try to answer your question or will arrange for you to speak to Dr. Yuan-Ling Ng (Telephone number: [REDACTED]).

Thank you very much for reading this information.



UCL Eastman Biobank for Studying Health and Disease

PARENT/GUARDIAN CONSENT FORM

For further information please email eastmanbiobank@ucl.ac.uk

DONOR NAME:

HOSPITAL NUMBER:

DONOR D.O.B:

If you wish to participate, please complete this section by initialling the boxes and then signing at the bottom of the page.

- | | |
|--|---|
| <p>1. I confirm that I have read and understood the relevant information sheet, version 3 dated 25th May 2017, and have had sufficient opportunity to ask questions.</p> <p>2. I give permission for my child's clinical data including imaging from any hospitals that my child attend, to be stored on a database in an anonymised format, and made available for ethically approved research, in the UK.</p> <p>3. I give permission for my child's tissue (surplus to diagnostic requirements) from any hospitals that my child attend to be made available for ethically approved research, including genetic analysis, in the UK.</p> <p>4. I give permission for my child's saliva to be made available for research, including genetic analysis, in the UK.</p> <p>5. I understand that all data and samples of my child will be coded for anonymity and all research projects will be approved by an ethical committee.</p> <p>6. I understand that my child's participation is voluntary, and can be withdrawn at any time without giving a reason. This will not affect my child's medical treatment or legal rights.</p> <p>7. I understand that my child and I will not receive feedback on the findings from my child's donated sample(s)</p> | <p><small>Please initial box</small></p> <input type="checkbox"/>
<input type="checkbox"/>
<input type="checkbox"/>
<input type="checkbox"/>
<input type="checkbox"/>
<input type="checkbox"/>
<input type="checkbox"/> |
|--|---|

CONSENT FOR BLOOD DONATION

In addition to the above, we may also ask for blood samples from your child. Please indicate below if you agree for blood samples of up to 50ml (5-8 teaspoons) to be taken from your child. If a blood sample for research purposes is taken from your child we will do our best to take it either when your child is under anaesthetic or when a blood sample is collected for diagnostic tests, however this may not always be possible. We may ask for blood on a number of separate occasions, but you or your child may refuse any time without giving a reason, and this will not affect your child's medical treatment or legal rights.

My child wish / do not wish to donate blood for research

Parent/Guardian signature:

Print full name:

Date: / /

Relationship to child:

Staff signature:

Institution:

Print name:

Date: / /



UCL Eastman Biobank for Studying Health and Disease

ASSENT FORM FOR YOUNG DONORS

For further information please email eastmanbiobank@ucl.ac.uk

DONOR'S NAME:

Donor (or parent/guardian on their behalf) to circle all they agree with*

Do you understand what this project/biobank is about? Yes No

Have you asked all the questions you want and had them answered in a way you understand? Yes No

Do you understand it's OK to stop taking part at any time? Yes No

When we ask you to donate blood, do you understand you can say no at any time without giving a reason? Yes No

Would you like to take part? Yes No

If any of the answers are 'no' or you don't want to take part, don't sign your name.
If you do want to take part, please write your name below*

Your name _____ Date _____

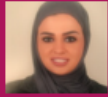
Your parent or guardian also needs to sign*

Print Name _____ Sign _____ Date _____

The doctor who explained this project to you needs to sign too*

Institution _____

Print Name _____ Sign _____ Date _____



The Use of Optical Coherence Tomography as a Diagnostic Tool for Dental Caries

R. Al-khuwaitem¹, S. Siddiqui², S. Parekh¹ and L. Bozec²

¹ Department of Paediatric, UCL Eastman Dental Institute, 256 Gray's Inn Road, London WC1X 8LD • www.ucl.ac.uk/eastman
² Department of Biomaterials, UCL Eastman Dental Institute, 256 Gray's Inn Road, London WC1X 8LD • www.ucl.ac.uk/eastman



Introduction

Dental caries is one of the most common human diseases, 60-90% of school children worldwide have dental cavities¹. White spot lesions (WSL) are the clinical presentation of early caries. Different diagnostic tools used to assess caries include; clinical examination, radiographic investigation and Enhanced Visual examination/International Caries Detection and Assessment System (ICDAS) as shown in table 1.

To date, no universal diagnostic tool can reliably detect carious lesions at the very early stages.

Optical Coherence Tomography (OCT) is a non-invasive and ionising radiation free technique that has been used in dentistry but not to diagnose caries.

ICDAS	Description	Visual appearance
0	Sound tooth surface	
1	Opacity or discoloration only visible after air drying	
2	Opacity or discoloration directly visible without air drying	
3	A white or brown spot lesion with localized enamel breakdown	
4	Irregularly shaped shallow dentine with or without localized enamel breakdown	
5	Distinct cavity with visible dentine	
6	Extensive cavity with visible dentine	

Table 1: Enhanced visual/ICDAS scores

Aim of the study:

"Can optical coherence tomography be used as a diagnostic tool for dental caries?"

Objectives

- To investigate the use of OCT imaging in dentistry as a diagnostic tool for dental caries
- To compare OCT imaging with clinical measures ICDAS and radiographic imaging of carious teeth
- To develop a standardised marker for each ICDAS score

Materials and Methods

Ethical approval was obtained from Eastman Biobank- study number 1702. A total of 180 primary and permanent teeth were collected from patients, according to the inclusion and exclusion criteria. All the samples were assessed (figure 1a) and categorised into six categories according to the ICDAS scoring system. All teeth were then imaged radiographically (figure 1b). Additionally, occlusal surfaces of teeth were imaged using the OCT (VivoSight, Michelson Diagnostics, Kent, UK shown in figure 1c).

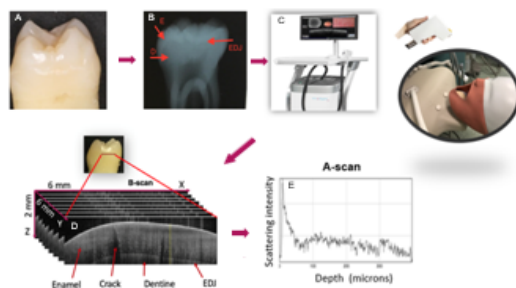
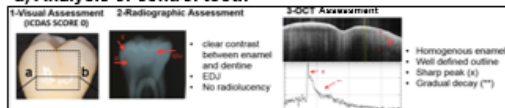


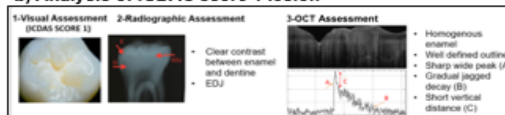
Figure 1: A) Control tooth B) Radiograph C) OCT D) B-scan E) A-scan

Results

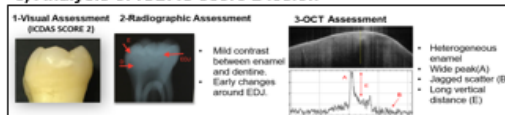
a) Analysis of control tooth



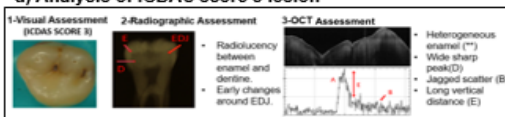
b) Analysis of ICDAS score 1 lesion



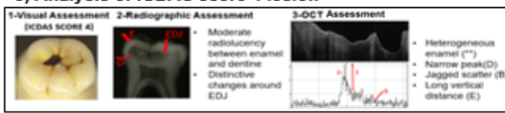
c) Analysis of ICDAS score 2 lesion



d) Analysis of ICDAS score 3 lesion



e) Analysis of ICDAS score 4 lesion



f) From scattering markers to diagnosis

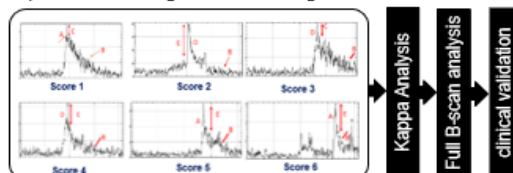


Figure 2: OCT a- scans of samples with markers, A indicates narrow peak, B jagged scatter, C short vertical distance, D wide peak and E long vertical distance.

Discussion

- Conventional methods of diagnosing caries do not give enough information on the extent of the lesion
- The abnormality of enamel destruction was clearly seen in OCT images

Conclusion

- This study showed that OCT imaging can be used to assess the extent of a caries lesion, proving the potential of OCT as a diagnostic tool
- OCT is a promising non-invasive and patient safe technique
- For deeper enamel lesions, it is likely that ICDAS/X-ray may still be the preferred diagnostic approach

References

- PETERSEN, P. E. 2003. The World Oral Health Report 2003: continuous improvement of oral health in the 21st century—the approach of the WHO Global Oral Health Programme. Community Dentistry and oral epidemiology, 31, 3-24.

Acknowledgement

Ministry of Health, Kuwait

PP2.089: The Use of Optical Coherence Tomography as a Diagnostic Tool for Dental Caries

R. Al-khuwaitem¹, S. Siddiqui², S. Parekh¹ and L. Bozec³

¹ Department of Paediatric, ² Department of Biostatistics, UCL Eastman Dental Institute, London WC1X 3LD * www.ucl.ac.uk/eastman
³ Faculty of Dentistry, University of Toronto, Toronto, Canada



Introduction

Dental caries is one of the most common human diseases, 80-90% of school children worldwide have dental cavities¹. Different diagnostic tools used to assess caries include: clinical examination, radiographic investigation and Enhanced Visual examination/International Caries Detection and Assessment System (ICDAS) as shown in table 1.

To date, no universal diagnostic tool can reliably detect carious lesions at the very early stages. Optical Coherence Tomography (OCT) is a non-invasive and ionising radiation free technique that has been used in dentistry, but not to diagnose caries.



Table 1: Enhanced visual/ICDAS scores

Aim of the study:

"Can optical coherence tomography be used as a diagnostic tool for dental caries?"

Objectives

- To investigate the use of OCT imaging as a diagnostic tool for dental caries
- To compare OCT imaging with ICDAS and radiographic imaging of carious teeth
- To develop a standardised marker for each ICDAS score

Materials and Methods

Ethical approval was obtained, a total of 180 primary and permanent teeth were collected from patients, according to the inclusion and exclusion criteria. All the samples were assessed (figure 1a) and categorised into six categories according to the ICDAS scoring system. All teeth were then imaged radiographically (figure 1b). Additionally, occlusal surfaces of teeth were imaged using the OCT (VivoSight, Michelson Diagnostics, Kent, UK shown in figure 1c).

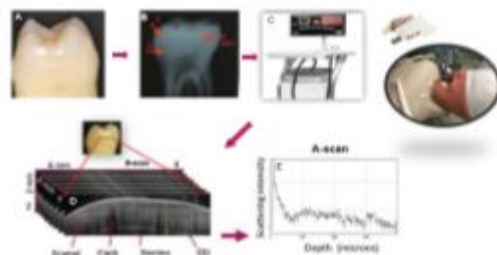


Figure 1: A) Control tooth B) Radiograph C) OCT D) B-scan E) A-scan

Results

a) Analysis of control tooth



b) Analysis of ICDAS score 1 lesion



c) Analysis of ICDAS score 2 lesion



d) Analysis of ICDAS score 3 lesion



e) Analysis of ICDAS score 4 lesion



f) From scattering markers to diagnosis

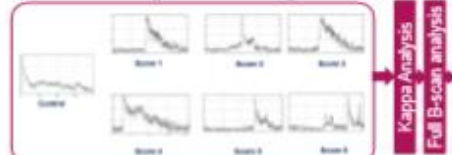


Figure 2: OCT a-scans of control and ICDAS scores samples with markers.

Discussion

- Conventional methods of diagnosing caries do not give enough information on the extent of the lesion
- The abnormality of enamel destruction was clearly seen in OCT images

Conclusion

- This study showed that OCT imaging can be used to assess the extent of a caries lesion, proving the potential of OCT as a diagnostic tool
- OCT is a promising non-invasive and patient safe technique
- For deeper enamel lesions, it is likely that ICDAS/X-ray may still be the preferred diagnostic approach

References

1. PETERSEN, P. E. 2003. The World Oral Health Report 2003: continuous improvement of oral health in the 21st century—the approach of the WHO Global Oral Health Programme. Community Dentistry and oral epidemiology, 31, 3-24.

Acknowledgement

Ministry of Health, Kuwait

